Supporting Information for

Lysine-Targeting Reversible Covalent Inhibitors with Long Residence Time

Rahi M. Reja, Wenjian Wang, Yuhan Lyu, Fredrik Haeffner, and Jianmin Gao*

Email: jianmin.gao@bc.edu

Department of Chemistry, Boston College, 2609 Beacon Street, Chestnut Hill, MA 02467, United States

Contents

1. Materials and Methods

All chemicals, reagents and amino acids were purchased from the commercially available sources. Hexane, Methanol, Dichloromethane, Ethyl acetate, N,N-Dimethylformamide were purchased from the commercially available sources and used without further distillation. Silica gel (230-400 mesh) was used for column chromatography. The chemicals used for the biological experiments were purchased as biological grades from the commercial's sources. The Ph.D.-C7C Phage Display Peptide Library Kit and the E. coli K12 ER2738 strain were purchased from New England Biolabs. The *S. aureus* (ATCC 6358) was purchased from Microbiologic as a lyophilized pellet. Peptide synthesis was carried out on a Tribute Peptide Synthesizer from Protein Technologies. All final peptides were purified by reverse phase HPLC. ^{1}H (600 MHz) and ^{13}C (150 MHz) NMR spectra were recorded using the residual solvent signal as internal standards. All the NMR spectra in 1× PBS were carried out using water suppression. Chemical shifts (δ) and coupling constants (J) are reported in parts per million (ppm) and Hz respectively.^{11}B NMR was recorded in 500 MHz NMR instrument using $BF_3.Et_2O$ as internal ^{11}B reference. Mass-spec data for the small molecules as well as peptides were generated using an Agilent 6230 LC-TOF mass spectrometer. UV spectra were collected on a Nanodrop UV-Vis spectrometer. The fluorescence anisotropy experiments for the binding curve and the competition assay were carried out using Spectra Max M5 plate reader. Fluorescence images were taken using Zeiss Axiovert Fluorescence Microscope. Flow cytometry was carried out using BD Accuri C6 Plus instrument. The following methods were used to analyze the purity of the samples in the LC-MS instrument.

Solvent A contains 100% water (0.1% formic acid) and solvent B contains 100% acetonitrile (0.1% formic acid).

Method A:

Time (Min)	A [%]	B[%]	Flow [mL/Min]
0	95.0	5.0	0.2
1	95.0	5.0	0.2
7	5.0	95.0	0.2
9	5.0	95.0	0.2
12	95.0	5.0	0.2
16	95.0	5.0	0.2

Method B:

Time (Min)	A [%]	B[%]	Flow [mL/Min]
0	95.0	5.0	0.2
5	95.0	5.0	0.2
24	5.0	95.0	0.2
27	5.0	95.0	0.2
28	95.0	5.0	0.2
33	95.0	5.0	0.2

Method C:

Time (Min)	A [%]	B[%]	Flow [mL/Min]
0	95.0	5.0	0.2
3	95.0	5.0	0.2
10	5.0	95.0	0.2
18	5.0	95.0	0.2
20	95.0	5.0	0.2
25	95.0	5.0	0.2

2. Synthetic Procedures

Scheme S1 (Compound **1)**:

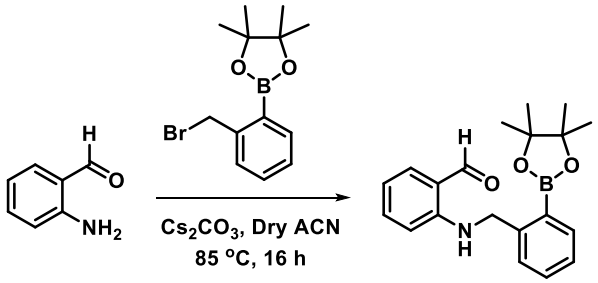

1

2-Amino benzaldehyde (242 mg, 2 mmol) was dissolved in 5 mL of dry acetonitrile. To this, 2-bromomethylphenylboronic acid pinacol ester (594 mg, 2 mmol) and anhydrous cesium carbonate (650 mg, 2 mmol) were added at room temperature. Then, the reaction mixture was refluxed at 85 °C for about 12h. After completion of the reaction (confirmed by TLC), solvent was evaporated and directly subjected for column chromatography and purified using EtOAc/hexane as a solvent. Yield: 300 mg (44.3%)

^{1}H NMR (600 MHz, $CDCl_3$) δ 9.82 (s, 1H), 7.86 (d, *J* = 6 Hz, 1H), 7.45 (dd, *J* = 7.8, 1.8 Hz, 1H), 7.38 – 7.35 (m, 2H), 7.33 – 7.31 (m, 1H), 7.27-7.24 (m, 2H), 6.76 (d, *J* = 8.4 Hz, 1H), 6.67 (t, *J* = 7.8 Hz, 1H), 4.73 (s, 2H), 1.34 (s, 12H). **^{13}C NMR** (150 MHz, $CDCl_3$) δ 193.88, 150.77, 144.89, 136.75, 135.79, 131.36, 127.60, 126.69, 118.77, 115.11, 111.85, 84.00, 46.69, 25.00. **MS-ESI$^+$:** *m/z* calculated for $C_{20}H_{24}BNO_3$ $[M+H]^+$ 338.1927, found 338.1770

Scheme S2 [Compound **2** (**RMR1**)]:

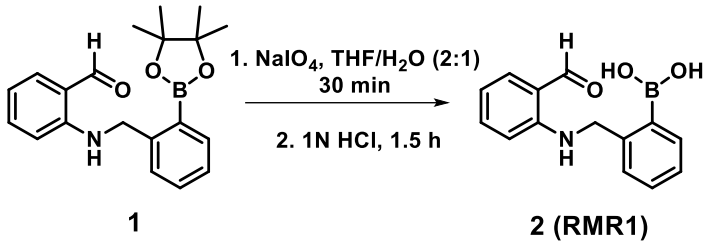

The pinacol ester of compound **1** was deprotected using reported protocol.[1] Briefly, compound 1 (338 mg, 1 mmol) was dissolved in 1 mL of THF/H_2O (4:1). To this solution, $NaIO_4$ (639 mg, 3 mmol) was added to it and stirred for about 30 min at room temperature. After that, 1.5 mL of 1N HCl solution was added and stirred for another 2 h at room temperature. After completion of the reaction (confirmed by TLC), THF was evaporated under vacuum and the aqueous solution was extracted with EtOAc (3 × 30 mL). Then the combined organic layer was washed with brine (3 × 30 mL) and dried over anhydrous Na_2SO_4. The crude compound was purified through column chromatography using EtOAc/hexane solvent system. Yield: 135 mg (53%)

^{1}H NMR (600 MHz, DMSO-d_6/D_2O) δ 9.60 (s, 1H), 8.54 (t, *J* = 6 Hz, 1H), 7.47 (dd, *J* = 7.8, 1.2 Hz, 1H), 7.40 (dd, *J* = 7.2, 1.8 Hz, 1H), 7.30-7.25 (m, 3H), 7.18 (td, *J* = 7.2, 1.8 Hz, 1H), 6.67 (d, *J* = 8.4 Hz, 1H), 6.64 – 6.61 (m, 1H). **^{13}C NMR** (150 MHz, DMSO-d_6/D_2O) δ 197.10, 144.09, 138.73, 138.11, 135.09, 131.18, 129.42, 128.36, 122.42, 119.68, 117.21, 113.06, 113.03, 47.74. **MS-ESI$^+$:** *m/z* calculated for $C_{14}H_{14}BNO_3$ $[M+H]^+$ 256.1145, found 256.1022

Scheme S3 [Compound **4** (**RMR2**)]:

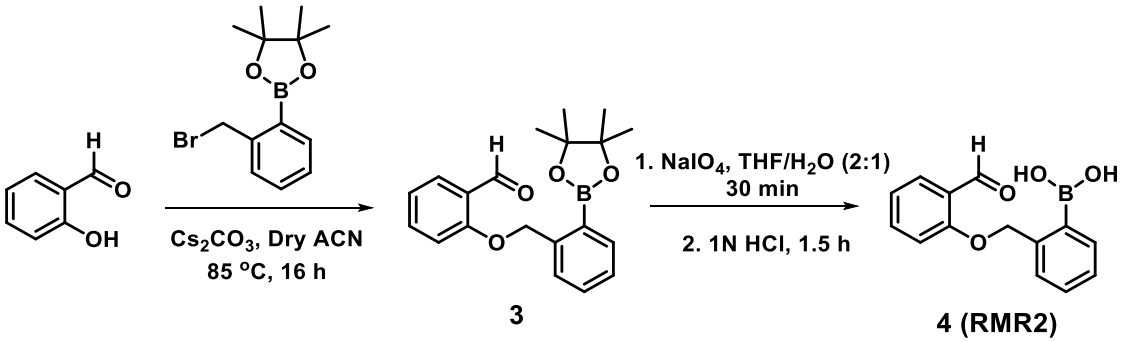

Compound **4** was synthesized by same protocol as mentioned for the compound **2**(RMR1). Instead of 2-Amino benzaldehyde, salicylaldehyde was used.

Compound **3**: **^{1}H NMR** (600 MHz, $CDCl_3$) δ 10.54 (s, 1H), 7.90 (dd, *J* = 7.2, 1.8 Hz, 2H), 7.85 (dd, *J* = 7.8, 1.8 Hz, 2H), 7.55-7.52 (m, 2H), 7.48 (td, *J* = 7.48, 1.2 Hz, 2H), 7.36 (td, *J* = 7.2, 1.2 Hz, 1H), 7.10 (d, *J* = 12 Hz, 1H), 7.02 (t, *J* = 12 Hz, 1H), 5.46 (s, 2H), 1.27 (s, 12H). **^{13}C NMR** (150 MHz, $CDCl_3$) δ 190.23, 161.81, 142.46, 136.48, 135.99, 131.48, 128.28, 127.75, 127.56, 125.20, 120.71, 113.35, 83.95, 70.38, 24.98. **MS-ESI$^+$:** *m/z* calculated for $C_{20}H_{23}BO_4$ $[M+H]^+$ 339.1767, found 339.1688

Compound **4** (**RMR2**):**^{1}H NMR** (600 MHz, CD_3OD) δ 10.46 (s, 1H), 7.81 (dd, *J* = 7.8, 1.8 Hz, 1H), 7.61-7.58 (m, 1H), 7.48 (d, *J* = 7.8 Hz, 1H), 7.45 – 7.40 (m, 2H), 7.37 (td, *J* = 7.5, 1.2 Hz, 1H),

7.23 (d, *J* = 8.4 Hz, 1H), 7.08 (t, *J* = 7.2 Hz, 1H), 5.32 (s, 2H). **^{13}C NMR** (150 MHz, CD_3OD) δ 191.24, 162.52, 141.08, 137.44, 133.21, 130.38, 129.99, 128.87, 128.70, 128.58, 126.26, 122.07, 114.58, 72.04. **MS-ESI$^+$:** *m/z* calculated for $C_{14}H_{13}BO_4$ $[M+Na]^+$ 279.0804, found 279.0676

Scheme S4 [Compound **5**(**RMR3**)]:

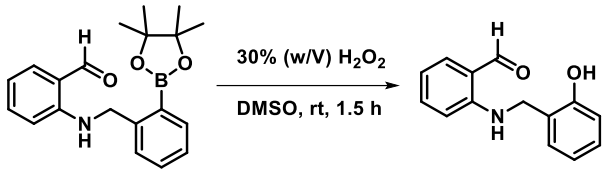

1 **5 (RMR3)**

Compound **5** was synthesized from compound **1**. Compound **1** (338 mg, 1mmol) was dissolved in 5 mL of DMSO. To this solution, 1 mL of 30% (wt/V) H_2O_2 was added. Then, the reaction mixture was stirred at room temperature for about 1.5 h. After completion of the reaction (confirmed by TLC), 30 mL of water was added to it. Then, the reaction mixture was extracted with EtOAc (3 × 30 mL). After that combined organic layer was washed with brine solution (3 × 30 mL) and dried over anhydrous Na_2SO_4. Then the crude compound was purified through silica gel column chromatography using EtOAc/hexane as a solvent. Yield: 200 mg (88.1%)

^{1}H NMR (600 MHz, $CDCl_3$) δ 9.86 (s, 1H), 7.53 (dd, *J* = 7.8, 1.8 Hz, 1H), 7.40-7.38 (m, 1H), 7.23-7.22 (m, 1H), 7.18 (td, *J* = 7.8, 1.8 Hz, 1H), 6.90 (td, *J* = 7.2, 1.2 Hz, 1H), 6.84 – 6.79 (m, 3H), 4.51 (s, 2H). **^{13}C NMR** (125 MHz, $CDCl_3$) δ 194.39, 154.61, 150.75, 136.82, 136.05, 128.96, 128.95, 123.91, 120.98, 119.66, 116.45, 116.09, 112.23, 43.68.**MS-ESI$^+$:** *m/z* calculated for $C_{14}H_{13}NO_2$ $[M+H]^+$ 228.1025, found 228.0893

Scheme S5 (Compound **6**):

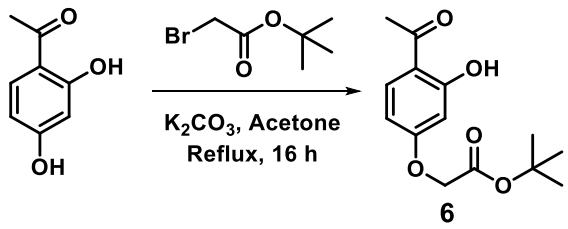

6

Compound **6** was synthesized using reported protocol.[2] Briefly, 2,4-Dihydroxyacetophenone (1.5 g, 10 mmol) was dissolved in 50 mL of acetone. To this solution, anhydrous K_2CO_3 (1.38 g, 10 mmol) and *tert*-butyl bromoacetate (1.2 mL, 10 mmol) was added. Then, the reaction mixture was refluxed at 85 °C for overnight. After completion of the reaction (confirmed by TLC), solvent was evaporated under vacuum and extracted with EtOAc (3 × 30 mL). After that the combined organic layer was washed with brine solution (3 × 30 mL) and dried over anhydrous Na_2SO_4. The crude

product was purified through silica gel column chromatography using EtOAc/hexane as solvent system. Yield: 2 g (77%)

^{1}H NMR (600 MHz, $CDCl_3$) δ 12.67 (s, 1H), 7.64 (d, *J* = 8 Hz, 1H), 6.47 (dd, *J* = 8.7, 2.4 Hz, 1H), 6.34 (d, *J* = 2.4 Hz, 1H), 4.53 (s, 2H), 2.54 (s, 3H), 1.48 (s, 9H). **^{13}C NMR** (150 MHz, $CDCl_3$) δ 202.82, 167.13, 165.14, 164.30, 132.57, 114.62, 107.83, 101.77, 83.00, 65.52, 28.14, 26.38. **MS-ESI$^+$:** *m/z* calculated for $C_{14}H_{18}O_5$ $[M+Na]^+$ 267.1232, found 267.1183

Scheme S6 (Compound **7**):

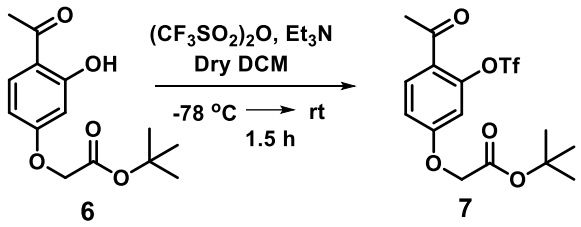

Compound **6** (2 g, 7.5 mmol) was dissolved in dry DCM. To this solution, triethylamine (1.4 mL, 10 mmol) was added at room temperature and stirred for 5 min. After that, triflic anhydride (1.7 mL, 10 mmol) was dropwise added to it at -78 °C. Then, the reaction mixture was stirred for another 1 h at room temperature. After completion of the reaction (confirmed by TLC), reaction was quenched with saturated $NaHCO_3$ solution and extracted with DCM (3 × 50 mL). The combined organic layer was washed with brine solution and dried over anhydrous MgSO4. The crude product was purified through silica gel column chromatography using EtOAc/hexane as solvent system. Yield: 2 g (67.1%)

^{1}H NMR (600 MHz, $CDCl_3$) δ 7.84 (d, *J* = 12 Hz, 1H), 6.94 (dd, *J* = 2.4, 9 Hz, 1H), 6.83 (d, *J* = 2.4 Hz, 1H), 4.58 (s, 2H), 2.59 (s, 3H), 1.49 (s, 9H). **^{13}C NMR** (150 MHz, $CDCl_3$) δ ^{13}C NMR (151 MHz, $cdcl_3$) δ 195.11, 166.65, 161.92, 148.50, 132.78, 125.02, 121.93, 119.80, 117.67, 115.55, 114.01, 109.69, 83.49, 65.97, 29.32, 28.11. **MS-ESI$^+$:** *m/z* calculated for $C_{15}H_{17}F_3O_7S$ $[M+Na]^+$ 421.0544, found 421.0294

Scheme S7 (Compound **8**):

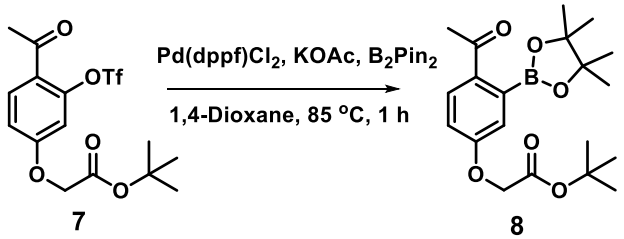

The compound **7** (800 mg, 2 mmol) was dissolved in 10 mL of dry dioxane. To this solution, potassium acetate (392 mg, 4 mmol), bis pinacolate diborane (1g, 4mmol) and $Pd(dppf)Cl_2$.DCM (81 mg, 10%) were added to it. Then, the solution was degassed for 30 mins. After that, it was heated at 85 °C for about 1 h. After completion of the reaction (confirmed by TLC), 30 mL of brine was added to it. Then the reaction mixture was extracted with EtOAc (3 × 30 mL). After that the

combined organic layer was washed with brine solution (3 × 30 mL) and dried over anhydrous Na_2SO_4. The crude product was purified through silica gel column chromatography using EtOAc/hexane solvent system. Yield: 400 mg (53.1%)

^{1}H NMR (600 MHz, $CDCl_3$) δ 7.78 (d, *J* = 12 Hz, 1H), 6.94 (d, *J* = 6 Hz, 1H), 6.89 (dd, *J* = 12, 6 Hz, 1H), 4.57 (s, 2H), 2.55 (s, 3H), 1.48 (s, 9H), 1.43 (s, 12H).**^{13}C NMR** (150 MHz, $CDCl_3$) δ 198.54, 167.46, 161.56, 134.40, 130.76, 117.92, 114.76, 83.80, 82.88, 65.84, 28.15, 25.05.**MS-ESI$^+$:** *m/z* calculated for $C_{20}H_{29}BO_6$ $[M+H]^+$ 377.2135, found 377.1871

Scheme S8 [Compound **9** (**APBA-Acid**)]:

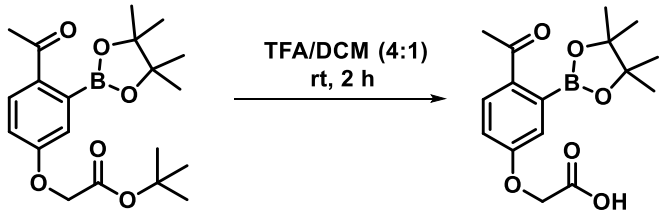

Compound **8** (376 mg, 1 mmol) was dissolved in 10 mL of TFA/DCM (4:1). Then, the reaction mixture was stirred for about 2 h at room temperature. After completion of the reaction (confirmed by LC-MS), TFA was evaporated under vacuum. Then, compound was precipitated using cold diethyl ether. The precipitation was centrifuged and dried in vacuum. The compound was directly used for coupling in solid phase peptide synthesis without any further purification. Yield: 250 mg (78.1%)

^{1}H NMR (600 MHz, DMSO-d_6) δ 13.09 (s, 1H), 7.96 (d, *J* = 12 Hz, 1H), 7.00 (dd, *J* = 3, 6 Hz, 1H), 6.87 (d, *J* = 6 Hz, 1H), 4.80 (s, 2H), 2.52 (s, 3H), 1.31 (s, 12H).**^{13}C NMR** (150 MHz, DMSO-d_6) δ 198.00, 169.76, 161.10, 133.50, 131.39, 117.79, 113.82, 82.92, 64.52, 25.01, 24.65.**MS-ESI$^+$:** *m/z* calculated for $C_{16}H_{21}BO_6$ $[M+H]^+$ 321.1590, found 321.1702

Scheme S9 (Compound **10**):

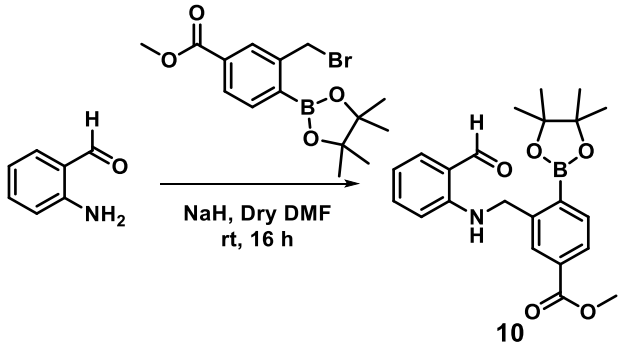

2-Amino benzaldehyde (605 mg, 5 mmol) was dissolved in 5 mL of dry DMF. To this solution, sodium hydride (240 mg, 10 mmol) was added under inert atmosphere. Then the reaction mixture was stirred for about 30 min at room temperature. After 30 min, methyl 3-(bromomethyl)-4-(4,4,5,5-tetramethyl-1,3,2-dioxaborolan-2-yl)benzoate (1.7 g, 5 mmol) was added to it . Then, the reaction mixture was stirred for about 16 h at room temperature under inert atmosphere. After completion of the reaction (confirmed by TLC), 30 mL of brine solution was added to it. Then, the reaction mixture was extracted with EtOAc (3 × 30 mL). After that the combined organic layer was washed with brine solution (3 × 30 mL) and dried over anhydrous Na_2SO_4. Then the crude compound was purified through silica gel column chromatography using EtOAc/hexane as solvent. Yield: 400 mg (20%)

^{1}H NMR (600 MHz, $CDCl_3$) δ 9.82 (s, *J* = 1 Hz, 1H), 8.01 (bs, 1H), 7.92 (dd, *J* = 3, 0.6 Hz, 2H), 7.46 (dd, *J* = 7.8, 1.8 Hz, 1H), 7.35-7.32 (m, 1H), 6.75 (d, *J* = 8.4 Hz, 1H), 6.68 (t, *J* = 7.8 Hz, 1H), 4.73 (s, 2H), 3.89 (s, 3H), 1.34 (s, 12H). **^{13}C NMR** (150 MHz, $CDCl_3$) δ 193.91, 167.10, 150.62, 145.34, 136.81, 136.78, 135.86, 132.41, 128.68, 127.66, 118.86, 115.32, 111.62, 84.43, 52.33, 46.69, 24.98. **MS-ESI$^+$:** *m/z* calculated for $C_{22}H_{26}BNO_5$ $[M+H]^+$ 396.1982, found 396.1782

Scheme S10 [Compound **11** (**RMR1-Acid**)]:

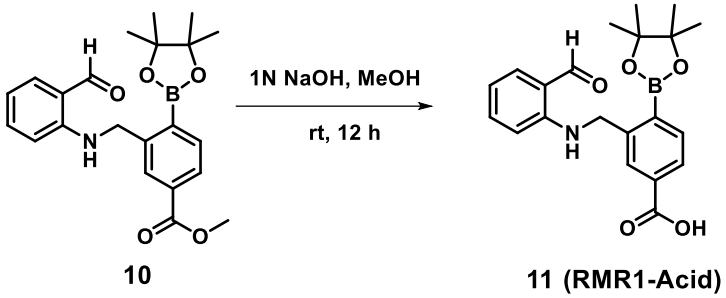

10 **11 (RMR1-Acid)**

Compound **10** (400 mg, 1 mmol) was dissolved in 35 mL methanol. To this solution, 5 mL of 1(N) NaOH solution was added drop wise. Then, the reaction mixture was stirred for about 12 h. After completion of the reaction (confirmed by TLC), methanol was evaporated and the aqueous layer was acidified with 5% HCl solution. Then, aqueous layer was mixture was extracted with EtOAc (3 × 30 mL). After that the combined organic layer was washed with brine solution (3 × 30 mL) and dried over anhydrous Na_2SO_4. Then the crude compound was purified through silica gel column chromatography using EtOAc/hexane as solvent. Yield: 150 mg (40%)

^{1}H NMR (600 MHz, CD_3OD) δ 9.80 (s, 1H), 8.06 (bs, 1H), 7.94 – 7.90 (m, 2H), 7.54 (dd, *J* = 7.8, 1.8 Hz, 1H), 7.41-7.38 (m, 1H), 6.85 (d, *J* = 4.5 Hz, 1H), 6.71 (t, *J* = 7.2 Hz, 1H), 4.73 (s, 2H), 1.35 (s, 12H). **^{13}C NMR** (150 MHz, CD_3OD) δ 195.50, 169.58, 151.74, 146.76, 137.92, 137.55, 137.00, 130.11, 128.71, 120.04, 116.33, 112.42, 85.57, 47.21, 25.16. **MS-ESI$^+$:** *m/z* calculated for $C_{21}H_{24}BNO_5$ $[M+H]^+$ 382.1825, found 382.1631

Scheme S11 (Compound **12**):

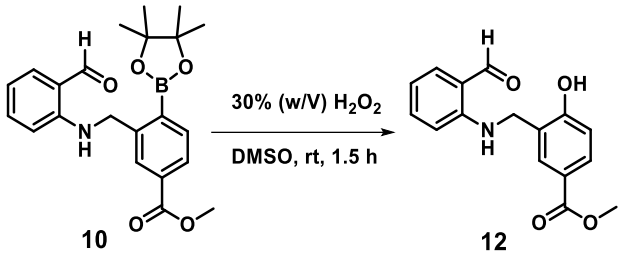

Compound **12** was synthesized from compound **10**. Compound **10** (396 mg, 1mmol) was dissolved in 5 mL of DMSO. To it, 1 mL of 30% (wt/V) H_2O_2 was added. The reaction mixture was stirred at room temperature for about 1.5h. After completion of the reaction (confirmed by TLC), 30 mL of water was added to it. Then, the reaction mixture was extracted with EtOAc (3 × 30 mL). After that, the combined organic layer was washed with brine solution (3 × 30 mL) and dried over anhydrous Na_2SO_4. Then the crude compound was purified through silicagel column chromatography using EtOAc/hexane as solvent. Yield: 200 mg (70.1%)

^{1}H NMR (600 MHz, $CDCl_3$) δ 9.87 (s, 1H), 7.95 (d, *J*= 1.8 Hz, 1H), 7.89 (dd, *J* = 8.4, 2.4 Hz, 1H), 7.55 (dd, *J* = 6.6, 1.2 Hz, 1H), 7.42-7.39 (m, 1H), 6.87-6.85 (m, 2H), 6.82 (d, *J* = 8.6 Hz, 1H), 4.53 (s, 2H), 3.87 (s, 3H). **^{13}C NMR** (150 MHz, $CDCl_3$) δ 194.57, 167.03, 159.40, 150.54, 136.92, 136.23, 131.15, 131.00, 123.81, 122.65, 119.88, 116.99, 116.09, 112.37, 52.11, 44.12.
MS-ESI$^+$: *m/z* calculated for $C_{16}H_{15}NO_4$ $[M+H]^+$ 286.1079, found 286.0894

Scheme S12 [Compound **13** (**RMR3-Acid**)]:

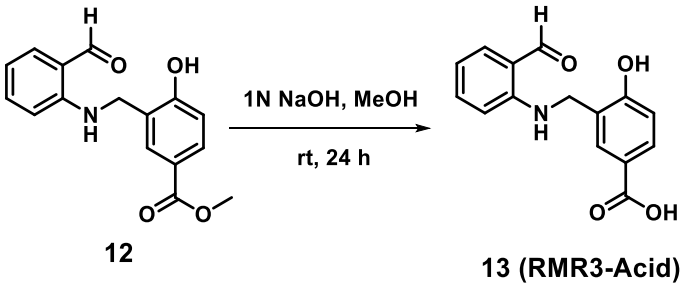

Compund **12** (200 mg, 0.7 mmol) was dissolved in 20 mL methanol. To this solution, 5 mL of 1(N) NaOH solution was added dropwise. Then the reaction mixture was stirred for about 24 hr. After completion of the reaction (confirmed by TLC), methanol was evaporated and the aqueous layer was acidified with 5% HCl solution. Then the aqueous layer was was extracted with EtOAc (3 × 30 mL). After that, the combined organic layer was washed with brine solution (3 × 30 mL) and dried over anhydrous Na_2SO_4. Then the crude compound was purified through silica gel column chromatography using EtOAc/hexane as solvent. Yield: 100 mg (52.7%)

^{1}H NMR (600 MHz, DMSO-d_6) δ 12.40 (bs, 1H), 10.60 (bs, 1H), 9.83 (s, 1H), 8.65 (t, *J* = 6 Hz, 1H), 7.78 (d, *J* = 1.8 Hz, 1H), 7.71 (dd, *J* = 8.4, 2.4 Hz, 1H), 7.61 (dd, *J* = 7.8, 1.8 Hz, 1H), 7.40-7.37 (m, 1H), 6.91 (d, *J* = 8.4 Hz, 1H), 6.74 (d, *J* = 9 Hz, 1H), 6.69 (t, *J* = 7.8, 1H), 4.44 (d, *J* = 6 Hz, 2H). **^{13}C NMR** (150 MHz, DMSO-d_6) δ 194.34, 167.15, 159.45, 149.90, 136.82, 135.91, 130.20, 129.97, 124.70, 121.33, 118.29, 114.92, 114.84, 111.11, 40.64. **MS-ESI$^+$:** *m/z* calculated for $C_{15}H_{13}NO_4$ $[M+H]^+$ 272.0922, found 272.1006

3. DFT Calculation for Mechanistic Study of the Conjugation Reaction

A mechanism of how the diazaborine compound RMR1 warhead is formed from RMR1 was determined using density functional theory (DFT) using the M06-2X functional and the 6-31+G* basis set. Water solvation was modeled by the polarizable continuum model PCM as well as by one explicit water molecule that helps facilitating proton transfer reactions. All stationary points were characterized by means of frequency calculations. The calculations were carried out using the Gaussian 16 computer program[3]. The relative standard enthalpies (298 K, 1 atm) are given in kcal/mol. The number of reactants of the reaction is two and the number of products is three. Consequently, the translational entropy part of the reaction entropy is positive to some extent. The reaction was modeled such that all geometries on the potential energy surface represent structure complexes held together via hydrogen bonding (a reasonable assumption given that the reaction takes place in water). The ground state of the reaction (see Figure S1 below) is modeled by a hydrogen bonded complex (GS). The aryl amine transfers a proton via the explicit water molecule (TS1) to one of the hydroxide anions bound to boron causing a ligand exchange; water leaves boron and the deprotonated aryl amine instead bonds to it forming intermediate I1. The enthalpy of activation is 18.7 kcal/mol and I1 is 15.4 kcal/mol higher in energy than GS. Next, the methylamine attacks the carbonyl of the RMR1 compound via TS2 (17.1 kcal/mol) forming the zwitterion ion intermediate I2 only 0.5 kcal/mol higher in energy than GS. Next, the two protons of the amino group of methylamine (now bonded to the carbonyl) are transferred, one at a time. One of them is transferred to the oxyanion (formed after addition of the methylamine to the carbonyl) via two water molecules (TS3) with a barrier of 12.7 kcal/mol generating intermediate I3 (13.3 kcal/mol). I3 is a minimum on the potential energy surface, see Figure S1) Then, via ligand exchange, I3 --> TS4 --> I4 --> single-bond rotation (see Figure S1) --> I5 --> TS5 intermediate I6 forms (7.7 kcal/mol). Thereafter the second proton is transferred to the aryl amine nitrogen via TS6 forming I7. Finally, the proton is transferred to the alcohol oxygen via the rate-determining step (TS7) with a barrier of 26.1 kcal/mol, forming a second water and the diazaborine product. The overall reaction is endothermic by 1.3 kcal/mol. The standard reaction entropy □S0rxn is challenging to compute, however, given the fact that the number of product molecules (3) is greater than the number of reactant molecules (2) it seems reasonable that the exergonicity of the reaction originates from this fact. The conversion of the reaction is also rather low (50% for Lysine), which shows that the exergonicity of the reaction is modest (the reaction is reversible) rationalizing the computed heat of reaction being close to zero.

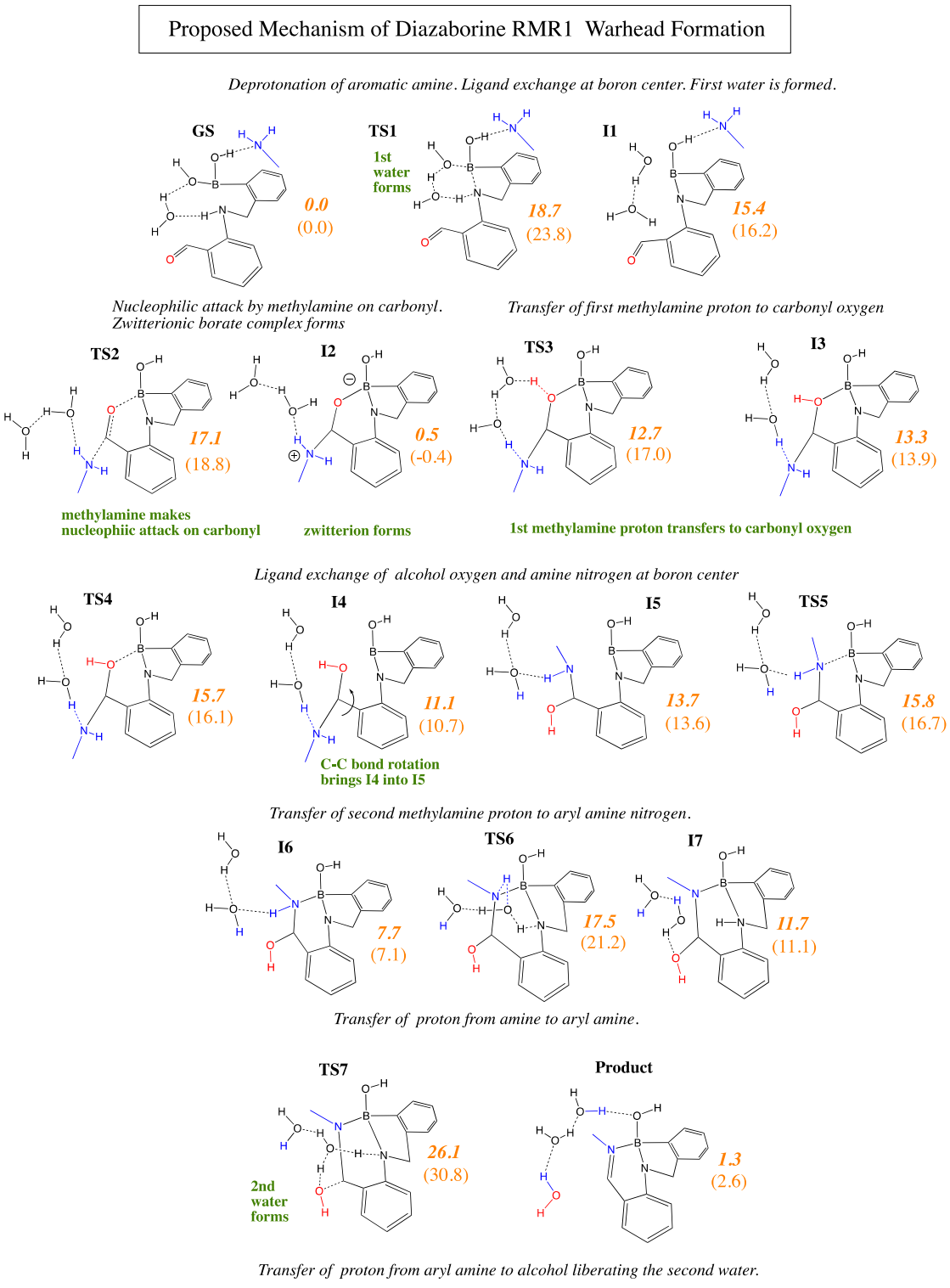

Figure S1: Relative reaction standard enthalpies computed at 298K and 1atm. SCF energies are included in parenthesis.

4. Procedure for Conjugation Reaction with Amines

^{1}H NMR study

All the conjugation reactions between RMR1 and amines were monitored by ^{1}H NMR. Typically, 10 mM of probe (RMR1) and amine (10 mM) were dissolved in DMSO-d_6/1 × PBS (containing 10% D_2O) as 2: 3 ratio. Then, pH of the reaction mixture was adjusted to 7.4 using 2N HCl. After that, the reaction was stirred for about 16 h to reach the equilibrium. The percentage of the product formation was calculated based on the peak integration of the aldehyde (around 9.9 ppm) and imine proton (around 8.5 ppm).

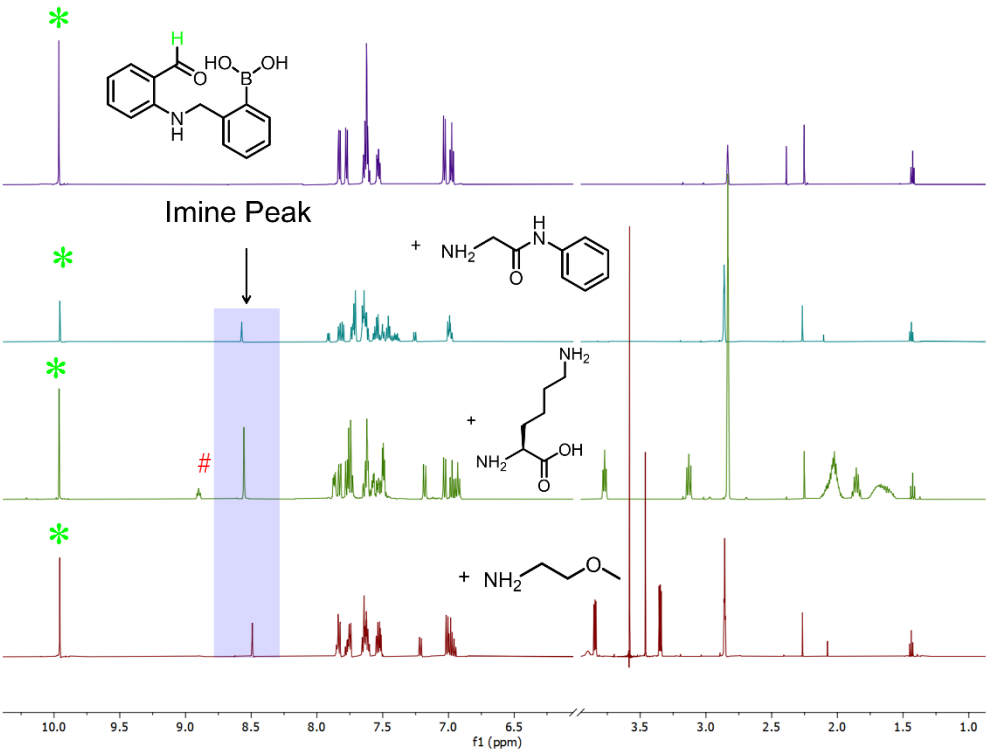

Figure S2: ^{1}H NMR spectra for the conjugation reaction mixture of RMR1 and amines. The green colored asterisks represent the peak for the aldehyde proton from RMR1 and the violet colored box represents the imine proton from the conjugates. The triplet peak at ~8.8 ppm (marked as #) represents the solvent exchangeable NH peak from RMR1 molecule.

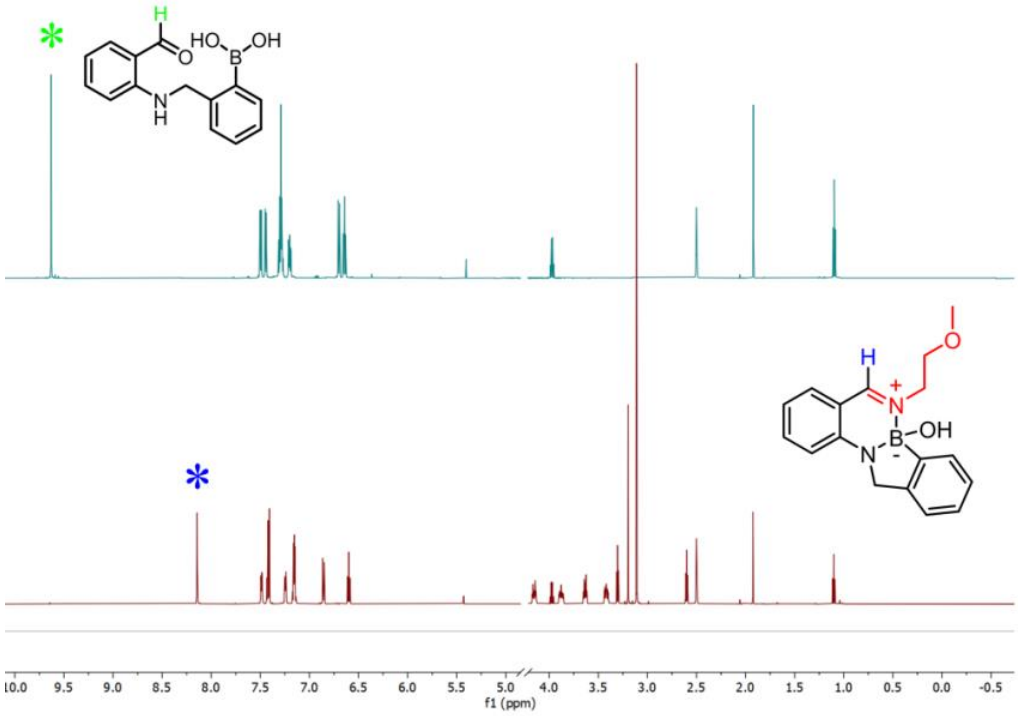

Figure S3: ^{1}H NMR spectra for the conjugation 100 mM reaction mixture of RMR1 and 2-MEA. The green colored asterisk represents the peak for the aldehyde proton from RMR1 and the blue colored asterisk represent the peak of imine proton from the RMR1-2MEA conjugate.

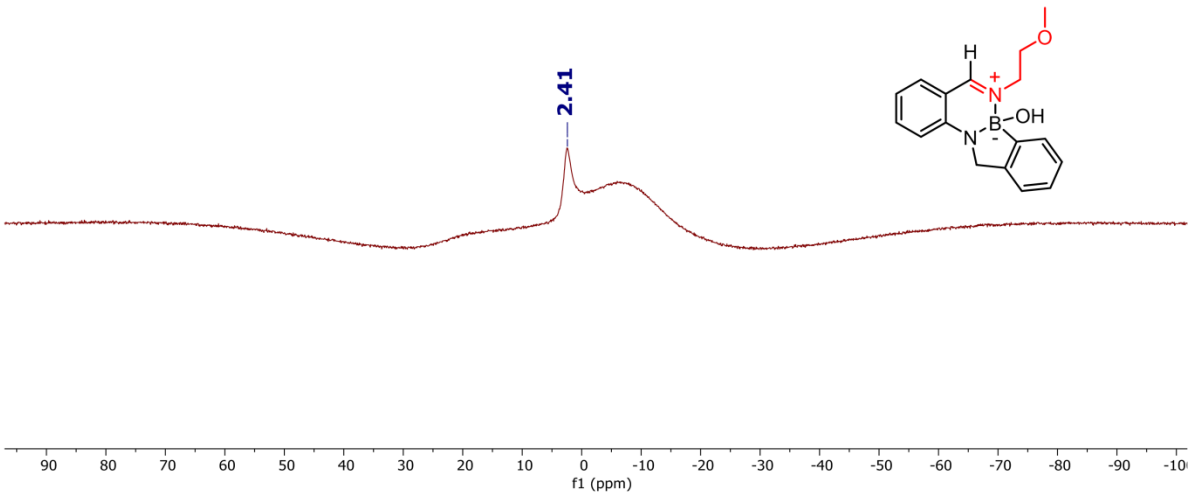

Figure S4: ^{11}B NMR spectra for the conjugation reaction for mixture of RMR1 (100 mM) and 2-MEA (100 mM).

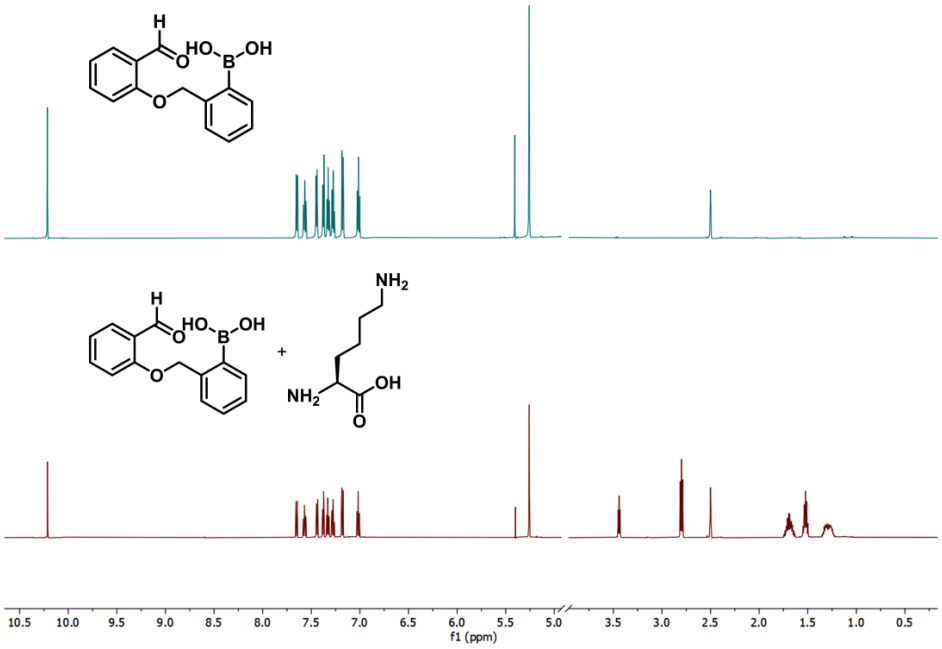

Figure S5: ^{1}H NMR spectra for the reaction mixture of RMR2 and Lys. Reaction condition: 10 mM reactants were dissolved in DMSO-d_6/1 × PBS (containing 10% D_2O) as 2: 3 ratio, 16 h, rt.

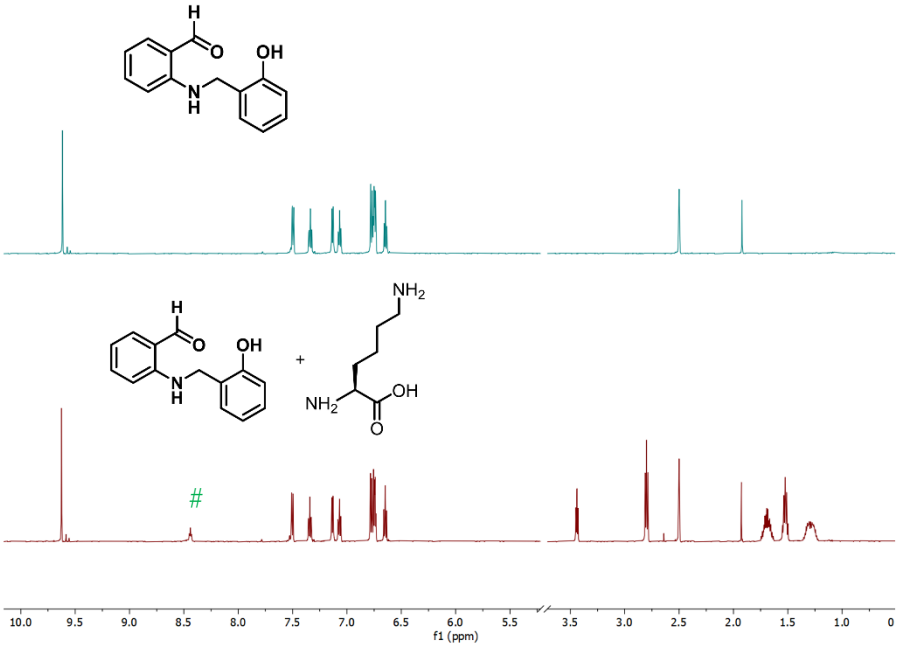

Figure S6: ^{1}H NMR spectra for the reaction mixture of RMR3 and Lys. Reaction condition: 10 mM reactants were dissolved in DMSO-d_6/1 × PBS (containing 10% D_2O) as 2: 3 ratio, 16 h, rt. The triplet peak at ~8.5 ppm (marked as #) represents the solvent exchangeable NH peak from RMR3 molecule.

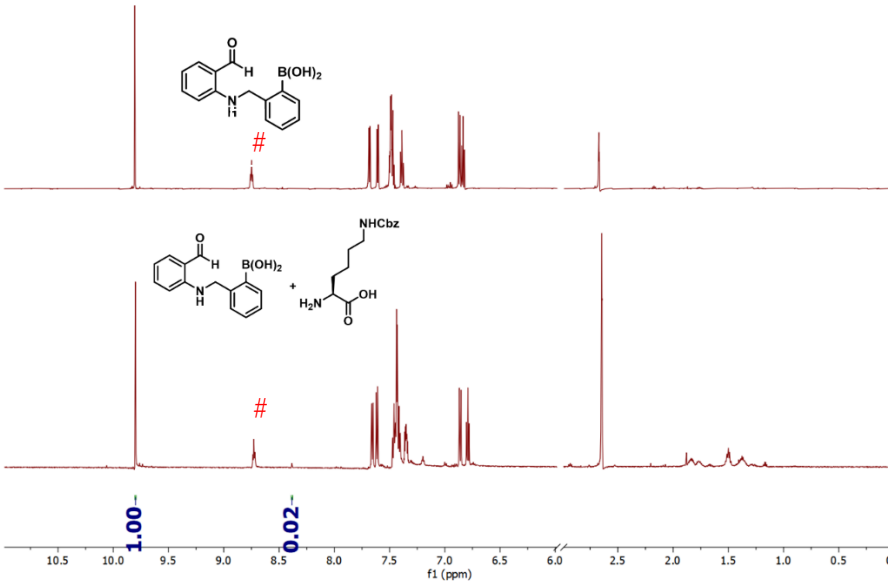

Figure S7: ^{1}H NMR spectra for the reaction mixture of RMR1 and H_2NLys(Cbz)COOH. Reaction condition: 10 mM reactants were dissolved in DMSO-d_6/1 × PBS (containing 10% D_2O) as 2: 3 ratio, 16 h, rt. The triplet peak at ~8.8 ppm (marked as #) represents the solvent exchangeable NH peak from RMR1 molecule. The NMR integration of singlet peak ~8.3 ppm shows ~2% of the conjugation formation.

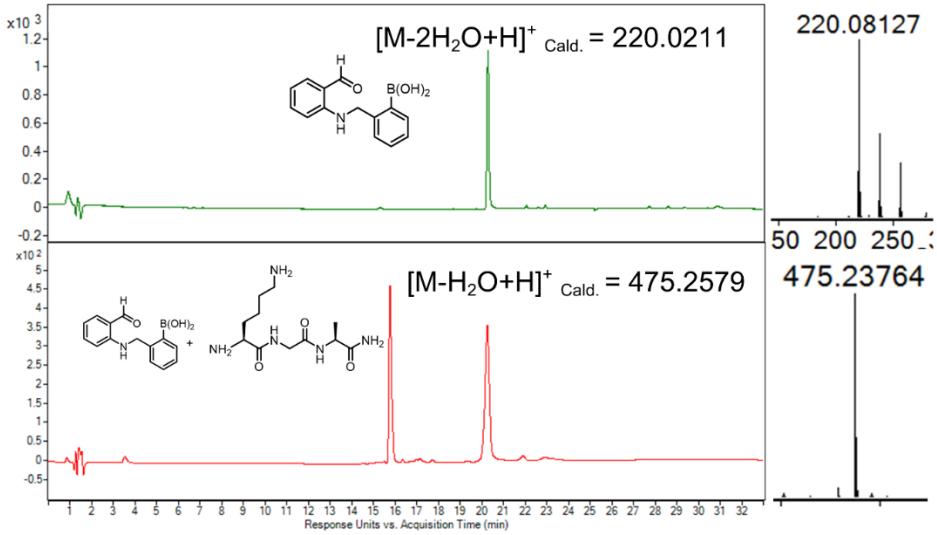

Figure S8: LC-MS trace of the mixture of RMR1 and H_2N-Lys-Gly-Ala-$CONH_2$. Reaction condition: 10 mM reactants were dissolved in DMSO-d_6/1 × PBS (containing 10% D_2O) as 2: 3 ratio, 16 h, rt. A single conjugation product was observed with unreacted RMR1 remaining, consistent with the sluggish reactivity of the α-amine observed in Figure S7.

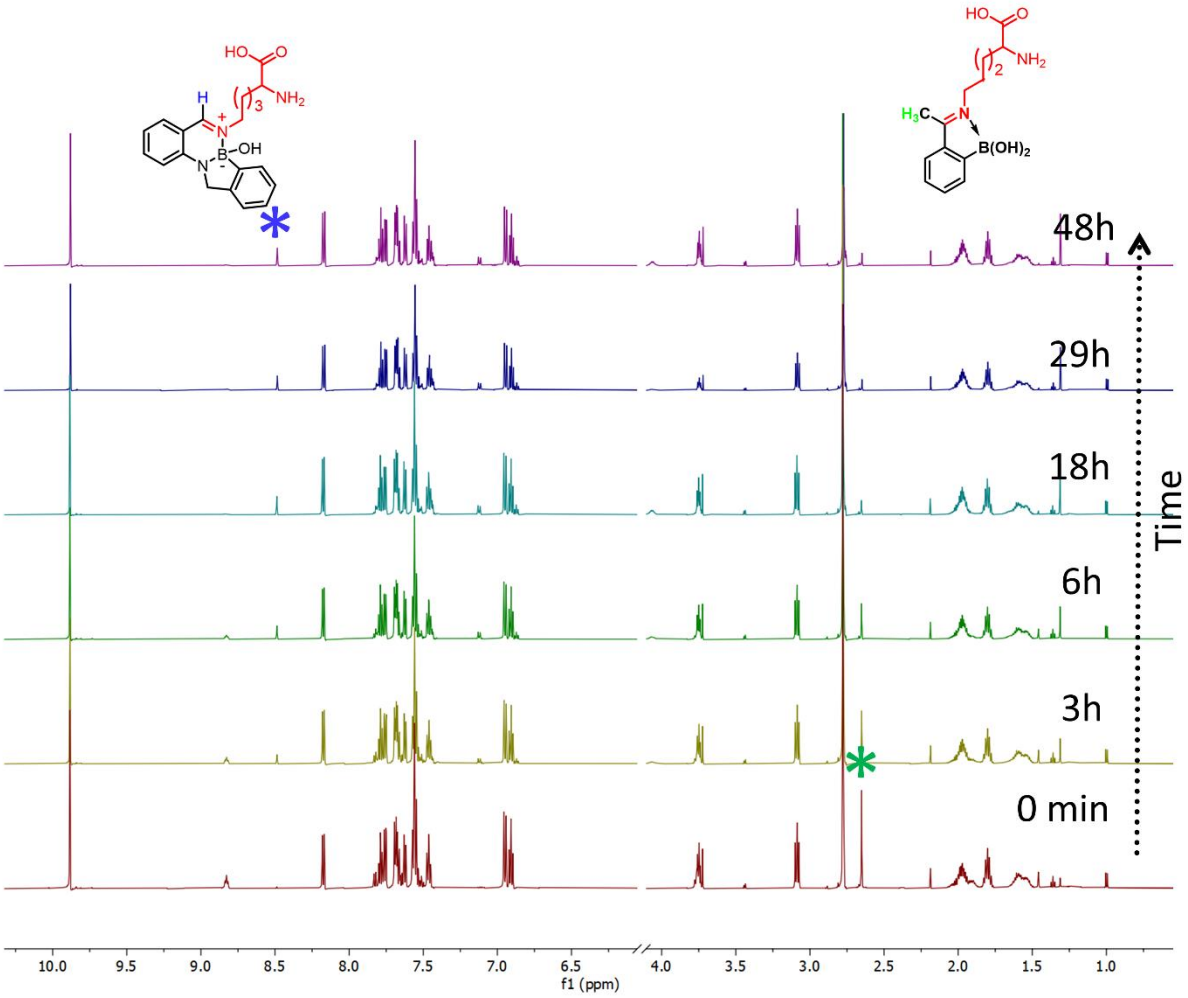

Figure S9: Time dependent ^{1}H NMR spectra for the competing experiment between 2-APBA and RMR1 with Lys. Reaction condition: 10 mM of each reactants were dissolved in DMSO-d_6/1 × PBS (containing 10% D_2O) as 2: 3 ratio, rt. The iminoboronate (from 2-APBA molecule) decreases from ~28% to ~5% and diazaborine (from RMR1) increases from ~0% to 16% over the time period of 48 h.

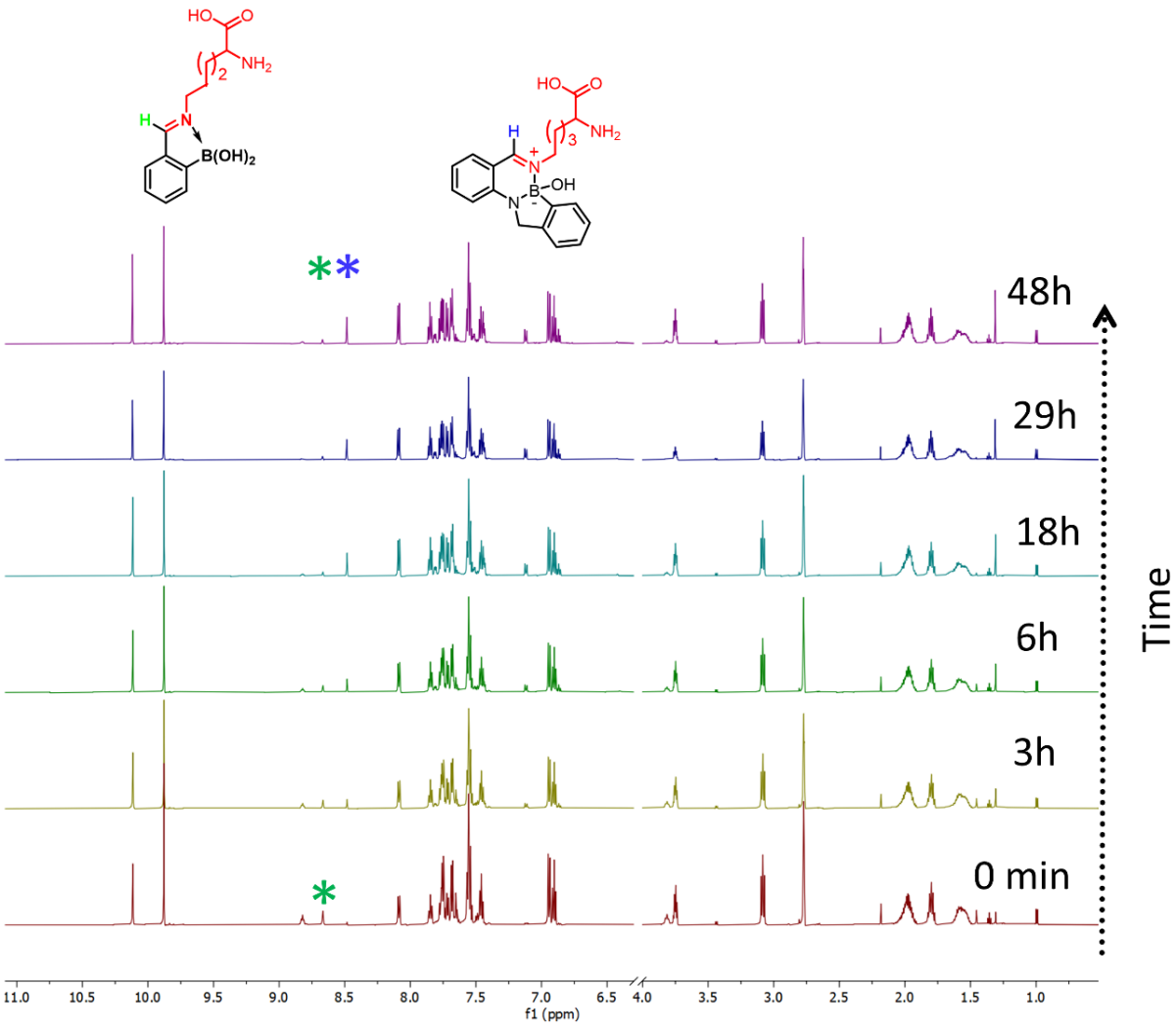

Figure S10: Time dependent ^{1}H NMR spectra for the competing experiment between 2-FPBA and RMR1 with Lys. Reaction condition: 10 mM of each reactants were dissolved in DMSO-d_6/1 × PBS (containing 10% D_2O) as 2: 3 ratio, rt. The iminoboronate (from 2-FPBA molecule) decreases from ~30% to ~7.5% and diazaborine (from RMR1) increases from ~1% to ~27% over the time period of 48 h.

LC-MS Analysis

The conjugation reaction between RMR1 and amines were further demonstrated by the LC-MS analysis. First, RMR1 (10mM) and amine (10mM) were mixed in DMSO/ 1 × PBS at 2:3 (v/v) ratio. Then the pH of medium was adjusted around 7.4 and stirred for about 16 h to reach the equilibrium. After 16h, 10 µL of 100 µM reaction mixture (diluted from the 10 mM reaction mixture) was directly injected in LC-MS and the formation of the conjugation was monitored by the UV-Vis trace. The peak for the conjugation product was further confirmed by the ESI-MS analysis.[4] The LC was run using the Method B mentioned in the instrumentation part.

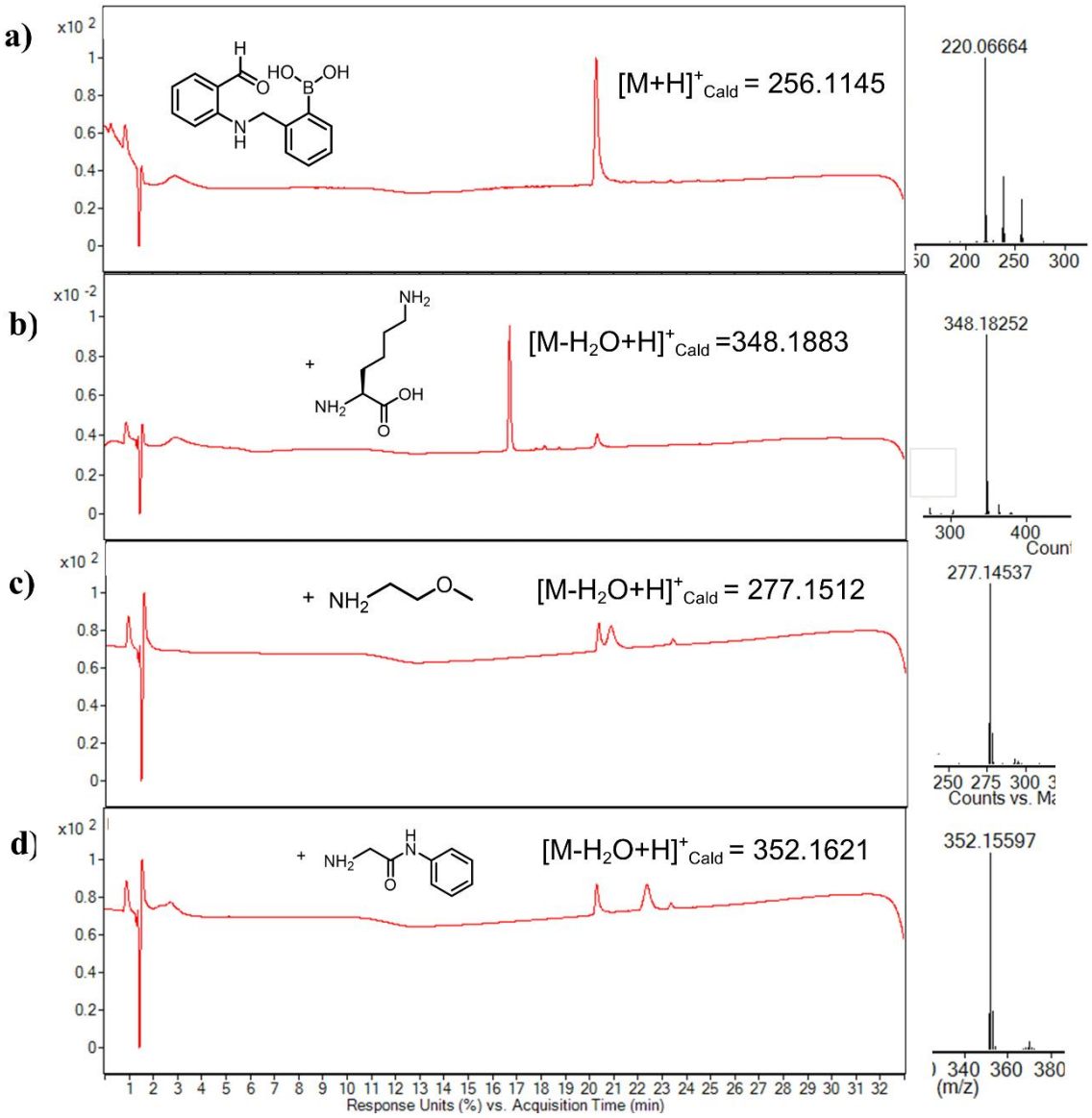

Figure S11: LC-MS analysis of the conjugation reaction between RMR1 and amines (b) Lys (C) 2-MEA (d) H_2NGlyNHPh. The right side of ESI-MS spectra indicates the formation of the diazaborine conjugated product.

5. X-Ray Crystal Structure of RMR1-2MEA Conjugate

First, 100 mM of RMR1 and 2-MEA were mixed together in DMSO-d_6/1× PBS (containing 10% D_2O), pH 7.4. Then, the reaction mixture was stirred for about 16h to reach the equilibrium. After 16 h, ^1H NMR was recorded. The NMR spectra (Figure S3) indicates the completion of the reaction at 100 mM. Then 100 mM conc. of RMR1 and 2-MEA were used for the crystallization trails. The X-ray diffraction quality crystals of RMR1-2MEA conjugate were grown from slow evaporation solution of methanol/water mixture. Briefly, RMR1 (100 mM) and 2-MEA (100mM) was dissolved in 3 mL of 1:1 Methanol/ Water mixture. Then the pH of the mixture was adjusted to 7.4 and kept it for slow evaporation. After several days some needle shaped crystals were grown. Bruker AXS SMART APEX CCD diffract meter was used for the collection of the X-ray data using Cu K_α radiation (λ = 1.54178Å)

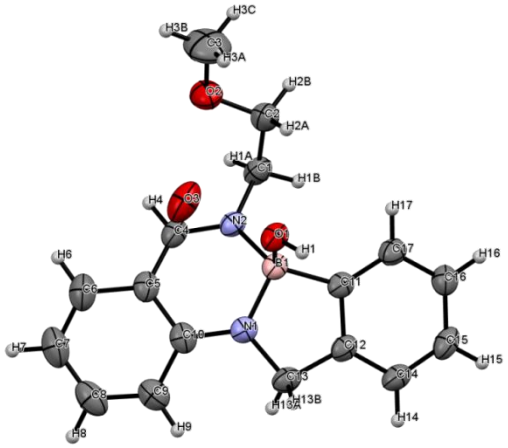

Figure S12: ORTEP diagram of RMR1-2-MEA conjugate. Ellipsoids are drawn at 50% probability (CCDC No: 2091359).

Table S1: Crystal data and structure refinement for RMR1_2-MEA (CCDC No: 2091359)

Identification code	RMR1_2-MEA
Empirical formula	C_{17} H_{19} B N_2 O_2, O
Formula weight	310.15
Temperature	173(2) K
Wavelength	1.54178 Å
Crystal system	Orthorhombic

Space group	P_{bca}
Unit cell dimensions	a=7.9459(2) Å, b=18.4587(5) Å, c=22.5948(5) Å
	α = 90°, β= 90°, γ= 90°
Volume	3314.00(14)
Z	8
Density (calculated)	1.243 g/cm^{-3}
Absorption coefficient	0.686mm^{-1}
F(000)	1312.0
Crystal size	0.220x 0.120x 0.080 mm^3
Theta range for data collection	3.913 to 66.635
Index ranges	-9<=h<=9, -21<=k<=21, -26<=l<=26
Reflections collected	40602
Independent reflections	40602 [R(int) = 0.0786]
Completeness to theta = 66.635°	99.6%
Max. and min. transmission	0.906 and 0.947
Absorption correction	Semi-empirical from equivalents
Refinement method	Full-matrix least-squares on F2
Goodness-of-fit on F2	1.030
Data / restraints / parameters	2916 / 211 / 0
Final R indices [I>2sigma(I)]	R1 = 0.0523, wR2 = 0.1386
	R2 = 0.0734, wR2 = 0.1524
Extinction coefficient	n/a
Largest diff. peak and hole	0.465 and -0.174e $Å^{-3}$

6. Procedure for K_d Determination between RMR1 and Amines

K_d was determined using titration experiment by monitoring the UV-Vis absorption. The UV-Vis absorption was measured using in 2mL quartz cuvette (10 mm path length) at room temperature. First, RMR1 (50 µM from a stock solution of 2mM in DMSO) was mixed with the different conc. of amine (25 µM to 50mM) in 1× PBS, pH 7.4 and the reaction mixture was stirred for 16h to reach the equilibrium. After 16h, absorbance spectra were recorded. Upon increase the conc. of amine, the peak at λ_{max}@380 nm gets red shifted. The appearance of new peak at λ_{max} at 423 nm (for Lys and 2-MEA) and 433 nm (for H_2NGlyNHPh) indicates the formation of the diazaborine conjugated product. All spectra collected during the titration were further background corrected by subtracting the value of the absorbance at λ_{max} at 423 nm and 433 nm for RMR1. The curve was then plotted as change in the absorbance at wavelength of λ_{max} at 423 nm (for Lys and 2-MEA) and 433 nm (for H_2NGlyNHPh) against the conc. of the amine. Hyperbola equation was used to fit the curve and the K_d values were extracted from the fitted curves.

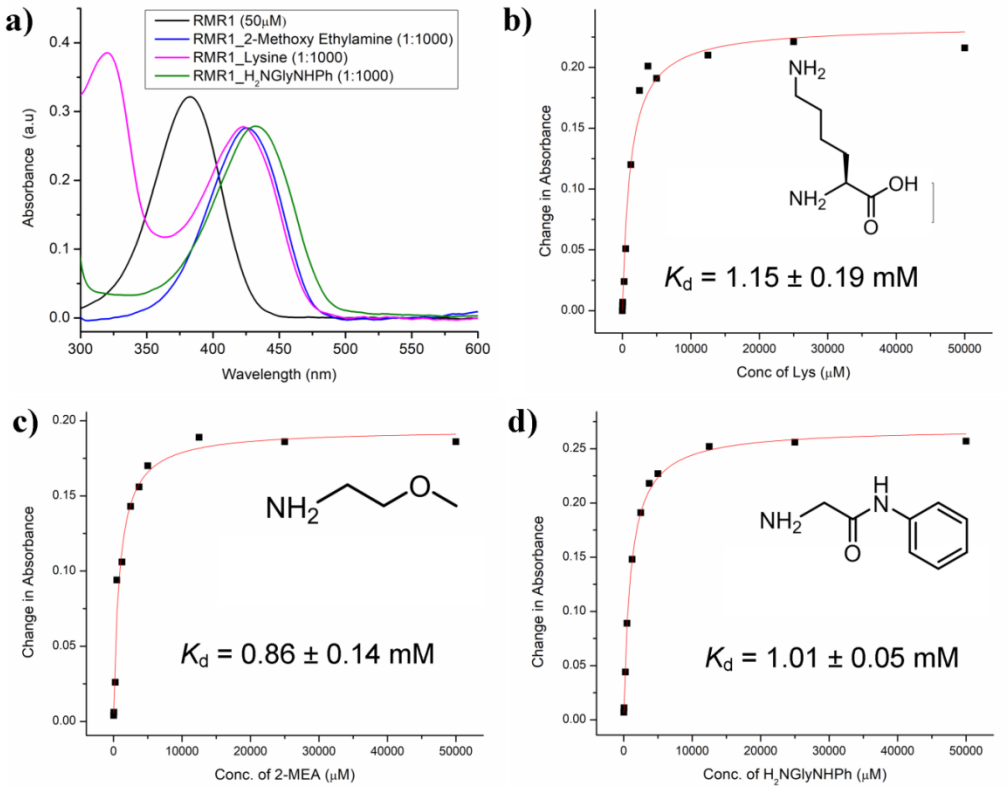

Figure S13: Thermodynamic characterization of the RMR1-amine conjugation. (a) UV-Vis spectra of RMR1 (50 µM) and reaction mixture of RMR1 and amines (1:1000 ratio). The red shifted spectrum upon reaction with amines indicates the formation of diazaborine conjugated products. (b)-(d) Titration plot for calculation of K_d for Lys, MEA and H_2NGlyNHPh respectively.

7. Procedure for Determination of Kinetic Parameters

The kinetic parameters of the conjugation reaction were derived from relaxation kinetics[2,5] by monitoring the absorbance of dissociation of the conjugated product using UV-Vis spectrometer. All spectra collected during the kinetics experiments were further background corrected by subtracting the absorbance value of RMR1 at λ_{max} at 423 nm and 433 nm. For the forward reaction rate constant (k_1) was derived from the dissociation rate constant (k_{-1}) using equations no (i)-(iii). For the dissociation kinetics, dilution experiments were performed. Briefly, 10mM of RMR1 and corresponding amine was mixed in DMSO/1× PBS (2:3), pH 7.4 and stirred for about 16h to reach the equilibrium. After the equilibrium is reached, reaction mixture was diluted to 50 μM and the absorbance at λ_{max} = 423 nm (for Lys and 2-MEA) and 433 nm (for H_2NGlyNHPh) were monitored over the time. The data was then fitted with the following equations and dissociation rate constant k_{-1} was calculated. Equations used for calculation of the kinetic parameters are as following

$$A + B \underset{k_{-1}}{\overset{k_1}{\rightleftharpoons}} C$$

$$Y = Y_0 + Ae^{-t/\tau} \quad \text{....(i)}$$

$$\tau = \frac{1}{\{k_{-1} + k_1 \times ([A] + [B])\}} \quad \text{....(ii)}$$

$$K_d = k_{-1}/k_1 \quad \text{....(iii)}$$

Where,

τ= Relaxation time

k_1= Rate of the forward reaction

k_{-1}= Rate of the backward reaction

K_d= Dissociation constant

[A] and [B] are conc. of RMR1 and amines in reaction mixture respectively.

The dilution experiment for the dissociation kinetics was further validated using ^{1}H NMR spectroscopy. Briefly, RMR1 and corresponding amines were mixed at conc. of 10mM in DMSO-d_6/1× PBS (containing 10% D_2O), pH 7.4. Then, the reaction mixtures were stirred for about 16h to reach the equilibrium. After the equilibrium is reached, reaction mixtures were diluted to 0.5 mM in1× PBS pH 7.4. Then ^{1}H NMR was recorded at different time points. The percentage yield of the conjugation was calculated based on the integration of the imine proton peak (around 8.5 ppm) and aldehyde proton peak (around 9.9 ppm).

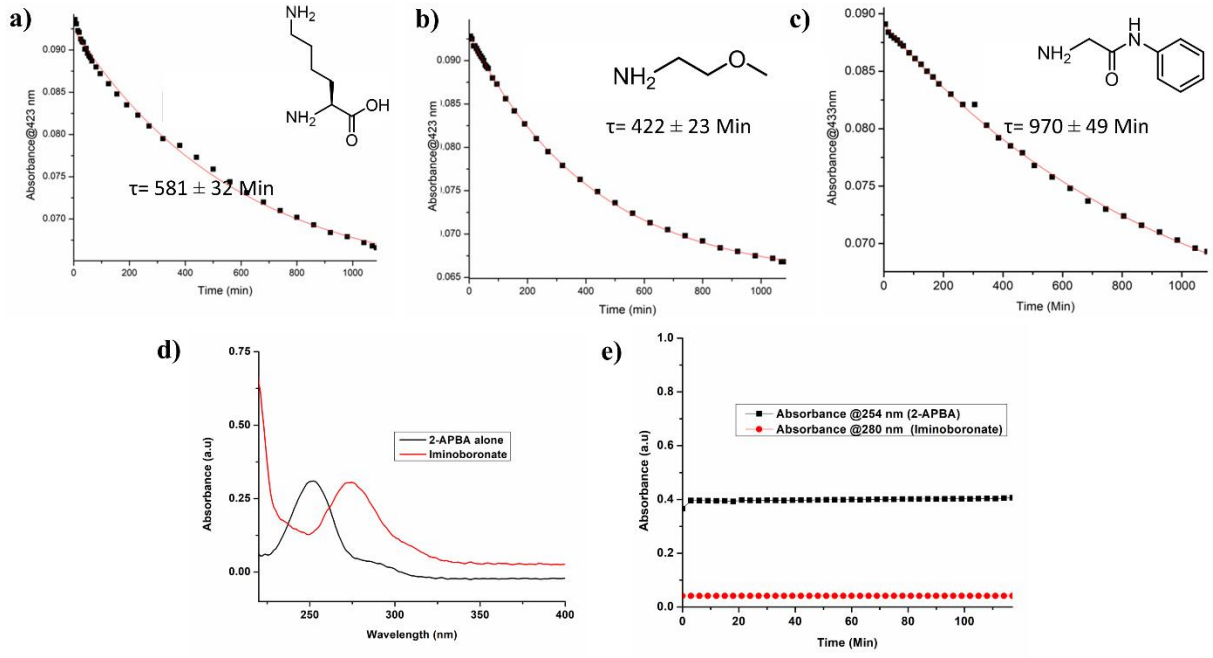

Figure S14: Dissociation kinetics recorded by diluting the conjugate of RMR1 with (a) Lys, (b) 2-MEA, and (c) H_2NGlyNHPh respectively. The dissociation was recorded by monitoring the UV-vis absorption of the diazaborines. Also shown for comparison is the dissociation kinetics of the iminoboronate conjugate of APBA and lysine, with the UV-vis absorption spectra shown in (d) and kinetic trace shown in (e). All dilutions were from 10 mM to 50 µM. These results collectively demonstrate the instantaneous dissociation of the iminoboronate in contrast to the slow dissociation of the diazaborines.

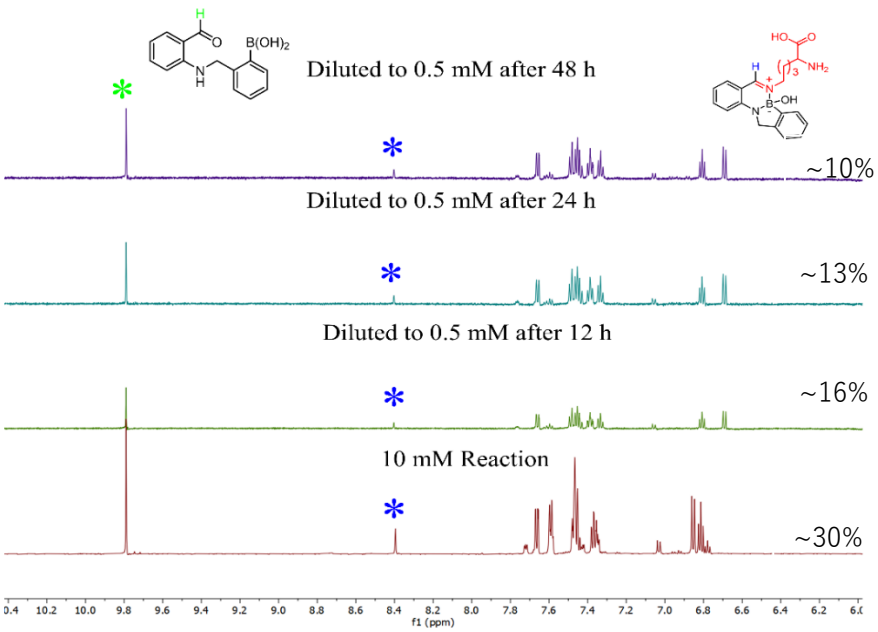

Figure S15: ^{1}H NMR spectra for the dilution experiment to show the reversibility of RMR1-Lys conjugation reaction. The % of the diazaborine conjugate, determined from integration of NMR spectra, is shown on each spectrum.

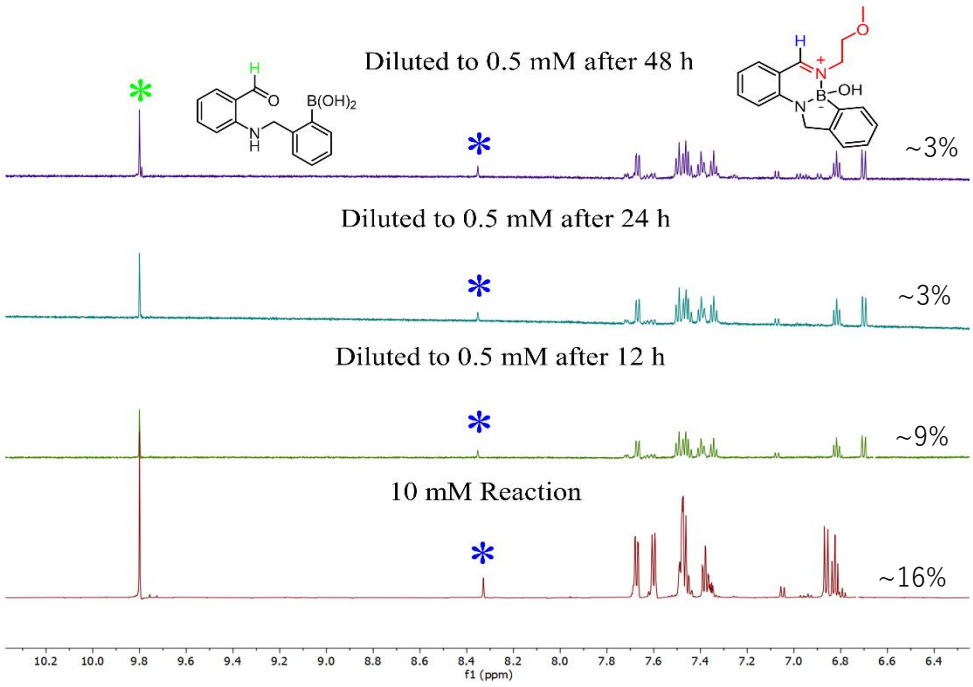

Figure S16: ^{1}H NMR spectra for the dilution experiment to show the reversibility of RMR1-2MEA conjugation reaction. The % of the diazaborine conjugate, determined from integration of NMR spectra, is shown on each spectrum.

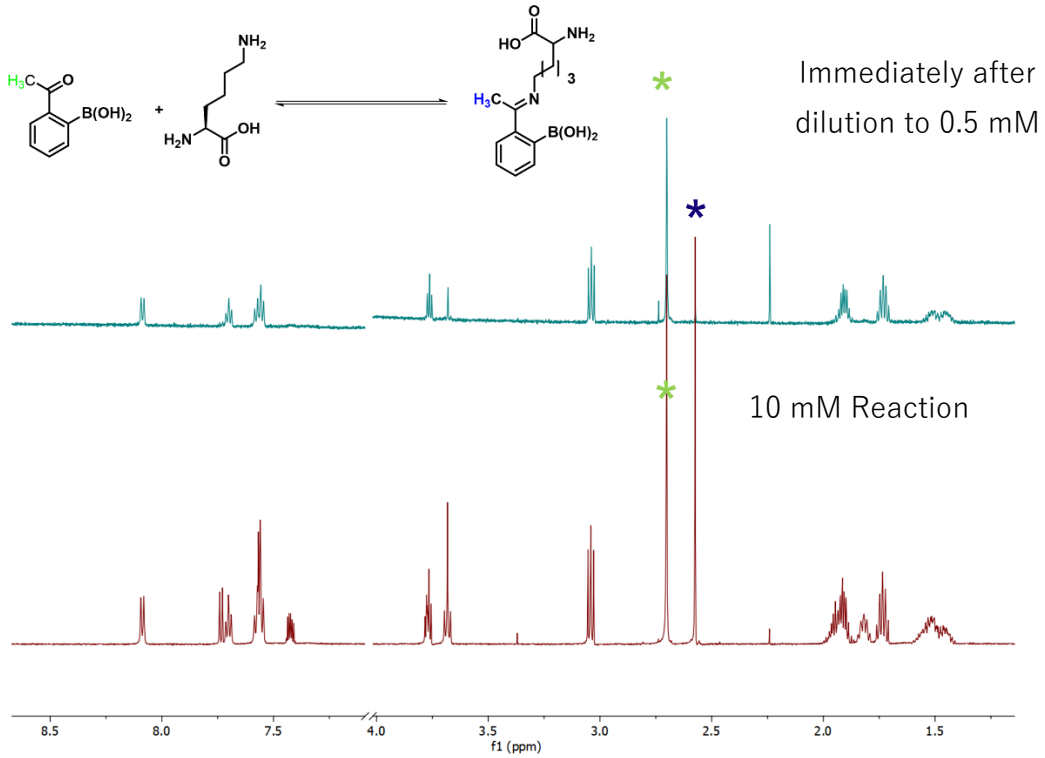

Figure S17: ^{1}H NMR spectra for the dilution experiment to show the instantaneous reversibility of APBA-Lys conjugation reaction. The ^{1}H NMR spectra were taken before and immediately after dilution to 0.5 mM. The disappearance of the iminoboronate acetyl peak demonstrates the fast kinetics of iminoboronate dissociation.

8. Peptide Synthesis

All the peptides were synthesized on solid support of Rink amide resin on 0.1 mmol scale using standard Fmoc based peptide synthesis chemistry. All coupling reactions were carried out in DMF solvent using HBTU as coupling reagents, 0.4 N-Methyl Morpholine in DMF as base. After each coupling, for the deprotection of the Fmoc group was done by using 20% piperidine in DMF. Alloc group was deprotected on N-terminal Fmoc protected resin (0.025 mmol) using $Pd(PPh_3)_3/PhSiH_3$ in DCM. After that the resins were thoroughly washed with DMF and DCM. Then 5(6)-Carboxyfluorescein or APBA-Acid or RMR1-Acid was coupled with Dap residue using HBTU as a coupling reagent and 0.4 N-Methyl Morpholine in DMF as a base. After completion of the coupling, N-Terminal Fmoc was deprotected and peptides were cleaved from resin using Reagent B. Then, the crude peptide was filtered through sintered glass funnel and precipitated out slowly by adding cold diethyl ether at 0 °C to give a solid product. For disulfide formation, crude peptide was dissolved in NH_4CO_3 buffer (20 mM, pH 8, peptide concentration 2mM) and stirred for 12 h in an open flask. After completion of the reaction (confirmed by LC-MS analysis), cyclic peptides were purified by reverse phase HPLC on a C18 column using ACN/H_2O (with 0.1% TFA) gradient

system. The acylation of the N-terminal of peptide P5 was carried out on purified N-terminal free P5 using 1 equivalent of acetic anhydride/pyridine in DMF. The purity of these peptides was further confirmed by LC-MS analysis (Method A mentioned in the instrument part was used for the analysis). Final pure peptides were lyophilized to get solid compound which was used for the different binding assays on protein and bacterial cells.

9. Expression of Sortase A

Sortase A plasmid of *S. aureus* was obtained from Addgene (pET28a-SrtAdelta59). The Sortase A over expression plasmid construct was transformed into the *Escherichia coli* strain BL21(DE3). For protein expression, the Sortase A plasmid contained E. coli BL21(DE3) was cultured in 1L of LB media containing 50 µg/mL kanamycin at 37 °C with vigorous shaking until the O.D. reaches 0.5-0.8. The production of Sortase A was then induced with 1mM IPTG for about 16 h incubation with vigorous shaking at room temperature. Then, the cells were harvested by centrifugation (5000 rpm for 20 min). The cell pallet was resuspended in 15 mL lysis buffer (containing 10 mM imidazole, 20 mM Tris, 300 mM NaCl) and lysied by sonication. The lysate is clarified by centrifugation at 7000 rpm for 40 min before purification with Ni-NTA agarose column and pd-10 desalting column. Furthermore, the purity of the Sortase a was confirmed by the LC-MS analysis (Method C mentioned in the instrumentation part was used)

Sequence of the expressed protein

MRGSSHHHHHHSSGLVPRGSHMQAKPQIPKDKSKVAGYIEIPDADIKEPVYPGPATPEQLNRG
VSFAEENESLDDQNISIAGHTFIDRPNYQFTNLKAAKKGSMVYFKVGNETRKYKMTSIRDVKPT
DVGVLDEQKGKDKQLTLITCDDYNEKTGVWEKRKIFVATEVK

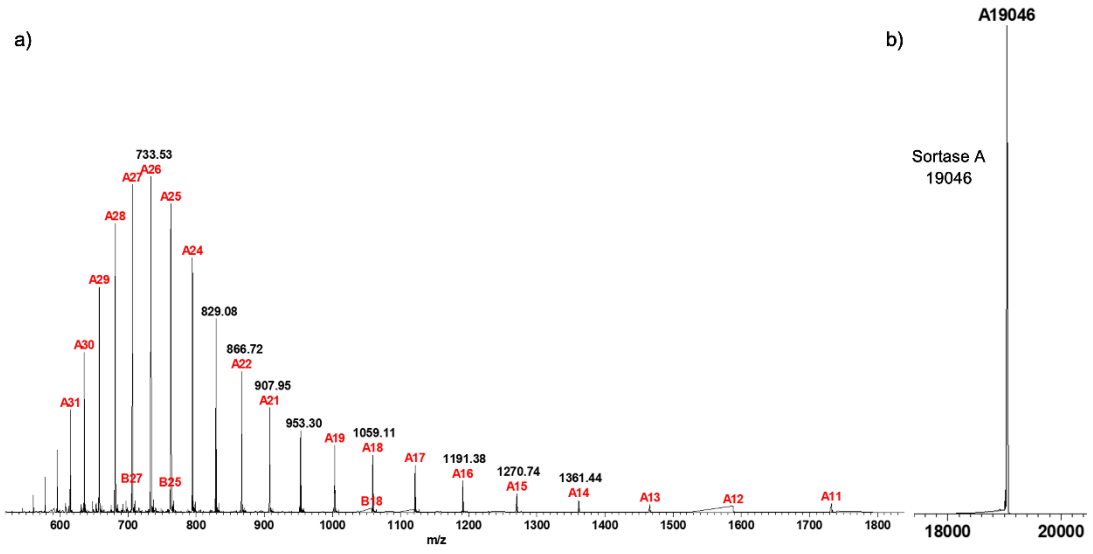

Figure S18: LC-MS data of Sortase A indicating the purity of the protein (a) and (b) are convoluted and deconvoluted mass spectra of Sortase A respectively.

10. Biotinylation of Sortase A

The Sortase A was biotinylated by incubation of 300 µM of protein in 1× DPBS, pH 7.4 with Biotin-NHS (300µM) for about 16 h at 4 °C. The biotinylation of Sortase A was further confirmed by LC-MS. analysis.

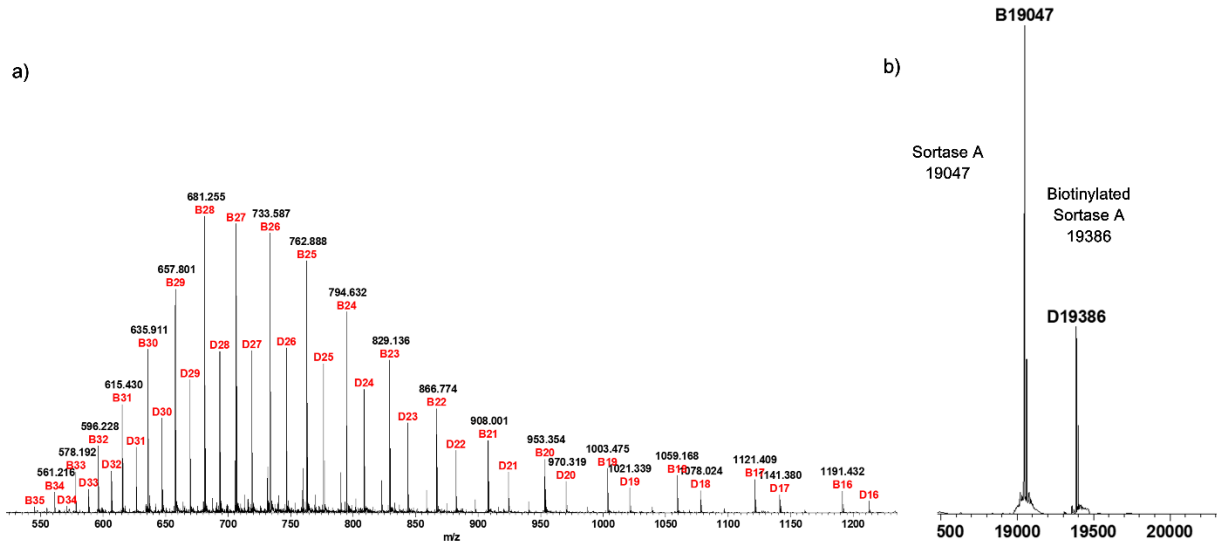

Figure S19: LC-MS data of biotinylated Sortase A. (a) and (b) are convoluted and deconvoluted mass spectra of biotinylated Sortase A respectively. The labeling reaction with Biotin-NHS yielded ~30% mono-biotinylated protein and a small amount of double biotinylated sortase.

11. Procedure for Phage Display Screening

The phage library was blocked in 200 µL of 1× DPBS containing 1% w/v BSA and 0.1% v/v Tween 20 for 30 min. Biotinylated Sortase A was immobilized on 20 µL magnetic streptavidin beads (Dynabeads M-280, Invitrogen Dynal Biotech) in 200 µL of 1× DPBS with 1% w/v BSA and 0.1% v/v Tween 20 for 30 min. The Sortase A immobilized beads were washed three times with 1 mL of 1× DPBS. The blocked phage was added to the Sortase A coated beads and incubated for another 30 min. Then, the beads were washed 10 times with 1mL 1× DPBS with 0.1% v/v Tween-20. The phage bound to the beads were eluted by 900 µL 150mM glycine, pH 2 for 10 min. the eluted phage is then neutralized with 90 µL of 1.5M Tris pH 8.8. The eluted phage was again incubated with 20 mL exponentially growing *E.coli* 2738 in LB media for about 4.5 h. Then the cells were harvested by centrifugation and the amplified phage in the supernatant was precipitated with 18.8% V/V PEG/NaCl and resuspended in 1× DPBS for the next round screening. After three rounds of panning we found the hit peptide W7 (ACLIPTWGGC)

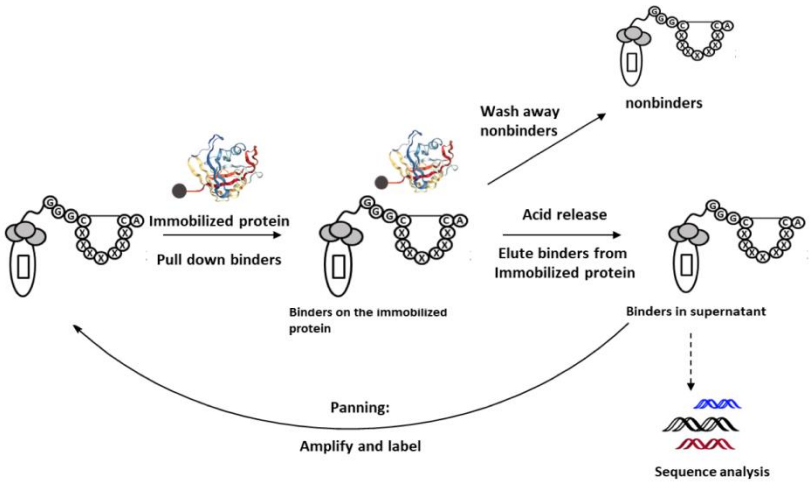

Figure S20: Schematic representation of panning against Sortase A using CX_7C phage library.

12. Procedure for Binding Assay between W7-F and Sortase A

The binding assay of peptide W7-F (with Sortase A was determined by the fluorescence polarization experiment. The assay was performed using peptide W7-F at a final conc. of 200 nM and incubated with increasing conc. of Sortase A (35 nM to 36 μM) in 1× DPBS, pH 7.4 for 30 min. After that, fluorescence polarizations were recorded by excitation at 485 nm and recording emission at 535 nm. Then the fluorescence polarization value was plotted against conc. of Sortase A. Furthermore, the curve was fitted using the following equation and K_d value was extracted from the fitted curve. The experiments were carried out in triplicate and plotted as an average of three trials with standard deviations.

$$y=FP_{min}+(FP_{max}-FP_{min})*(K_d+Lst+x-sqrt((K_d+Lst+x)^2-4*Lst*x))/(2*Lst)$$

Where,

FP_{min}= Lowest value of fluorescence polarization in the binding curve experiment

FP_{max}= Highest value of fluorescence polarization in the binding curve experiment

K_d= Dissociation constant for binding of peptide W7-F and Sortase A.

Lst= Conc. of W7-F peptide i.e. 200nM

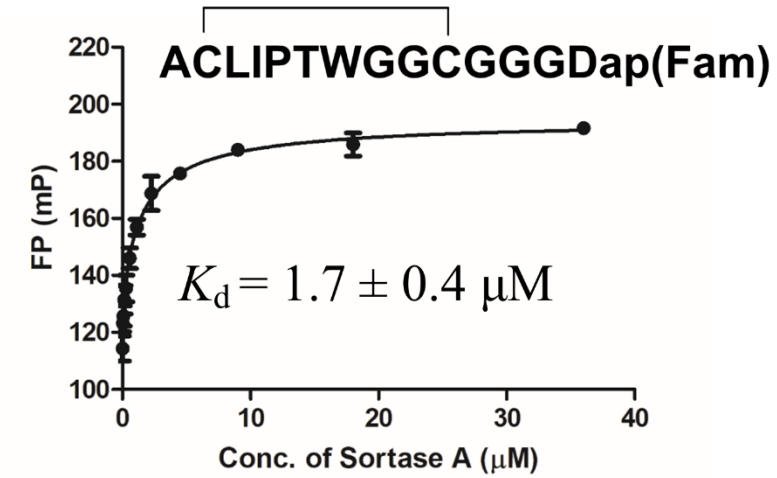

Figure S21: Binding curve between peptide W7-F and Sortase A.

13. Molecular Docking Calculations for Binding of Peptide W7 with Sortase A

A model of the cyclic peptide W7 was prepared using the Avogadro program and saved in pdb-file format. The Auto Dock Tool utility program prepare_ligand4.py (v 1.10) was used to create the ligand input file for the docking calculations in pdb qt file format. The Sortase A receptor structure was prepared from the Brookhaven Protein Databank file with code 1T2W. The protein crystal structure consists of a trimeric complex with subunits A, B, and C. The B and C units were discarded. The pentapeptide LPETG was removed from the active site of unit A. The molecular docking program Vina[6] (AutoDockVina 1.1.2 (May 11, 2011) was used for the molecular docking calculations. The molecular docking space was chosen to 40 by 40 by 40 Å, encompassing the entire receptor. All molecular docking parameters were set to their default values.

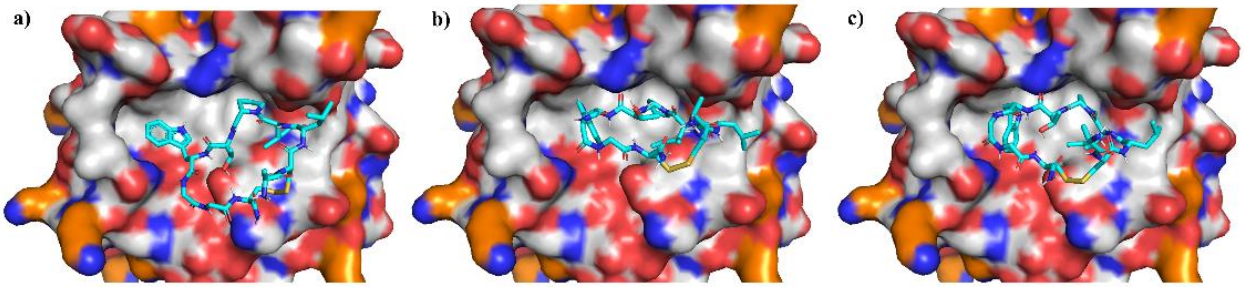

Figure S22: High-scoring conformers in which Trp and Pro residues are bound into the active site of Sortase A.

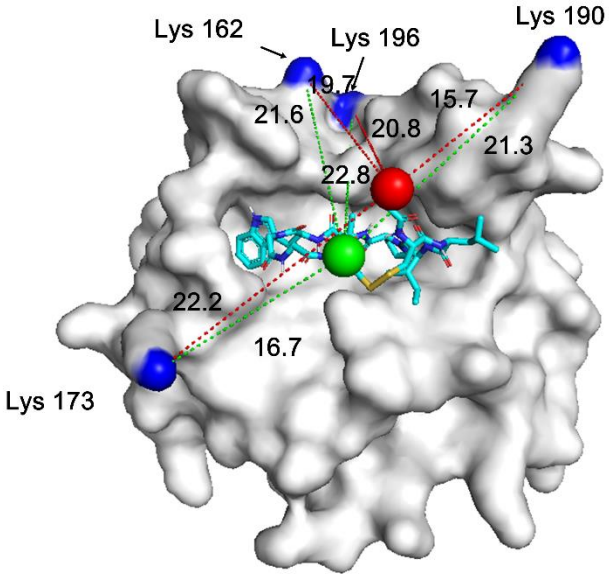

Figure S23: Measured distances between the N-/C- terminus of the docked W7 peptide and the lysine residues in close proximity of the enzyme's binding site. The N- and C-terminus are highlighted as red and green sphere respectively. The lysine side chain amines are colored blue.

14. Procedure for IC_{50} Value Determination of Peptides W7, W7-Linear and P1-P8

Competition assay was performed by measuring fluorescence polarization using reporter peptide W7-F. Briefly, fluorescent labeled peptide W7-F and Sortase A were added to different concentration of inhibitor peptides (P1-P8, W7) such a way that the final conc. of the fluorescent reporter peptide and Sortase A are 200 nM and 3 μM respectively. Then it was incubated for about 30 mins (for peptide W7, W7-Linear, P1-P4, P6-P7) or 5h (for peptides P5 and P8). After that, it was transferred to a Costar blk/clrbtm 96 well plate and fluorescence polarization was recorded using emission at 535 nm. upon excitation at 485 nm. The obtained fluorescence polarization value was then plotted against log scale of conc. of inhibitor peptide. The curve was fitted using the following equation and the IC_{50} values are extracted from it. The experiments were carried out in triplicate and plotted as an average of three trials with standard deviations.

$$Y=FP_{Lowest} + (FP_{Highest} - FP_{Lowest})/(1+10^{(X-LogIC_{50})})$$

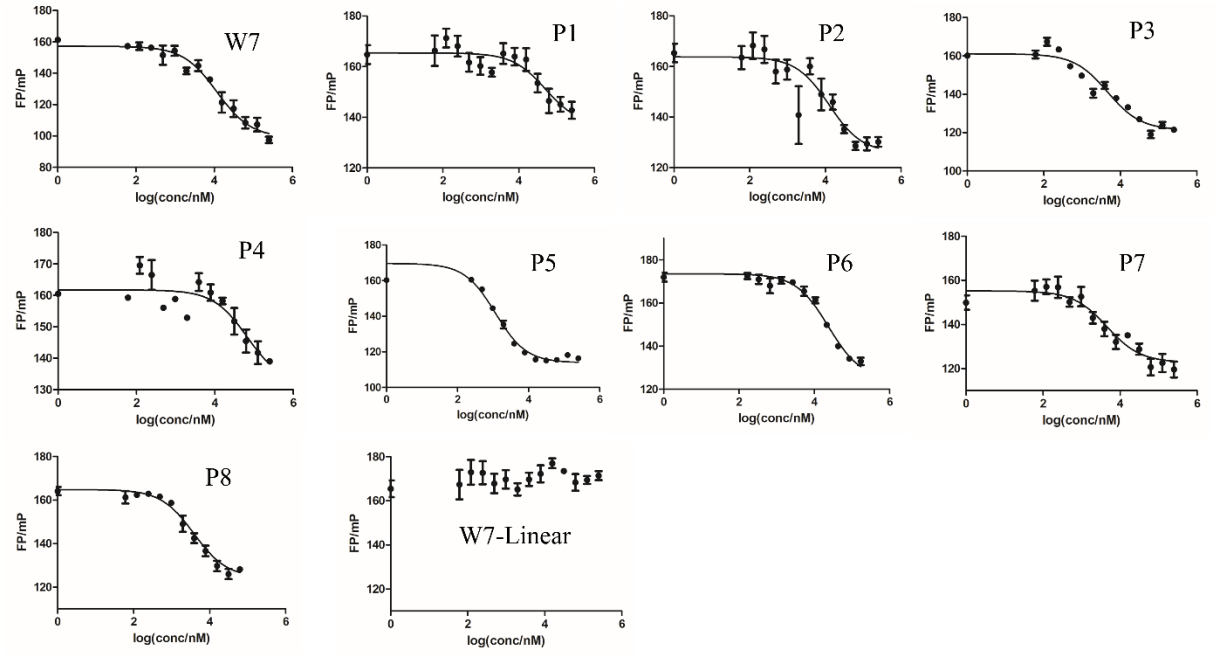

Figure S24: Titration curves obtained from the competition assay of W7, W7-Linear and P1-P8. IC_{50} values are given as Figure 4c in the main text.

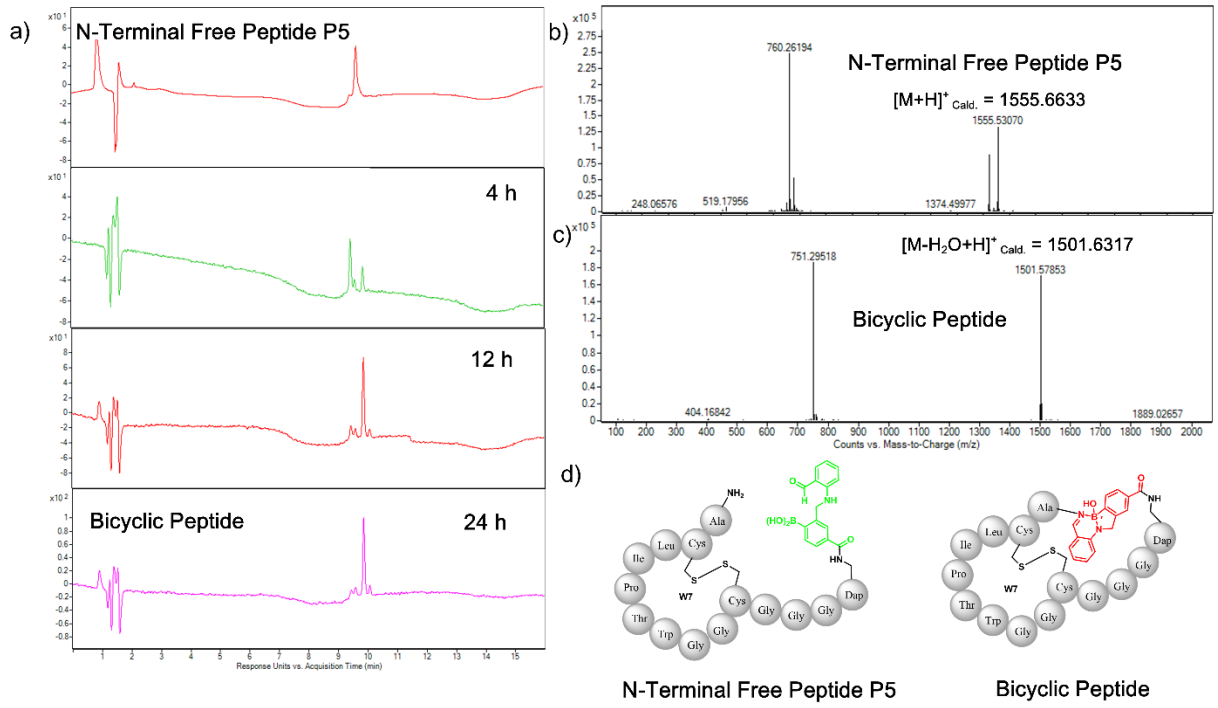

Figure S25: Bicyclic peptide formation by reaction between N-terminal NH_2 and RMR1 warhead from N-terminal free P5. (a) LC trace of bicyclization over the time in 1× PBS (pH7.4). (b) and (c) ESI-MS spectra of mono and bicyclic peptide. (d) Cartoon representation of N-terminal free P5 and diazaborine bicyclized peptide form P5.

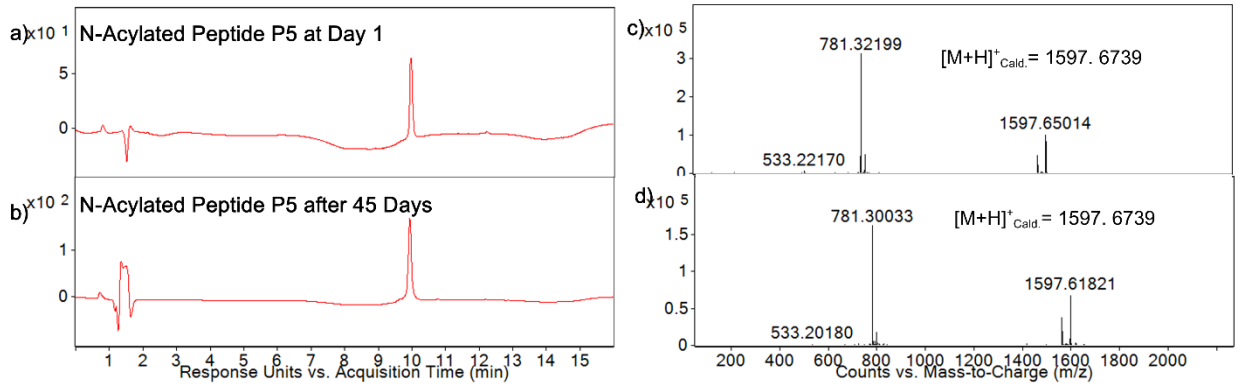

Figure S26: Stability of N-acylated peptide P5 over time in 1× PBS (pH7.4). (a) and (b) LC trace of N-acylated peptide P5 at day 1 and after 45 days respectively. (c) and (d) ESI-MS spectra of N-acylated peptide P5 at day 1 and after 45 days respectively.

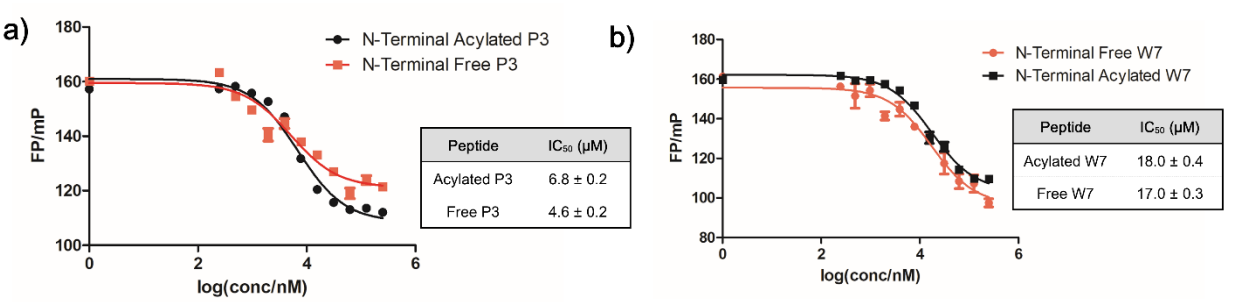

Figure S27: Titration curves obtained from the competition assay of inhibitor peptides of free and N-terminal acetylated peptide of W7 and P3 (IC_{50} values are given in the insert table).

15. Procedure for Determination of Kinetic Parameters between Peptide P3 and P5 with Sortase A:

The association and dissociation kinetics on Sortase A were determined by the fluorescence polarization experiment using a reporter peptide W7-F. The fluorescence polarization data were obtained by measuring emission at 535 nm upon excitation at 485nm. For the association experiments, first reporter peptide W7-F at final conc. of 200 nM was incubated with 3μM of Sortase A for 30 min. Then to this solution, 20 μM of peptide P3 or P5 (from a stock solution of 5 mM) were added and fluorescence polarization was recorded with time. Exemplary kinetic traces are shown in Figure 4e, f. As the reporter peptide was used at much lower concentrations in comparison to the enzyme and the peptide inhibitors, the IC_{50} value from the competition experiments can be considered as K_d value. Therefore, the kinetic parameters were calculated by fitting the curve using a relaxation kinetics equations (i)-(iii) mentioned earlier (section 7).

16. Procedure for Trypsin Digestion of Wildtype Sortase A and Sortase A-P5 Conjugates

First, Sortase A and peptide P5 at a conc of 75 µM were incubated for overnight to form Sortase A-P5 conjugate. The formation of the conjugate was confirmed by LC-MS analysis. The results indicate that ~85% of conjugates were formed (Figure S28). After that, the conjugates were denatured in 6M urea at 37 °C for 30 min. Then the free Cys of denatured SortaseA-P5 conjugates were alkylated by treating iodoacetamide for 30 min at rt. Then the alkylated SortaseA-P5 digested by treating with Trypsin Gold (Mass Spectrometry Grade, from Promega) at a ratio of 1:25 (enzyme: substrate) ratio for 2h at 37 °C. After 2h, the digestion reaction was quenched with formic acid (~5% of the final volume). The undigested pellets were removed by centrifuge and 10 µL of supernatant was directed injected into LC-MS. The modification site of the fragment was monitored by UV absorbance trace @ 425nm (the diazaborine absorbs at 425 nm). For control experiment, sortase A alone was digested with trypsin under the same conditions and then subjected to LC-MS analysis.

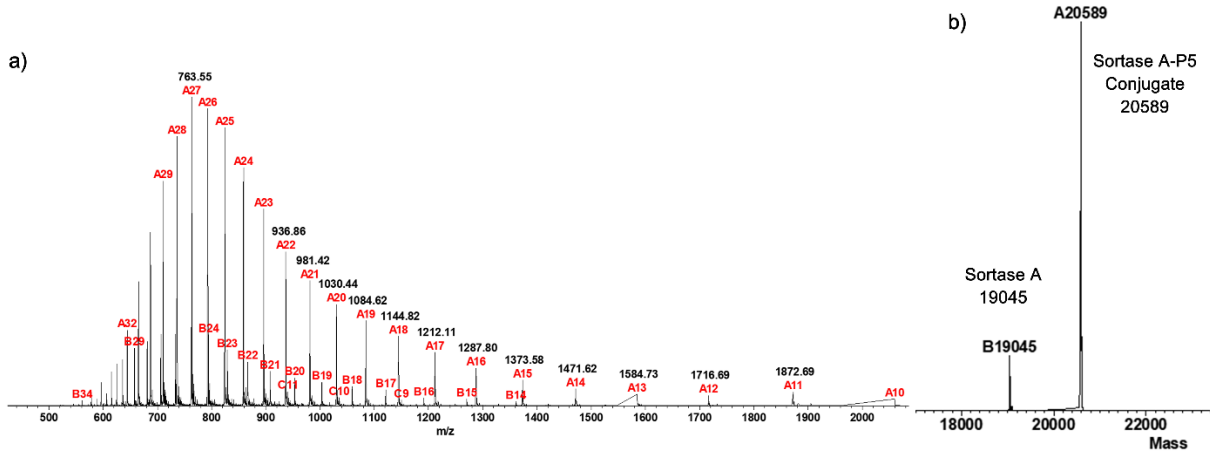

Figure S28: Covalent adduct of sortase A and P5. (a) and (b) are crude and deconvoluted mass-spec data demonstrating sortase-P5 conjugation formation.

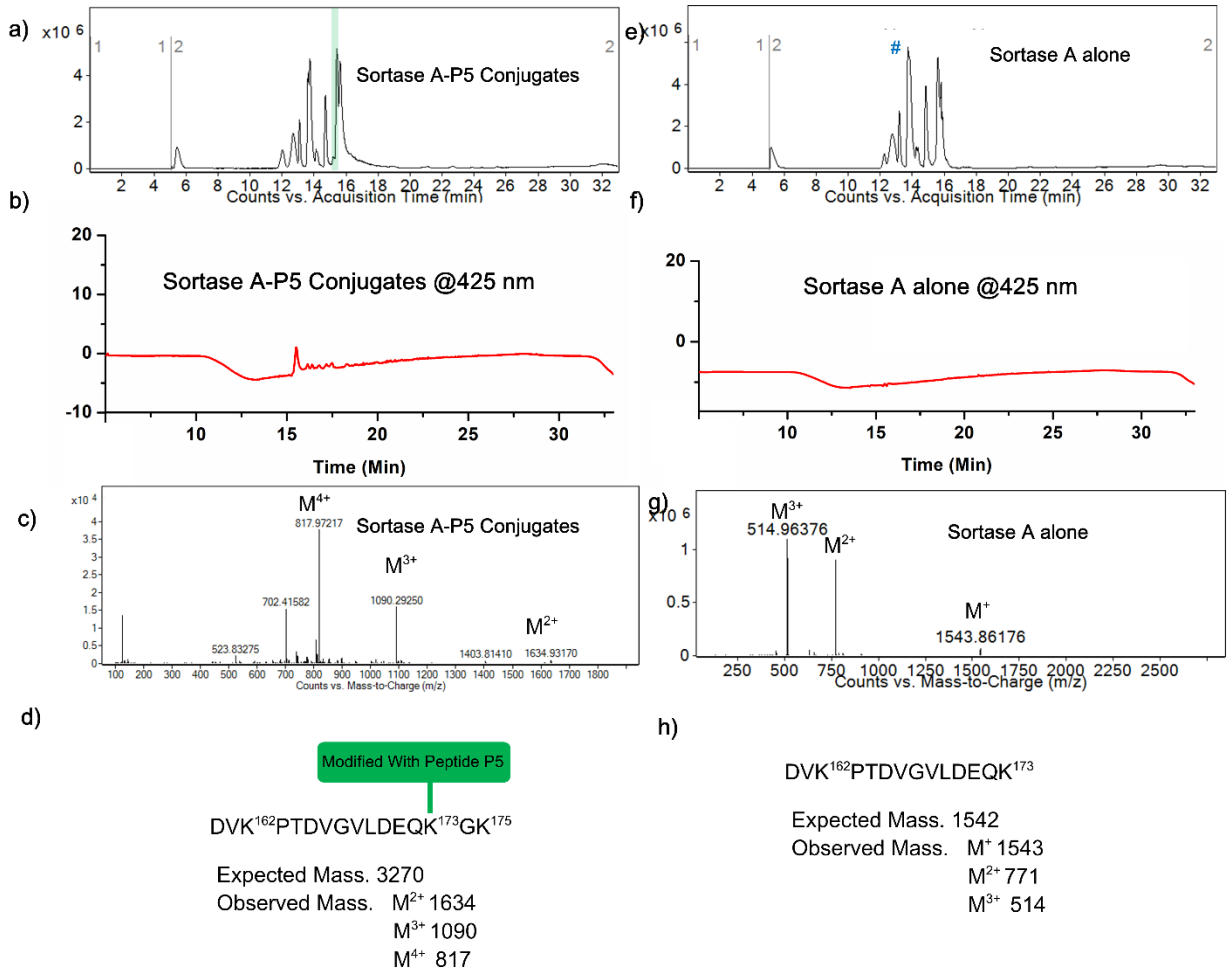

Figure S29: Peptide mapping to identify the conjugation site of P5 on sortase A. Shown for side-by-side comparison are the TIC (Total Ion Count) (a, e) and LC (b, f) traces of trypsin digested sortase-P5 conjugate (a, b) and sortase alone (e, f). Comparison of (b) and (f) shows a distinct peak (retention time: 15.5 min) with diazaborine absorption in the trypsin digested sortase-P5 mixed sample, which is absent from the trypsin digested sortase alone. Mass-spec data (c) of this distinct peak corresponds to the P5 conjugate of peptide D160-K175 (d). This peptide fragment contains two lysines K162 and K173. (g) shows the mass-spec data of sortase alone, specifically the peak marked with # in (e), which corresponds to peptide D160-K173 (h), which suggests that trypsin cleaves K173 of sortase, but not K162. Comparing the mass-spec data of sortase alone versus the sortase-P5 conjugate indicates ***P5 conjugation makes K173 no longer susceptible to trypsin cleavage***, hence, we conclude K173 is the conjugation site of P5 as a reversible covalent inhibitor.

17. Procedure for the Inhibition of Sortase A activity on S. aureus by Peptides W7, P3 and P5

a. Protocol for IC_{50} determination on live cells

The inhibitory effect of peptides W7, P3 and P5 on sortase activity on *S. aureus* cells was measured using a fluorescently labeled peptide substrate (FAM-GSLPETGGS).[7] First *S. aureus* cells (strain ATCC 6538) were cultured in 10 mL of LB media to reach OD=0.1. After that, the peptide substrate (0.3 mM) and an inhibitor peptide at varied concentrations (0.1 μM to 250 μM) were incubated together with the *S. aureus* cells in LB media for 6 h at 37 °C. Then the *S. aureus* cells were washed with 500 μL of 1× DPBS under 3700rpm, 5 min for 3 times. Then the fluorescence from the cells was quantified using flow cytometry analysis. Flow cytometry analysis were carried out by diluting cells to 10^6 cfu/mL in 1× DPBS (Exemplary crude data set shown in Figure S30). The median florescence intensity of FITC channel was normalized against that of positive control (no inhibitor), and then plotted against conc. of the inhibitor peptide (Figure 5c). The curves were fitted by the following the equation below to get the IC_{50} value. The flow cytometry measurements were carried out in triplicates and each data points in Figure 5c were plotted as an average of the triplicate samples.

$$Y=Bottom+ (Top - Bottom)/(1+10^{(X-LogIC_{50})})$$

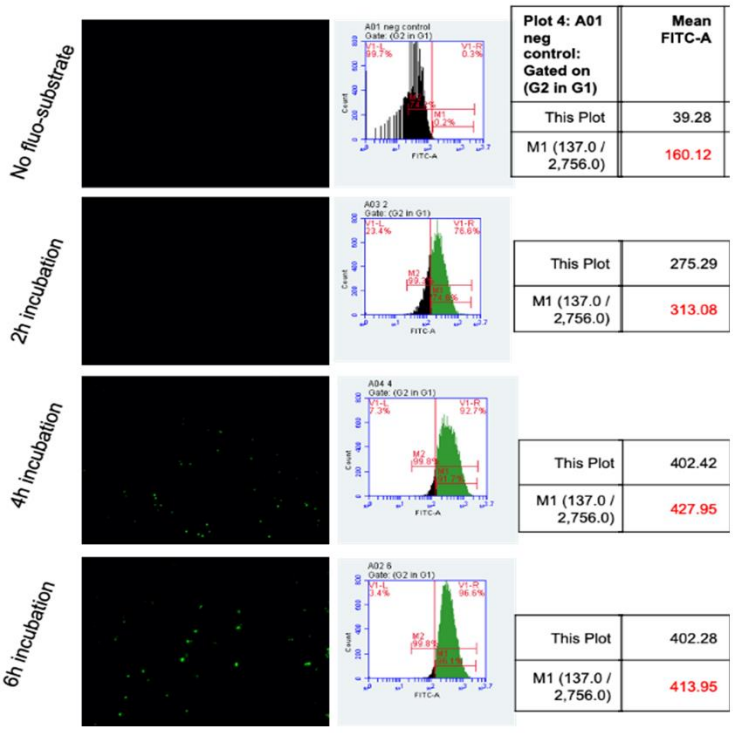

Figure S30: Flow cytometry analysis of Sortase A mediated fluorescence labeling of *S. aureus*.

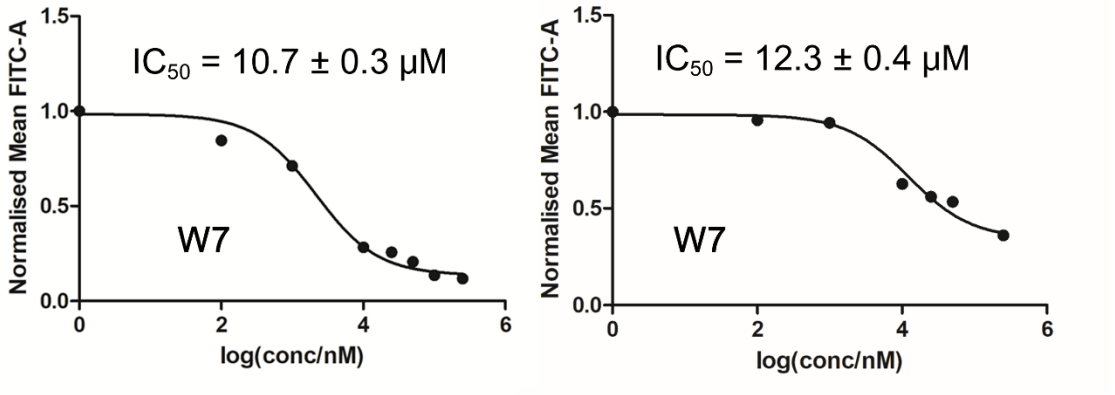

Figure S31: Sortase inhibition of W7 on live *S. aureus* cells. The replicate experiments carried out on different days gave consistent results.

b. Long Acting Inhibition from Peptide P5 on S. aureus:

S. aureus (strain ATCC 6538) was cultured in 10 ml LB to reach OD=0.1. Inhibitor peptides (W7, P3, and P5) at a conc. of 20 μM were incubated with the *S. aureus* culture with total volume 1mL for 4 h at room temperature. After that, *S. aureus* cells were thoroughly washed with 500 μL1× DPBS under 3700rpm, 5 min for 3 times to remove the non-covalently bound peptides. Then the cells were aging incubated with fluorescently labeled peptide substrate (0.3 mM) in M9 media for another 6 h at room temperature. After that, the cells were washed with 500 μL 1× DPBS under 3700rpm, 5 min for 3 times. Then the fluorescence from the cells was quantified using flow cytometry analysis. Flow cytometry analysis was carried out by diluting cells to 10^6 cfu/ml in 1× DPBS. The median florescence intensity of FITC channel was normalized against positive control and plotted. All experiments were carried out in triplicates and plotted as an average of three trials with standard deviations (Figure 5c).

c. Fluorescence Microscopy Sample Preparation:

For fluorescence microscopy images, *S. aureus* cells were diluted to OD=1 in 1× DPBS and 4 μL of the suspension was then placed on a glass slide. Then white light and fluorescent images were obtained on Zeiss microscope equipped with filter set 44 (excitation: BP 475/40, emission: BP 530/50). The images were captured using the 100x oil immersion with 1000 ms exposure time. All the images were further processed using Image J software with same parameters.

18. LC-MS trace and ESI-MS$^+$ of Purified Peptides

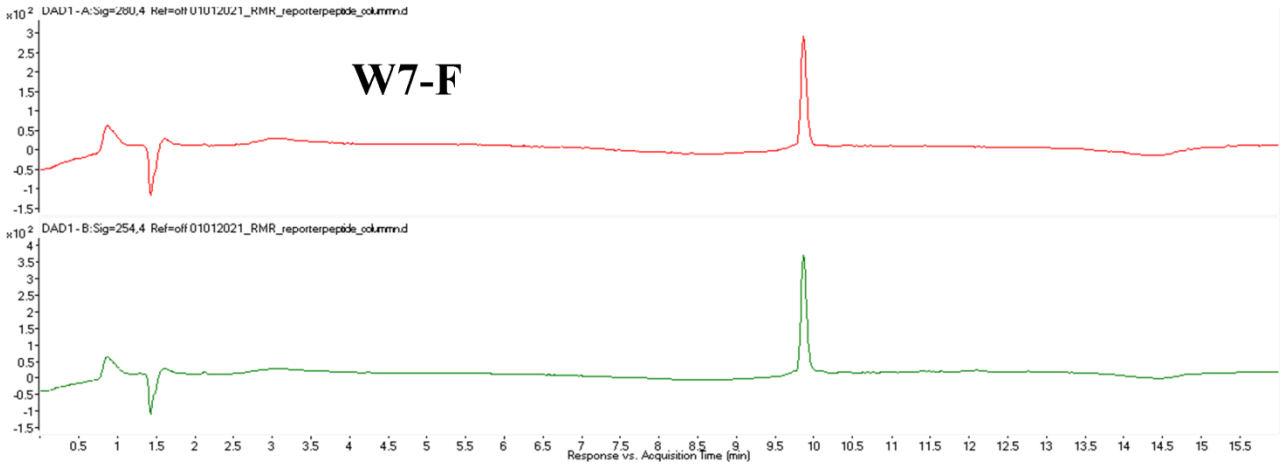

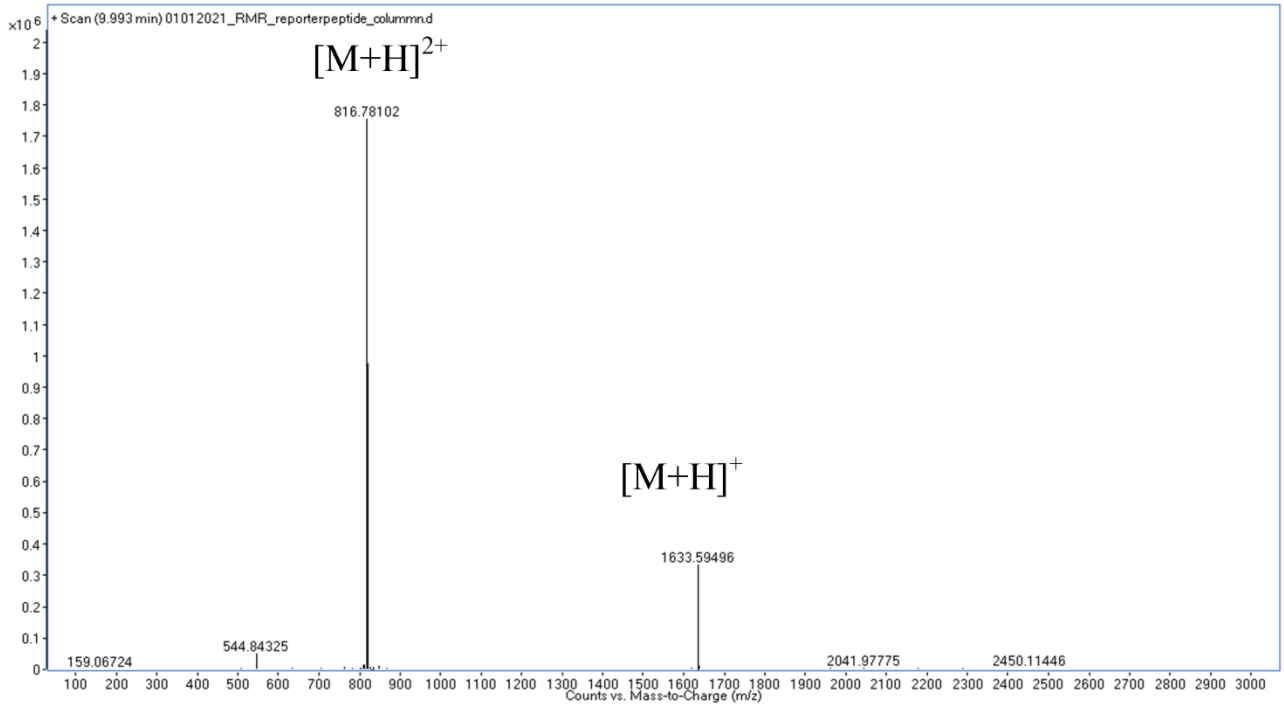

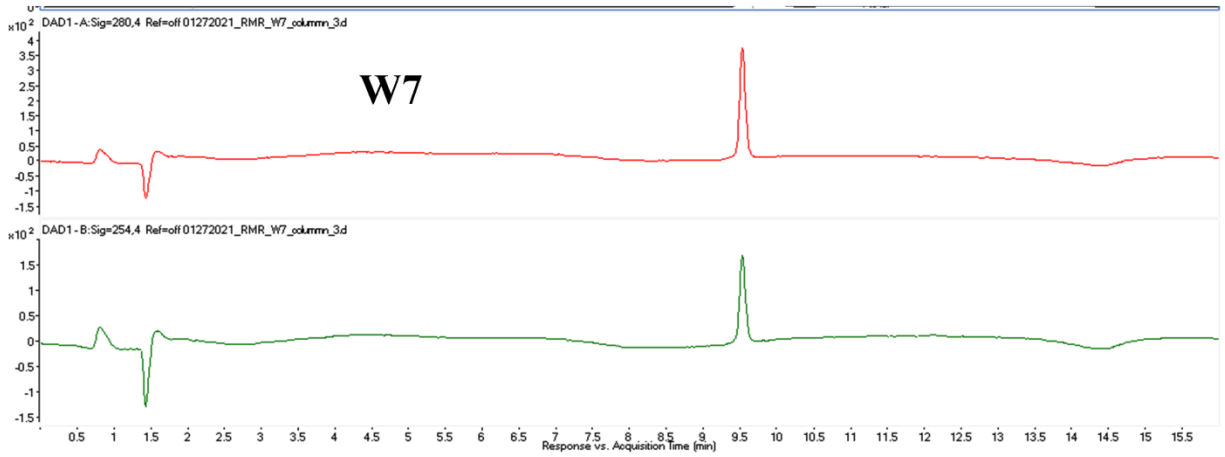
DAD1 - A:Sig=280,4 Ref=off 01272021_RMR_W7_columnn_3d
W7
DAD1 - B:Sig=254,4 Ref=off 01272021_RMR_W7_columnn_3d
Response vs. Acquisition Time (min)

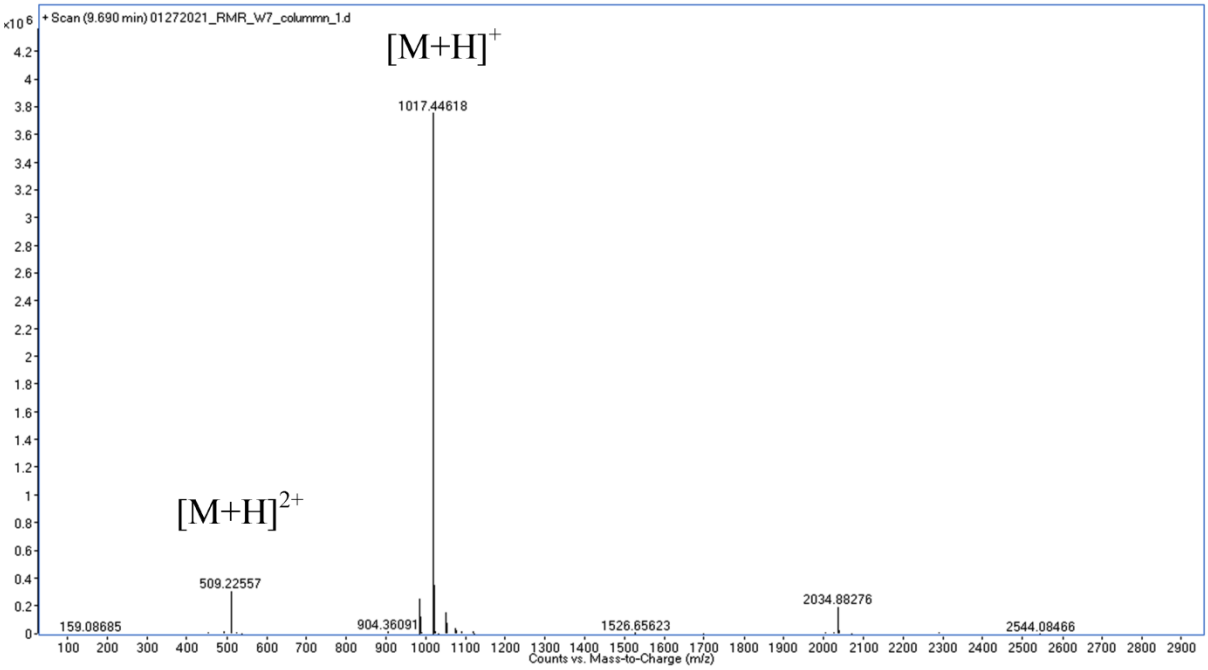
+ Scan (9.690 min) 01272021_RMR_W7_columnn_1.d
[M+H]+
1017.44618
[M+H]2+
509.22557
159.08685
904.36091
1526.65623
2034.88276
2544.08466
Counts vs. Mass-to-Charge (m/z)

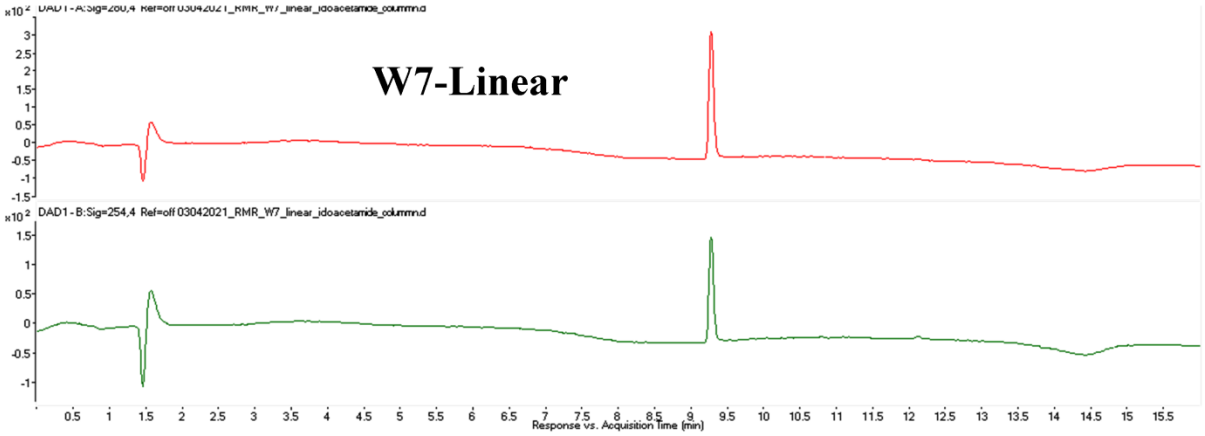
W7-Linear
DAD1 - B:Sig=254,4 Ref=off 03042021_RMR_W7_linear_idoacetamide_columm.d
Response vs. Acquisition Time (min)

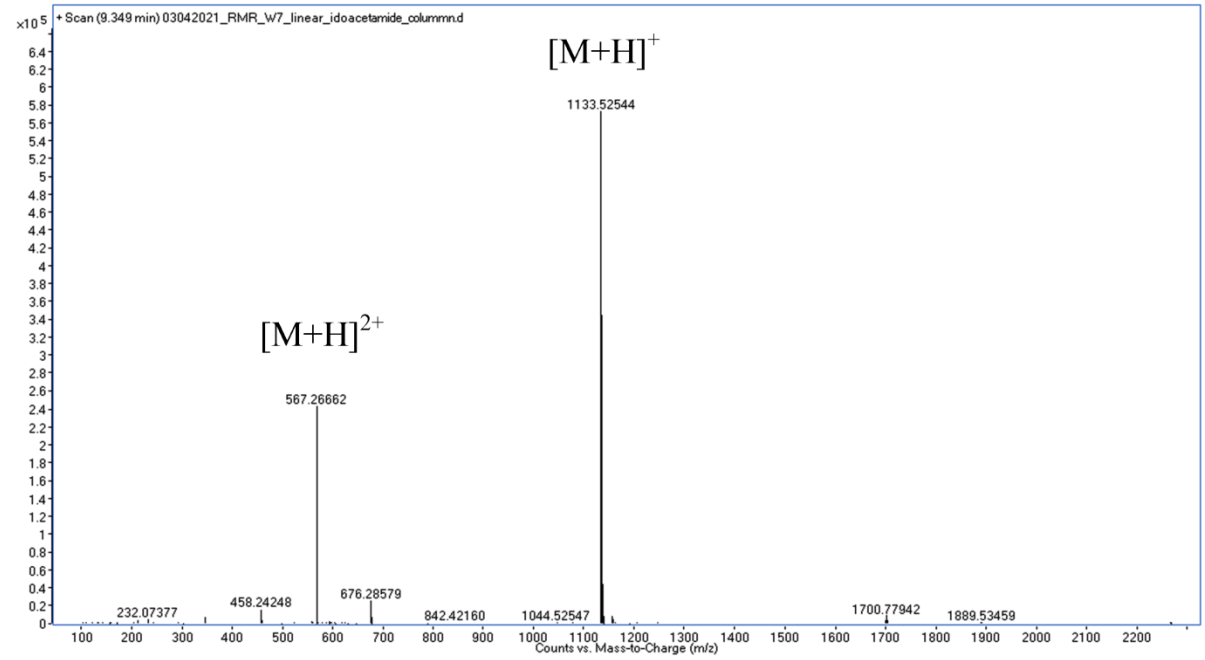
+ Scan (9.349 min) 03042021_RMR_W7_linear_idoacetamide_columm.d
[M+H]+
1133.52544
[M+H]2+
567.26662
458.24248
676.28579
232.07377
842.42160
1044.52547
1700.77942
1889.53459
Counts vs. Mass-to-Charge (m/z)

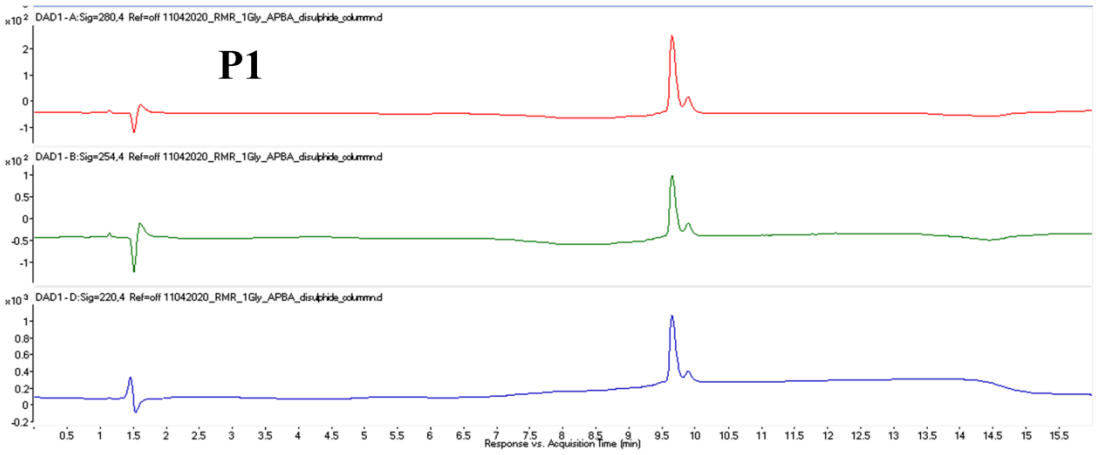
DAD1 - A:Sig=280,4 Ref=off 11042020_RMR_1Gly_APBA_disulphide_columnn.d
P1
DAD1 - B:Sig=254,4 Ref=off 11042020_RMR_1Gly_APBA_disulphide_columnn.d
DAD1 - D:Sig=220,4 Ref=off 11042020_RMR_1Gly_APBA_disulphide_columnn.d
Response vs. Acquisition Time (min)

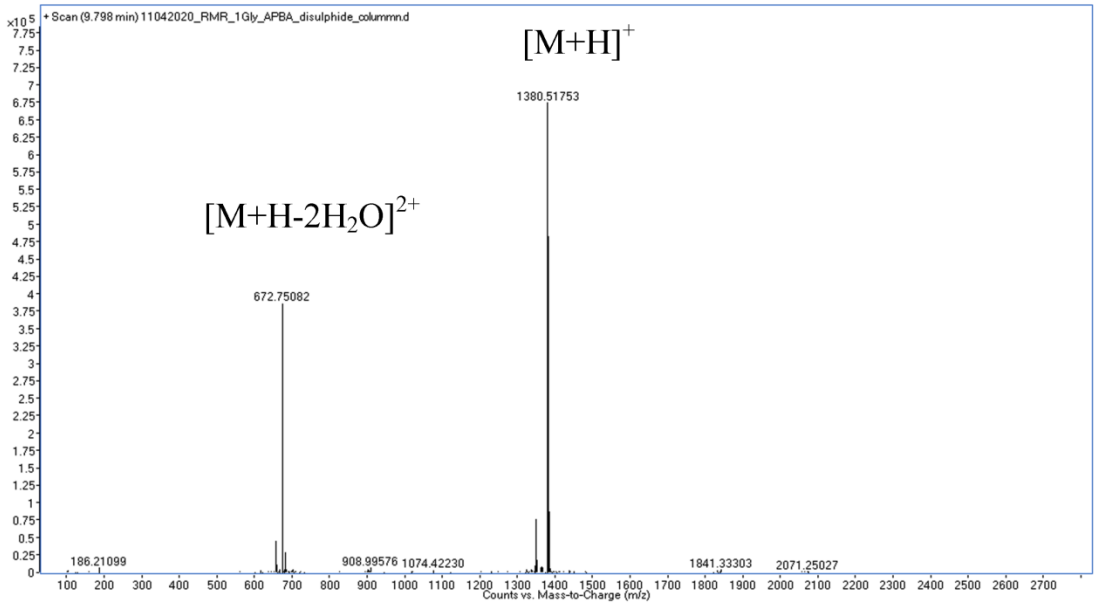
+ Scan (9.798 min) 11042020_RMR_1Gly_APBA_disulphide_columnn.d
[M+H]+
1380.51753
[M+H-2H2O]2+
672.75082
186.21099
908.99576
1074.42230
1841.33303
2071.25027
Counts vs. Mass-to-Charge (m/z)

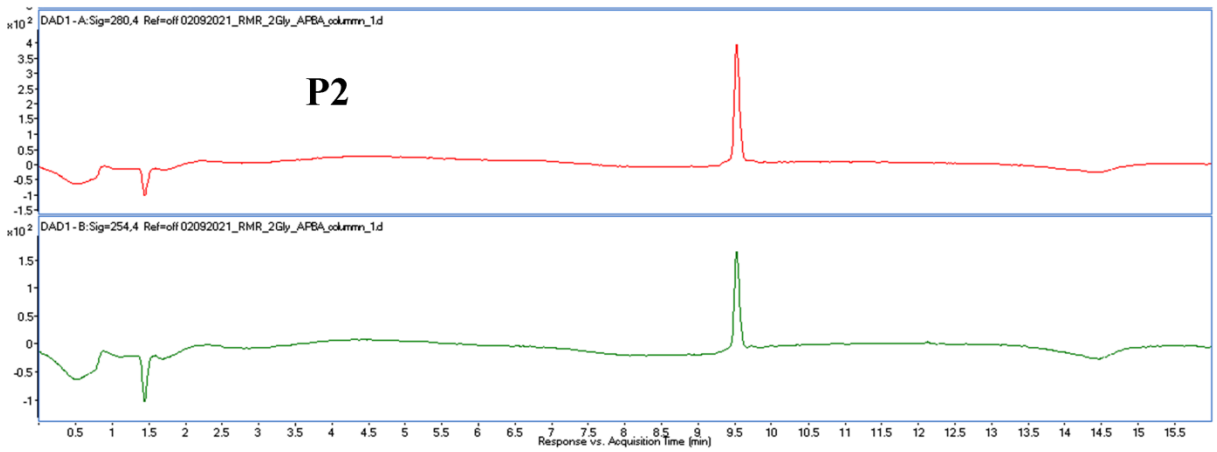
DAD1 - A:Sig=280,4 Ref=off 02092021_RMR_2Gly_APBA_columnn_1.d
P2
DAD1 - B:Sig=254,4 Ref=off 02092021_RMR_2Gly_APBA_columnn_1.d
Response vs. Acquisition Time (min)

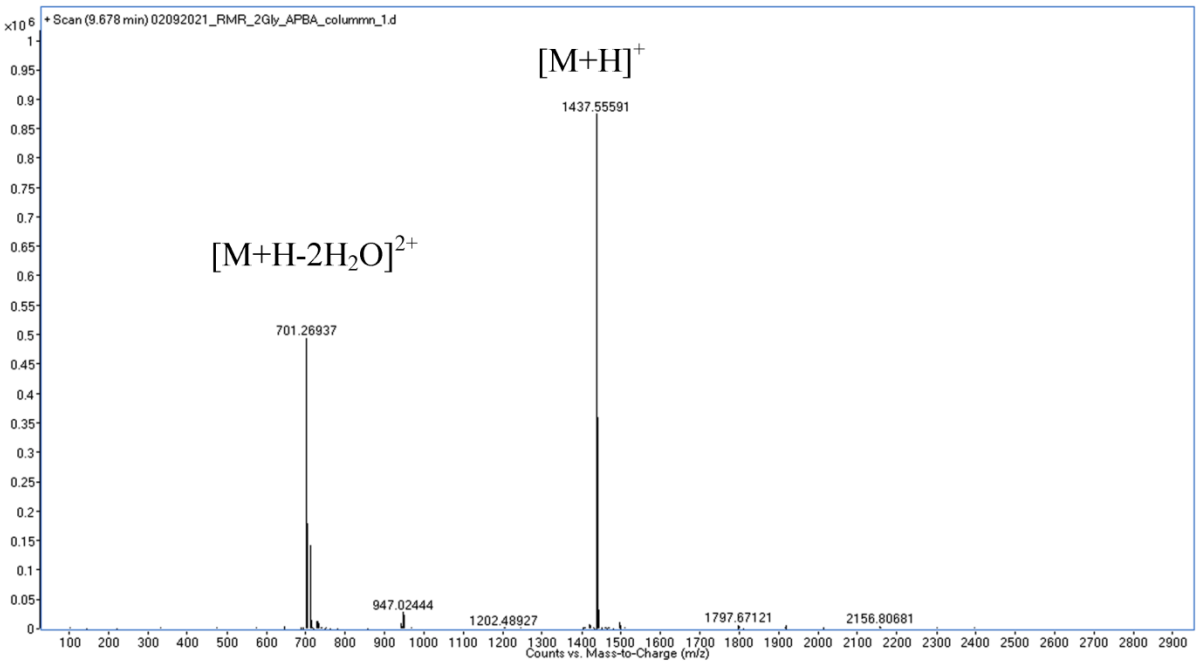
+ Scan (9.678 min) 02092021_RMR_2Gly_APBA_columnn_1.d
[M+H]+
1437.55591
[M+H-2H2O]2+
701.26937
947.02444
1202.48927
1797.67121
2156.80681
Counts vs. Mass-to-Charge (m/z)

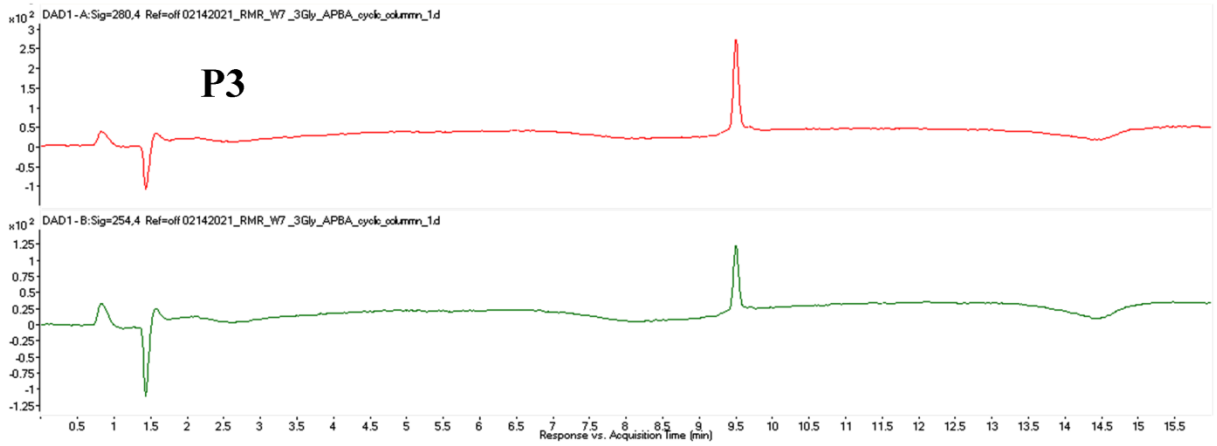
DAD1 - A:Sig=280,4 Ref=off 02142021_RMR_W7 _3Gly_APBA_cyclic_columnn_1.d
P3
DAD1 - B:Sig=254,4 Ref=off 02142021_RMR_W7 _3Gly_APBA_cyclic_columnn_1.d
Response vs. Acquisition Time (min)

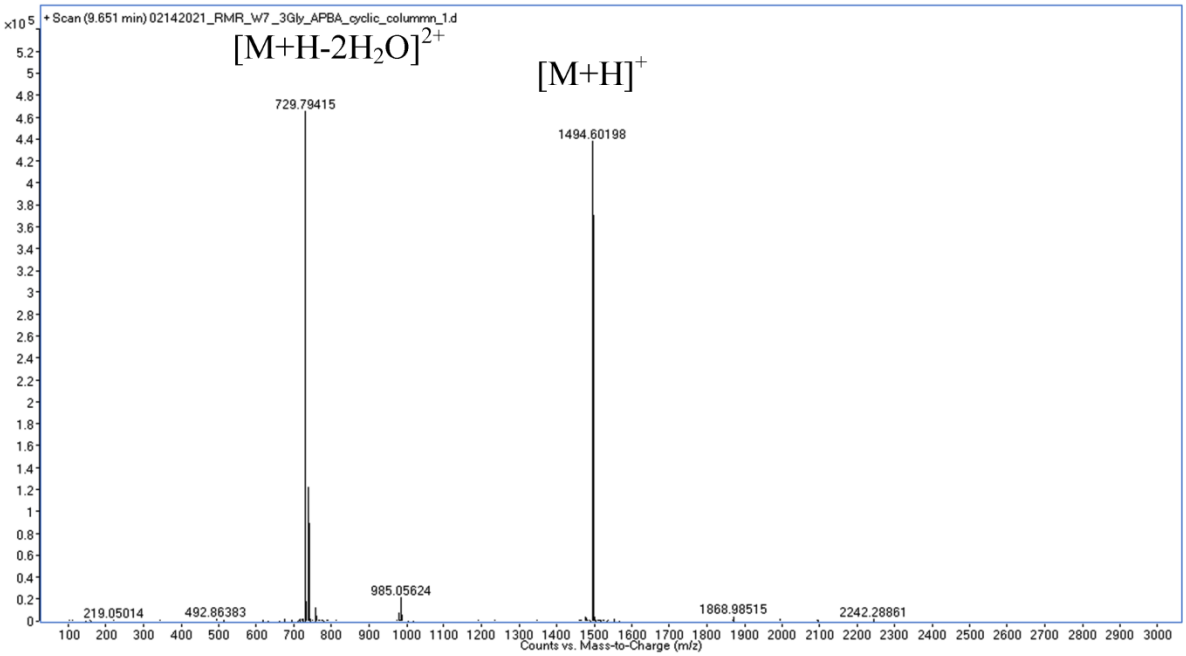
+ Scan (9.651 min) 02142021_RMR_W7 _3Gly_APBA_cyclic_columnn_1.d
[M+H-2H2O]2+
[M+H]+
729.79415
1494.60198
985.05624
219.05014
492.86383
1868.98515
2242.28861
Counts vs. Mass-to-Charge (m/z)

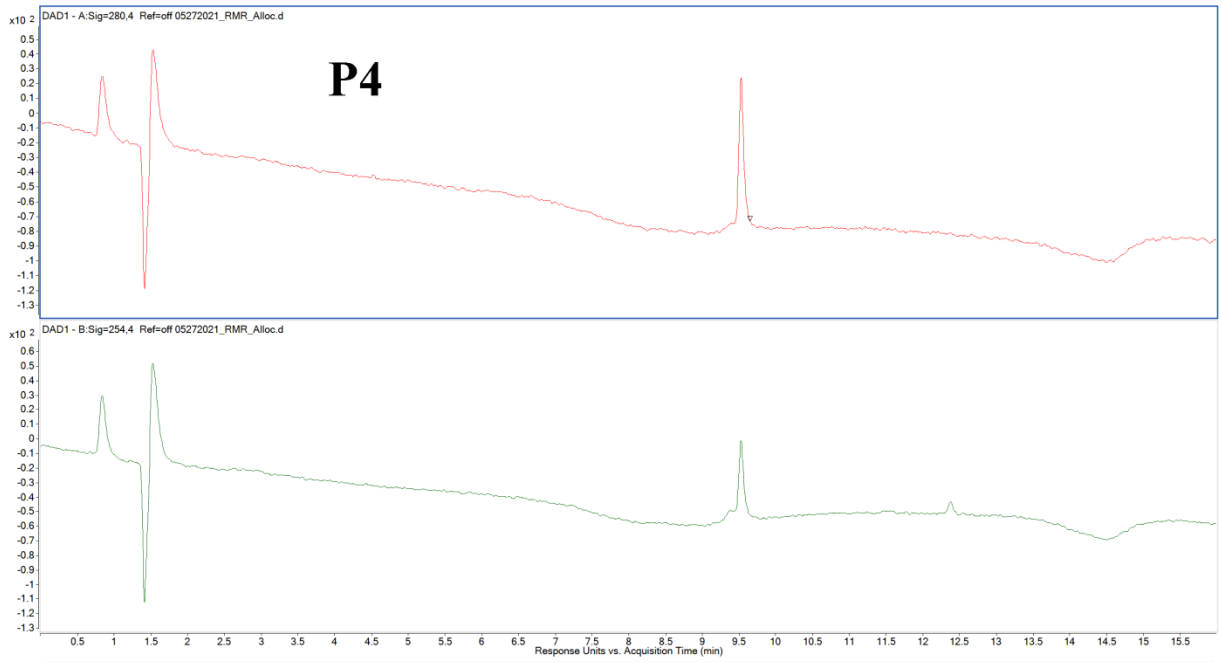
DAD1 - A:Sig=280,4 Ref=off 05272021_RMR_Alloc.d
P4
DAD1 - B:Sig=254,4 Ref=off 05272021_RMR_Alloc.d
Response Units vs. Acquisition Time (min)

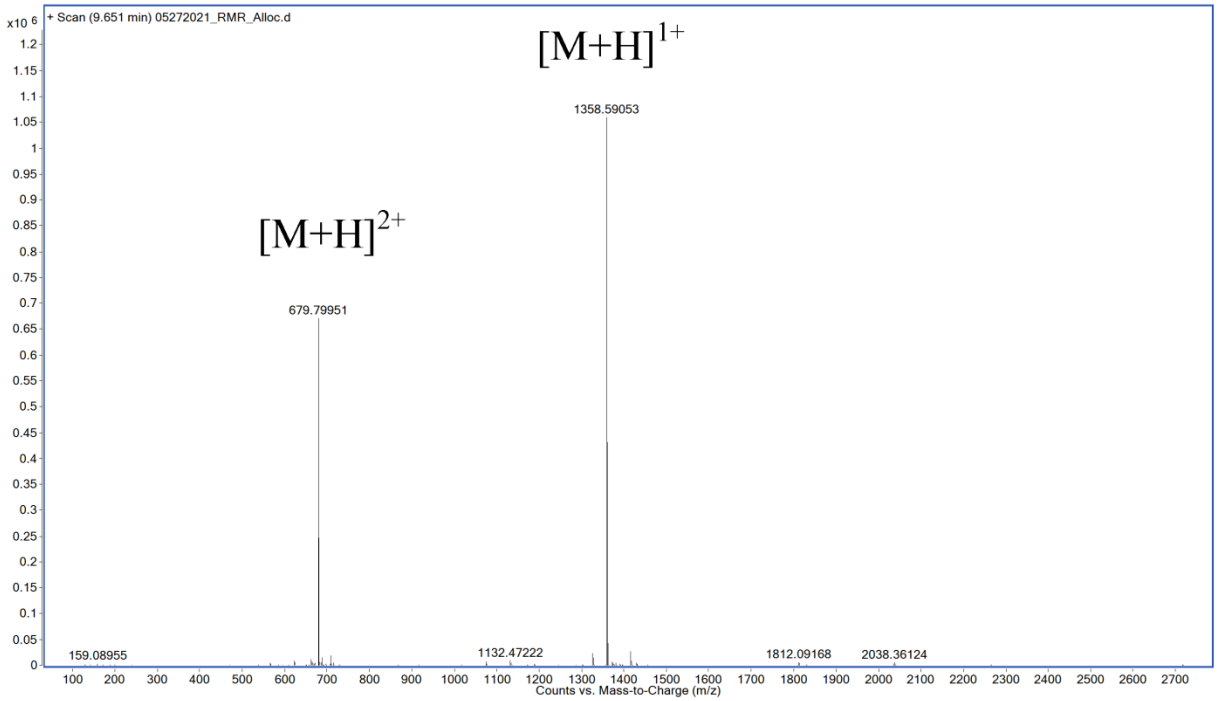
+ Scan (9.651 min) 05272021_RMR_Alloc.d
[M+H]1+
1358.59053
[M+H]2+
679.79951
159.08955
1132.47222
1812.09168
2038.36124
Counts vs. Mass-to-Charge (m/z)

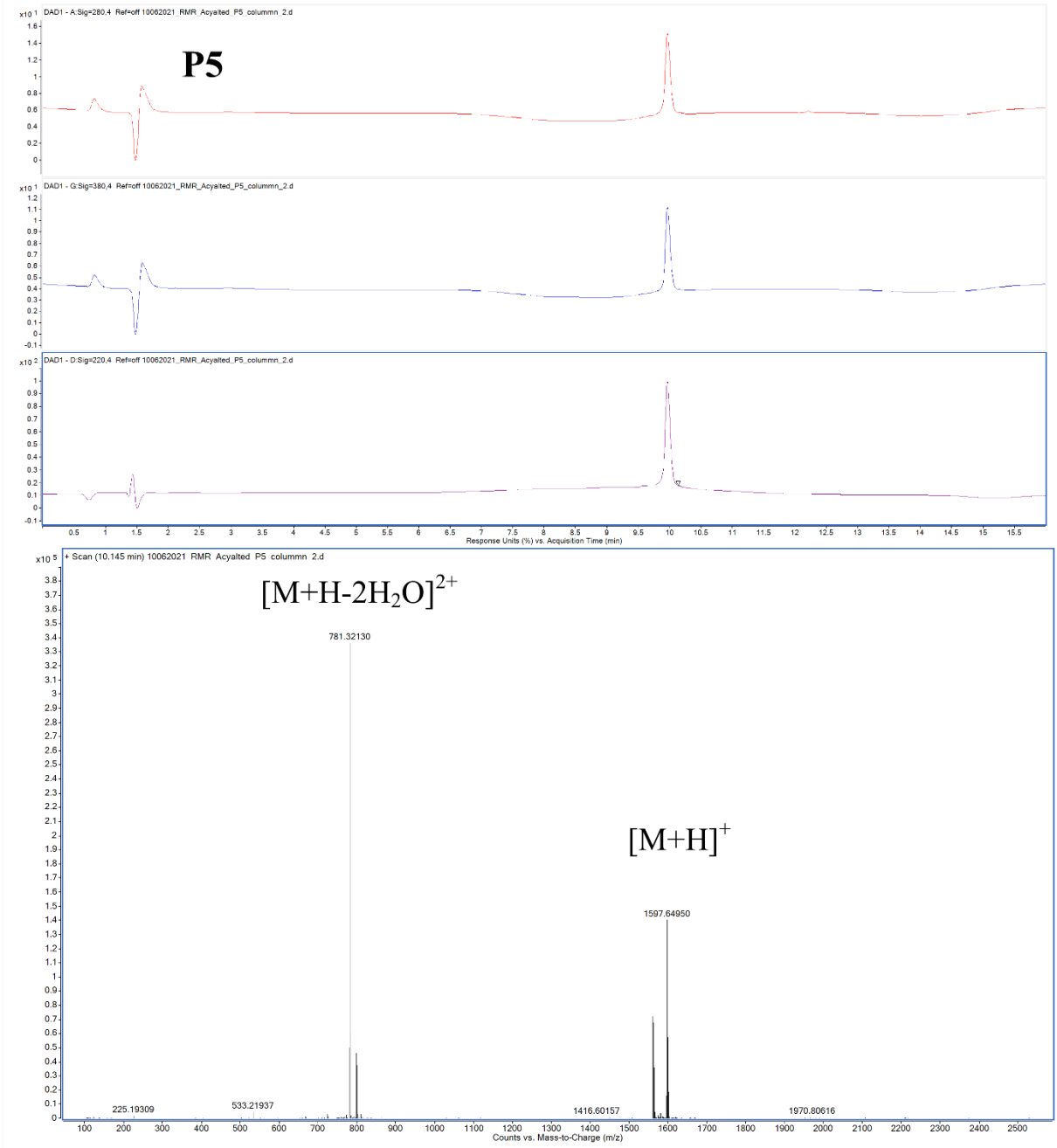
P5
DAD1 - A:Sig=280,4 Ref=off 10062021_RMR_Acyalted_P5_columnn_2.d
DAD1 - G:Sig=380,4 Ref=off 10062021_RMR_Acyalted_P5_columnn_2.d
DAD1 - D:Sig=220,4 Ref=off 10062021_RMR_Acyalted_P5_columnn_2.d
Response Units (%) vs. Acquisition Time (min)
+ Scan (10.145 min) 10062021_RMR_Acyalted_P5_columnn_2.d
[M+H-2H2O]2+
781.32130
[M+H]+
1597.64950
225.19309
533.21937
1416.60157
1970.80616
Counts vs. Mass-to-Charge (m/z)

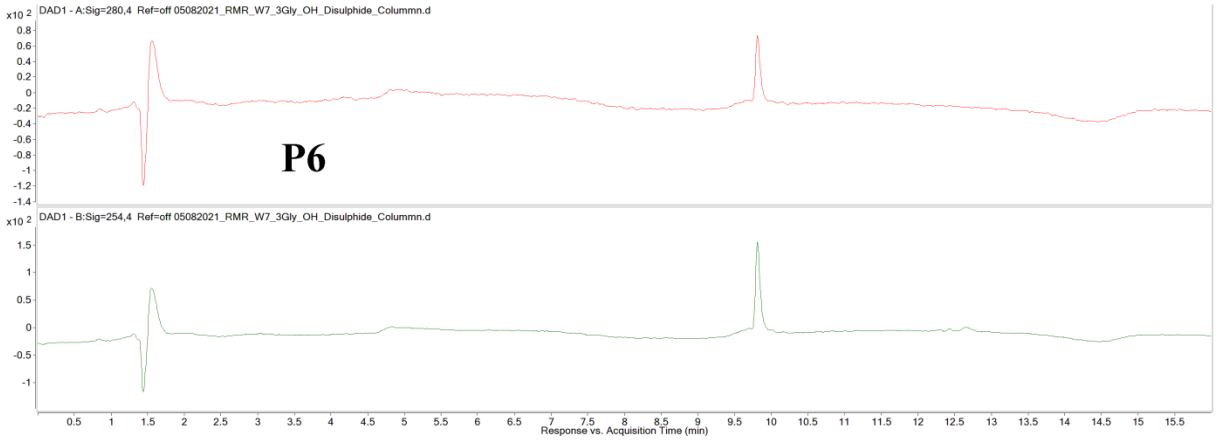
DAD1 - A:Sig=280,4 Ref=off 05082021_RMR_W7_3Gly_OH_Disulphide_Columnn.d
P6
DAD1 - B:Sig=254,4 Ref=off 05082021_RMR_W7_3Gly_OH_Disulphide_Columnn.d
Response vs. Acquisition Time (min)

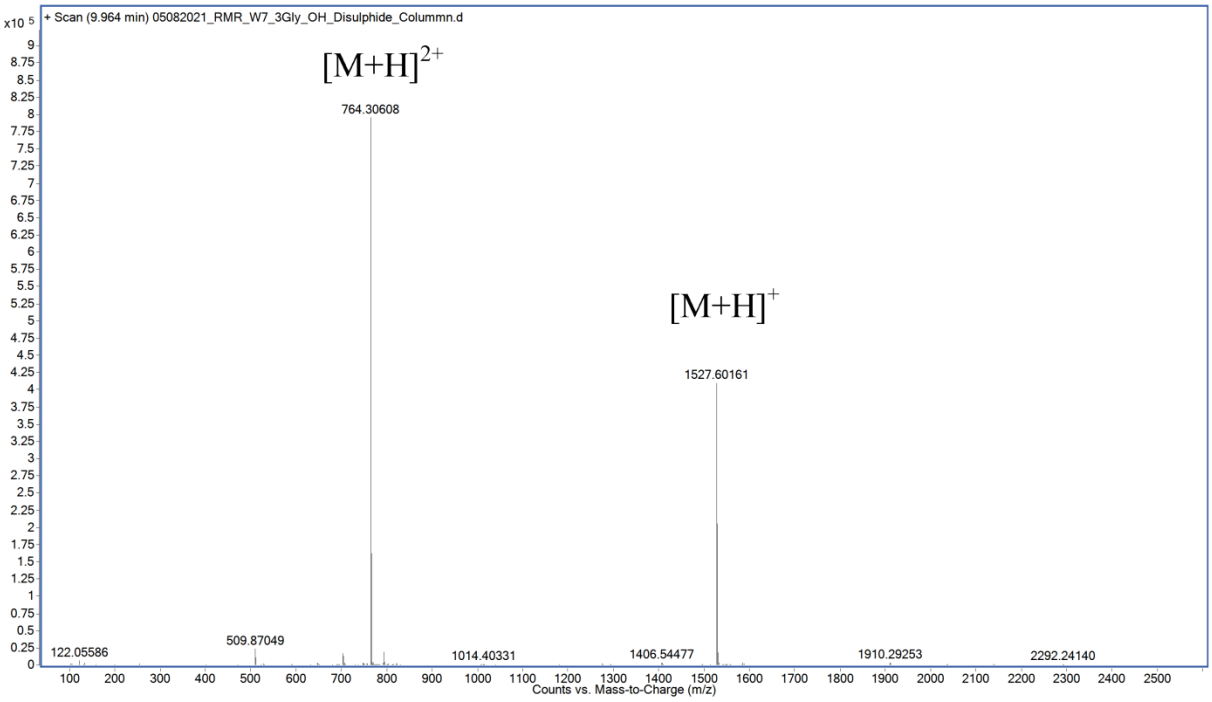
+ Scan (9.964 min) 05082021_RMR_W7_3Gly_OH_Disulphide_Columnn.d
[M+H]2+
764.30608
[M+H]+
1527.60161
122.05586
509.87049
1014.40331
1406.54477
1910.29253
2292.24140
Counts vs. Mass-to-Charge (m/z)

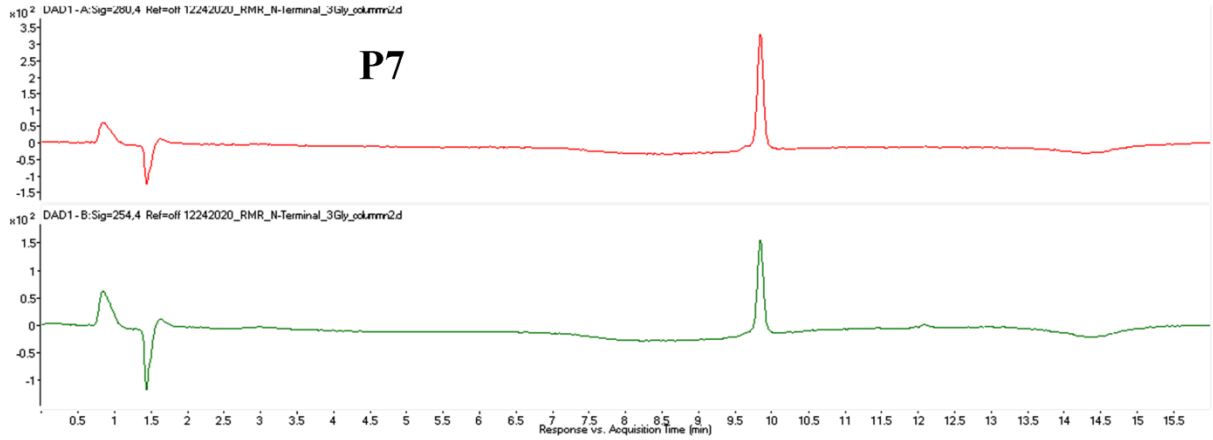
P7
DAD1 - A:Sig=280,4 Ref=off 12242020_RMR_N-Terminal_3Gly_columnn2.d
DAD1 - B:Sig=254,4 Ref=off 12242020_RMR_N-Terminal_3Gly_columnn2.d
Response vs. Acquisition Time (min)

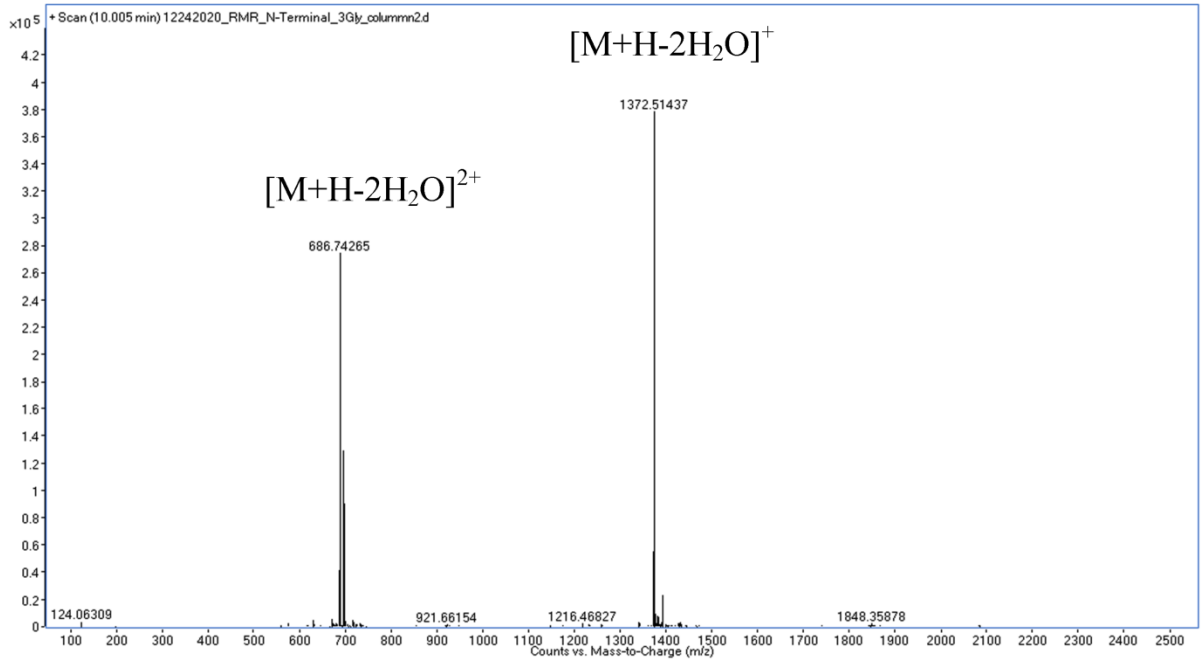
+ Scan (10.005 min) 12242020_RMR_N-Terminal_3Gly_columnn2.d
[M+H-2H2O]+
1372.51437
[M+H-2H2O]2+
686.74265
124.06309
921.66154
1216.46827
1848.35878
Counts vs. Mass-to-Charge (m/z)

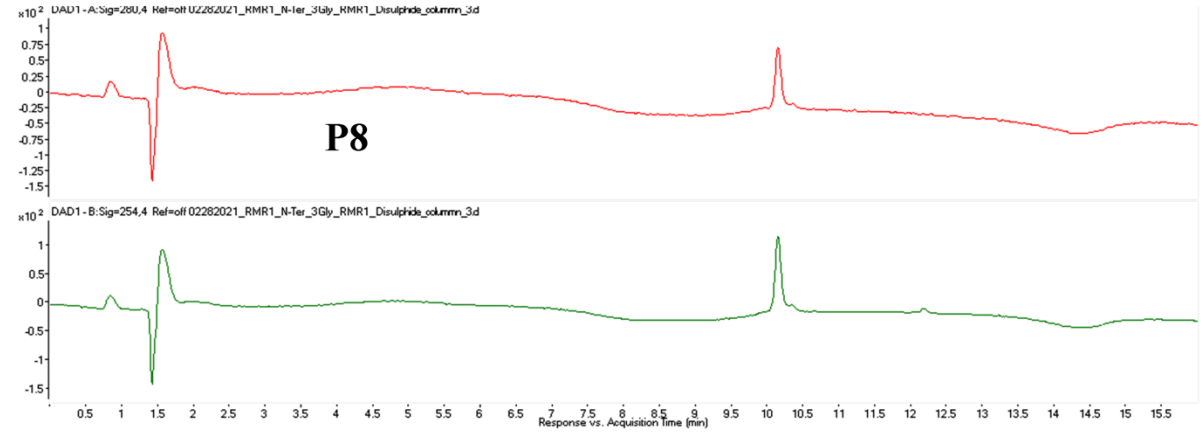
P8
DAD1 - B:Sig=254,4 Ref=off 02282021_RMR1_N-Ter_3Gly_RMR1_Disulphide_columnn_3d
Response vs. Acquisition Time (min)

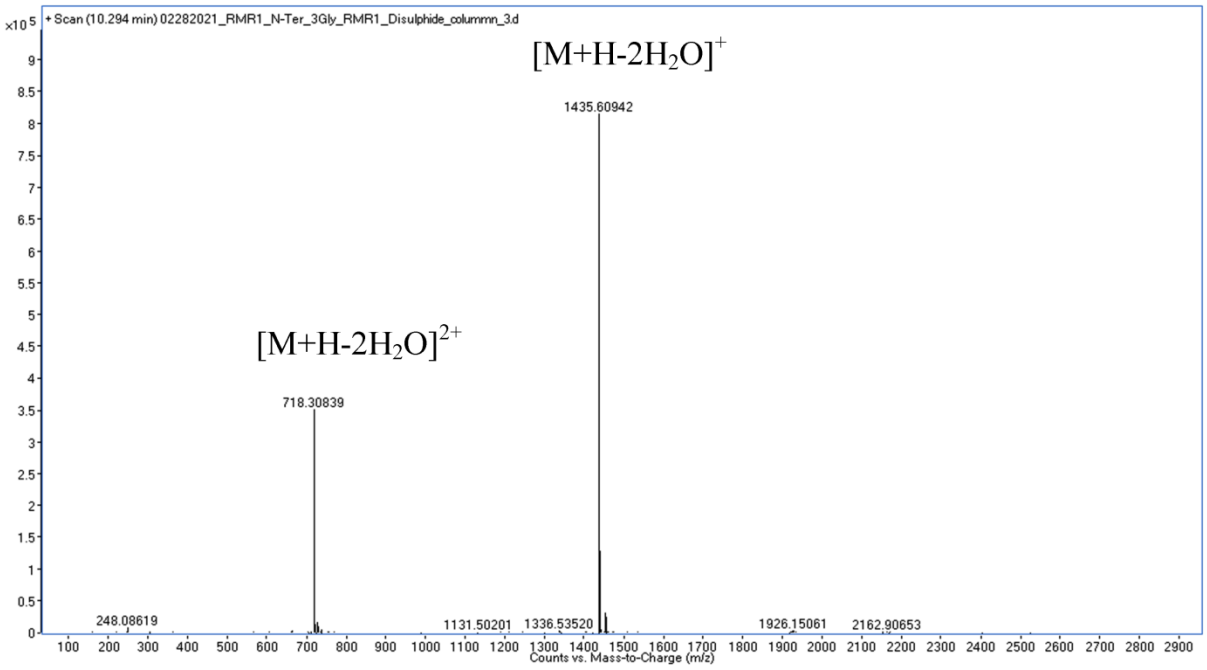
+ Scan (10.294 min) 02282021_RMR1_N-Ter_3Gly_RMR1_Disulphide_columnn_3d
[M+H-2H2O]+
1435.60942
[M+H-2H2O]2+
718.30839
248.08619
1131.50201
1336.53520
1926.15061
2162.90653
Counts vs. Mass-to-Charge (m/z)

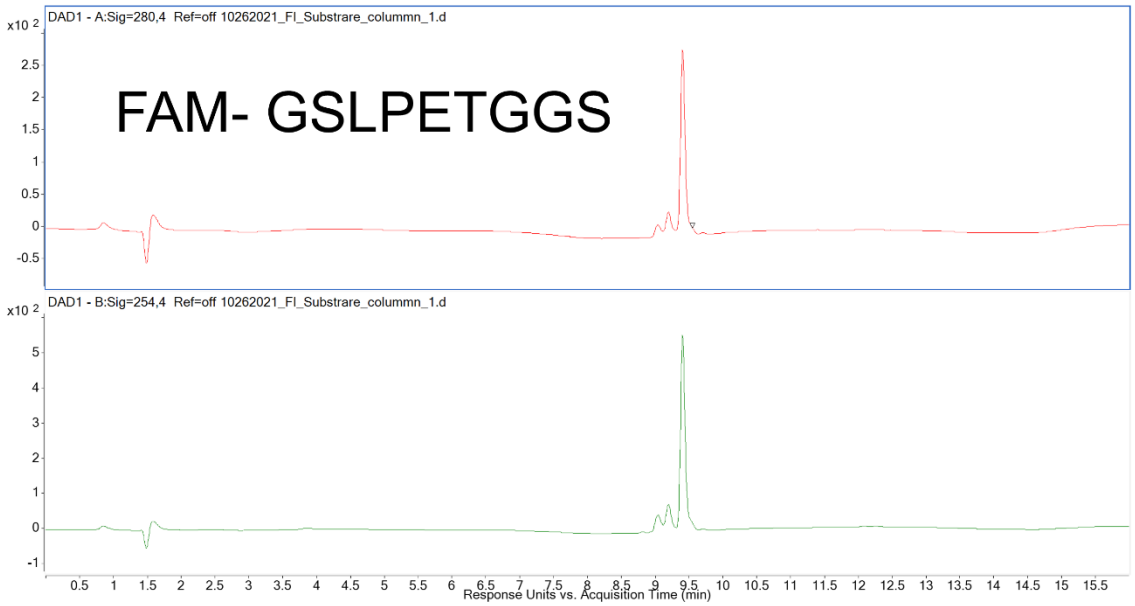
DAD1 - A:Sig=280,4 Ref=off 10262021_FI_Substrare_columnn_1.d
FAM- GSLPETGGS
DAD1 - B:Sig=254,4 Ref=off 10262021_FI_Substrare_columnn_1.d
Response Units vs. Acquisition Time (min)

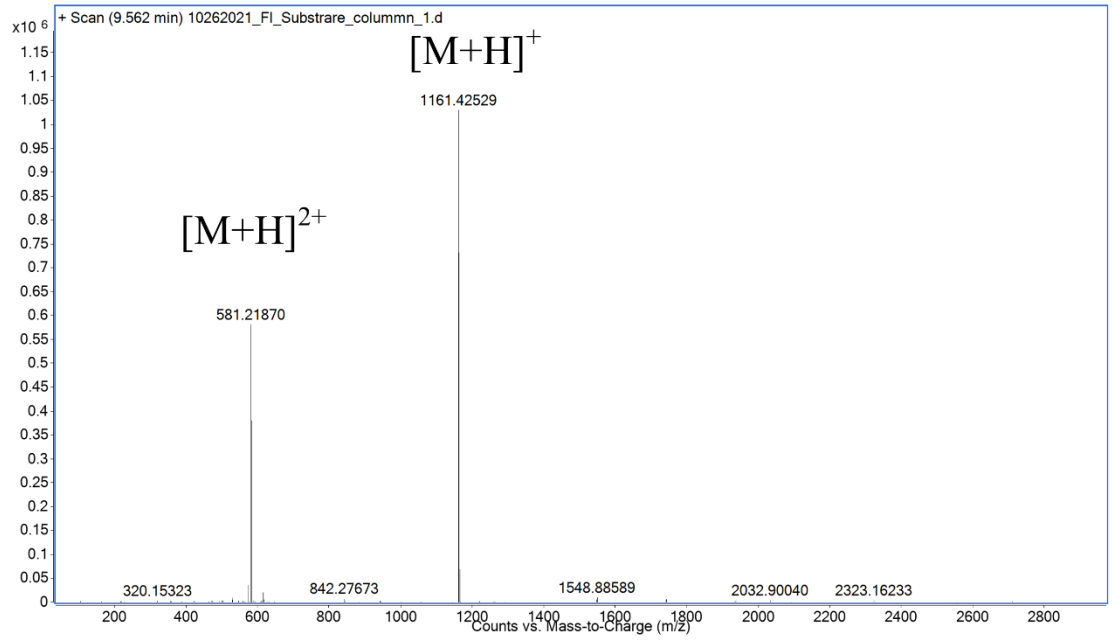
+ Scan (9.562 min) 10262021_FI_Substrare_columnn_1.d
[M+H]+
1161.42529
[M+H]2+
581.21870
320.15323
842.27673
1548.88589
2032.90040
2323.16233
Counts vs. Mass-to-Charge (m/z)

19. ^{1}H NMR and ^{13}C NMR Spectra

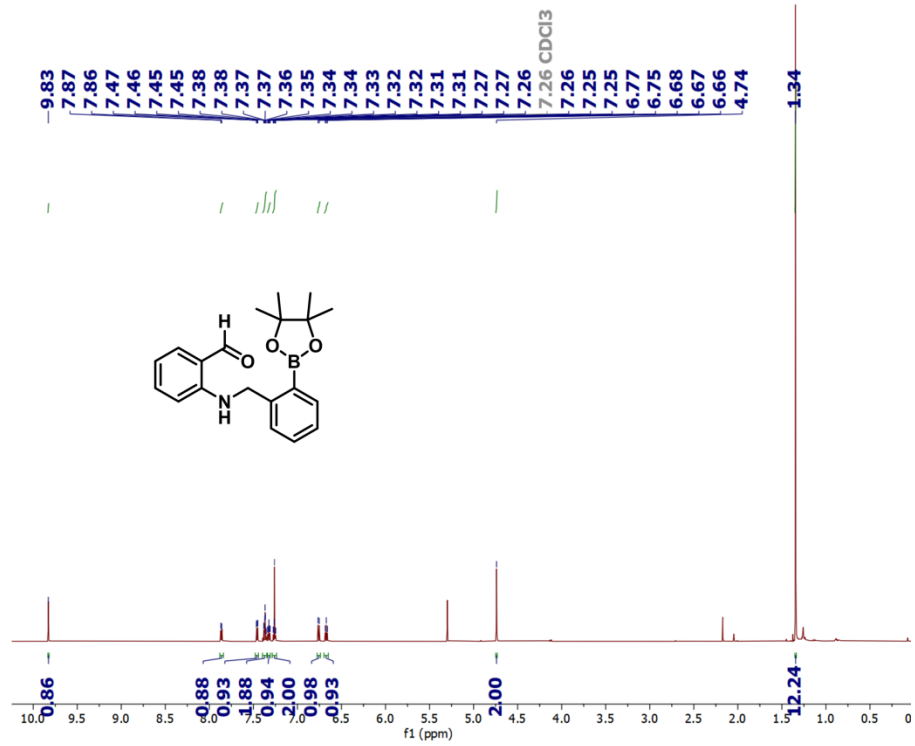

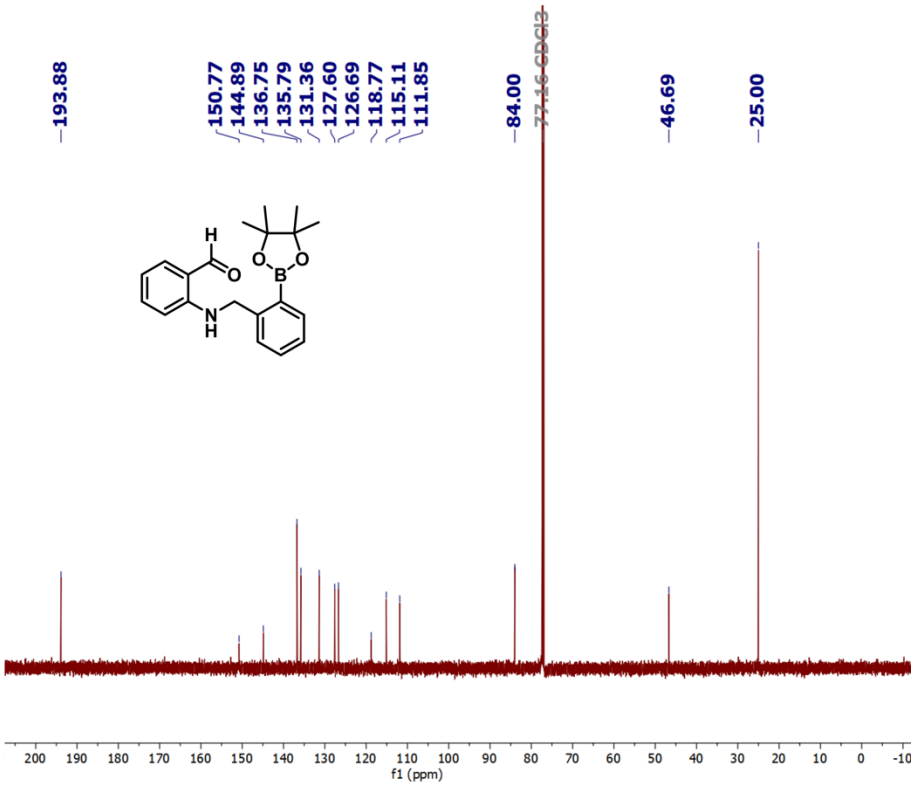

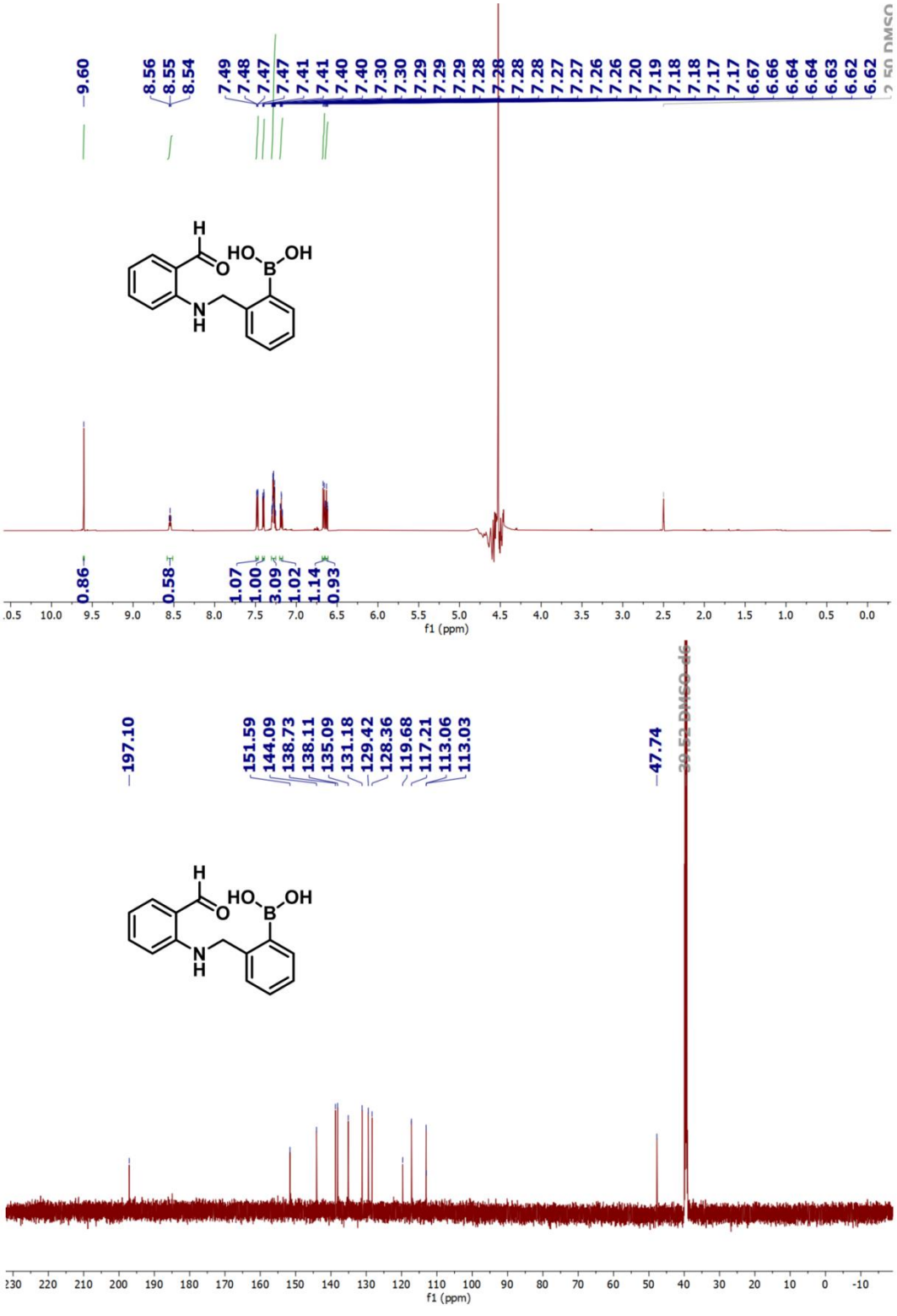
9.60
8.56
8.55
8.54
7.49
7.48
7.47
7.47
7.41
7.41
7.40
7.40
7.30
7.30
7.29
7.29
7.29
7.28
7.28
7.28
7.28
7.27
7.27
7.26
7.26
7.20
7.19
7.18
7.18
7.17
7.17
6.67
6.66
6.64
6.64
6.63
6.62
6.62
2.50 DMSO
0.86
0.58
1.07
1.00
3.09
1.02
1.14
0.93
f1 (ppm)
197.10
151.59
144.09
138.73
138.11
135.09
131.18
129.42
128.36
119.68
117.21
113.06
113.03
47.74
39.52 DMSO-d6
f1 (ppm)

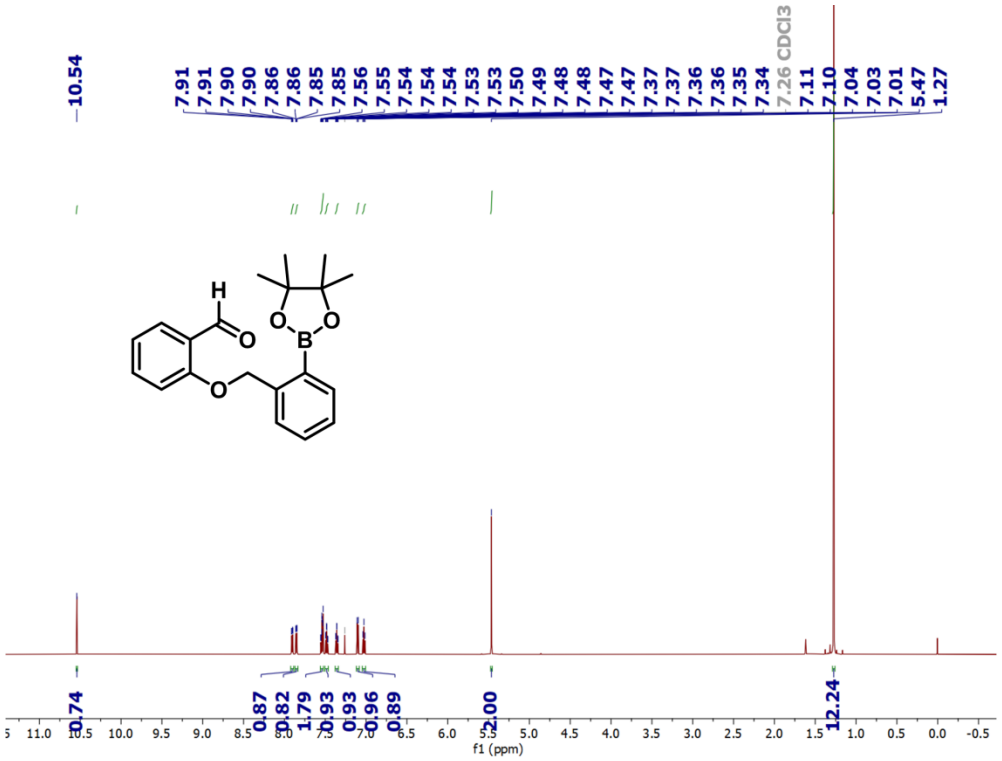
10.54
7.91
7.91
7.90
7.90
7.86
7.86
7.85
7.85
7.56
7.55
7.54
7.54
7.54
7.53
7.53
7.50
7.49
7.48
7.48
7.47
7.47
7.37
7.37
7.36
7.36
7.35
7.34
7.26 CDCl3
7.11
7.10
7.04
7.03
7.01
5.47
1.27
H
O
O
B
O
O
0.74
0.87
0.82
1.79
0.93
0.93
0.96
0.89
2.00
12.24
f1 (ppm)

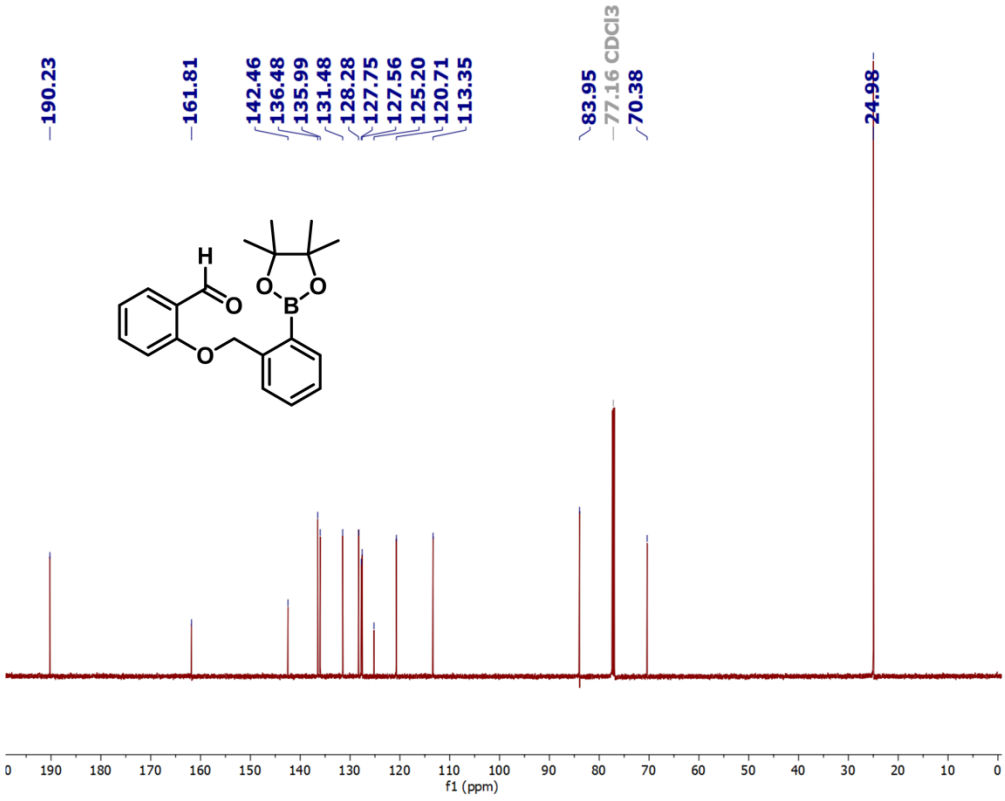
190.23
161.81
142.46
136.48
135.99
131.48
128.28
127.75
127.56
125.20
120.71
113.35
83.95
77.16 CDCl3
70.38
24.98
H
O
O
B
O
O
f1 (ppm)

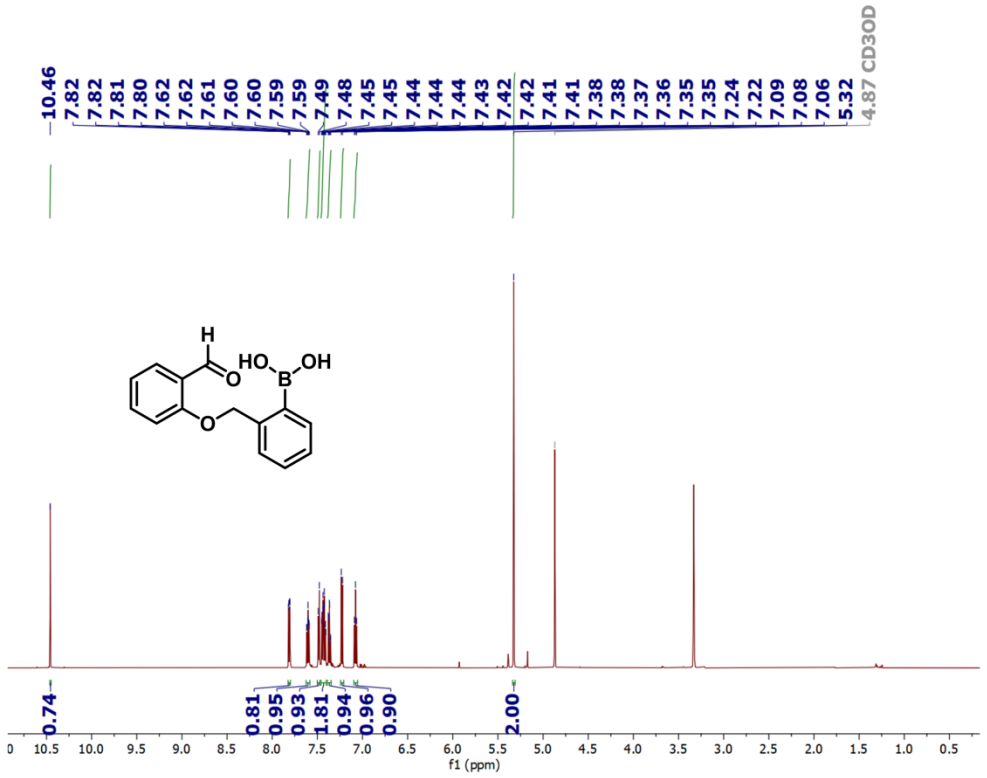
10.46
7.82
7.82
7.81
7.80
7.62
7.62
7.61
7.60
7.60
7.59
7.59
7.49
7.48
7.45
7.45
7.44
7.44
7.44
7.43
7.42
7.42
7.41
7.41
7.38
7.38
7.37
7.36
7.35
7.35
7.24
7.22
7.09
7.08
7.06
5.32
4.87 CD3OD
H
O
HO
B
OH
O
0.74
0.81
0.95
0.93
1.81
0.94
0.96
0.90
2.00
f1 (ppm)

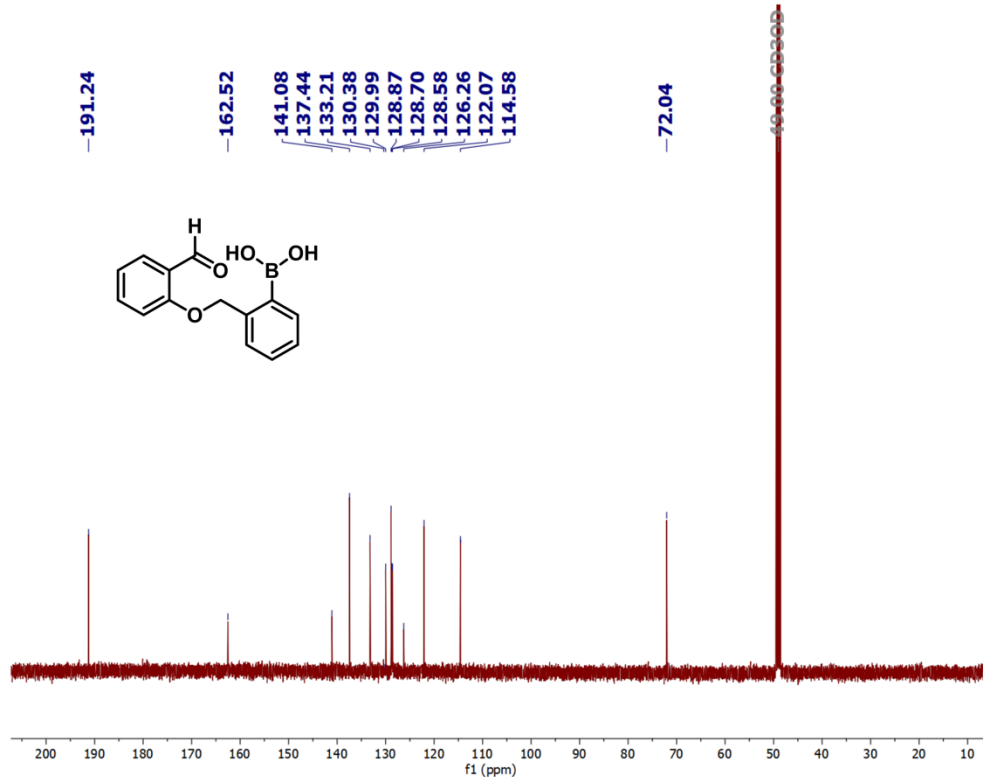
191.24
162.52
141.08
137.44
133.21
130.38
129.99
128.87
128.70
128.58
126.26
122.07
114.58
72.04
49.00 CD3OD
H
O
HO
B
OH
O
f1 (ppm)

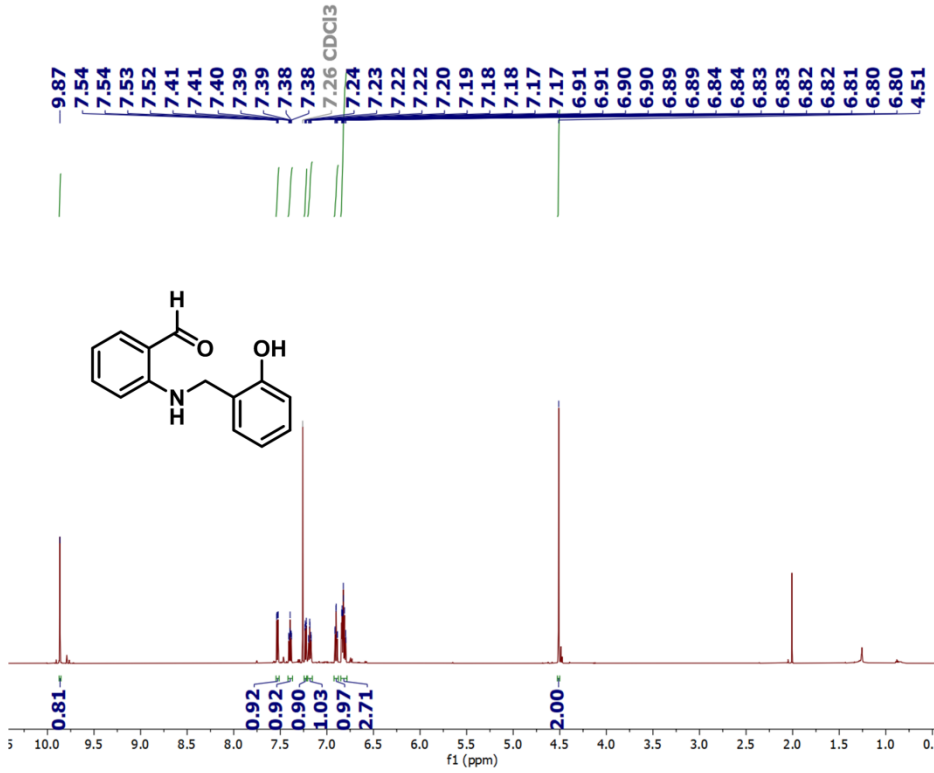
9.87
7.54
7.54
7.53
7.52
7.41
7.41
7.40
7.39
7.39
7.38
7.38
7.26 CDCl3
7.24
7.23
7.22
7.22
7.20
7.19
7.18
7.18
7.17
7.17
6.91
6.91
6.90
6.90
6.89
6.89
6.84
6.84
6.83
6.83
6.82
6.82
6.81
6.80
6.80
4.51
H
O
OH
N
H
0.81
0.92
0.92
0.90
1.03
0.97
2.71
2.00
f1 (ppm)

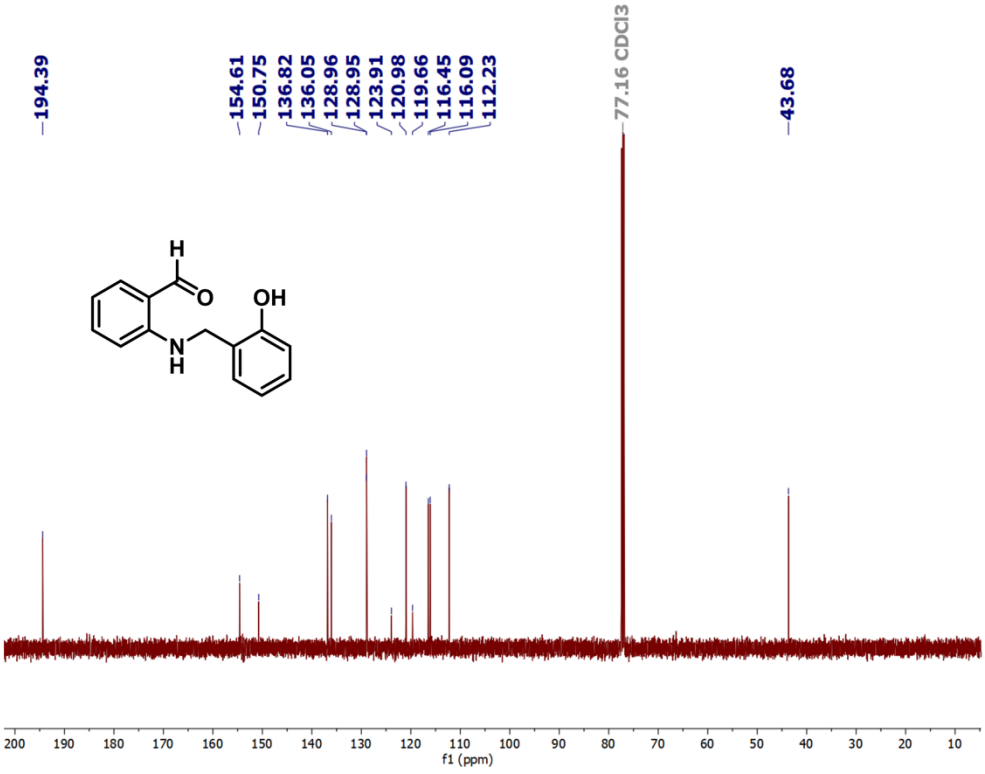
194.39
154.61
150.75
136.82
136.05
128.96
128.95
123.91
120.98
119.66
116.45
116.09
112.23
77.16 CDCl3
43.68
H
O
OH
N
H
f1 (ppm)

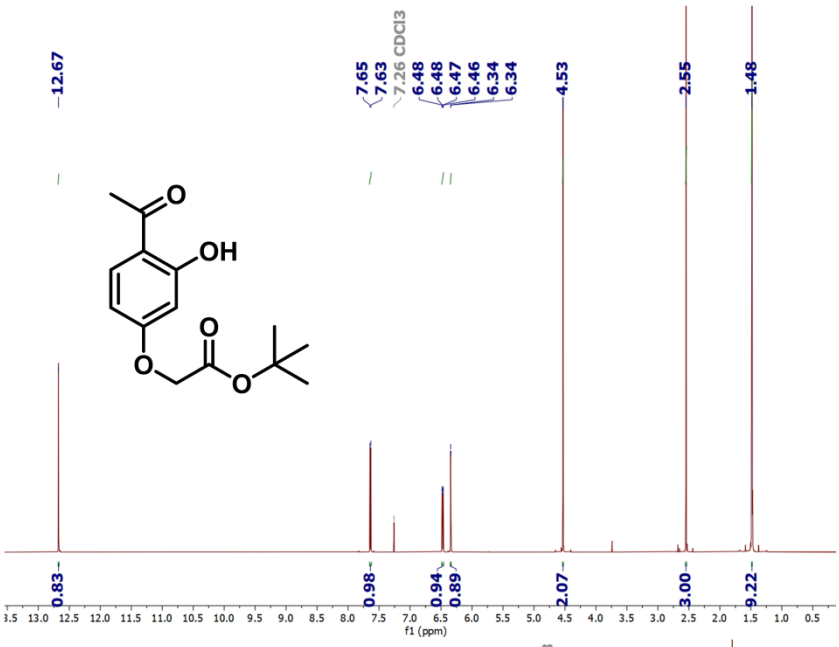
12.67
7.65
7.63
7.26 CDCl3
6.48
6.48
6.47
6.46
6.34
6.34
4.53
2.55
1.48
O
OH
O
O
O
0.83
0.98
0.94
0.89
2.07
3.00
9.22
f1 (ppm)

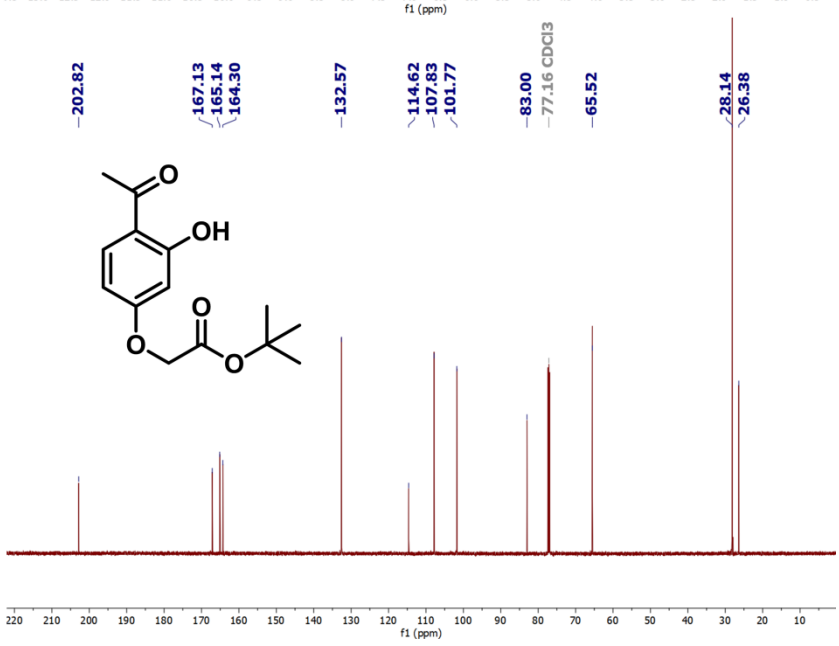
202.82
167.13
165.14
164.30
132.57
114.62
107.83
101.77
83.00
77.16 CDCl3
65.52
28.14
26.38
O
OH
O
O
O
f1 (ppm)

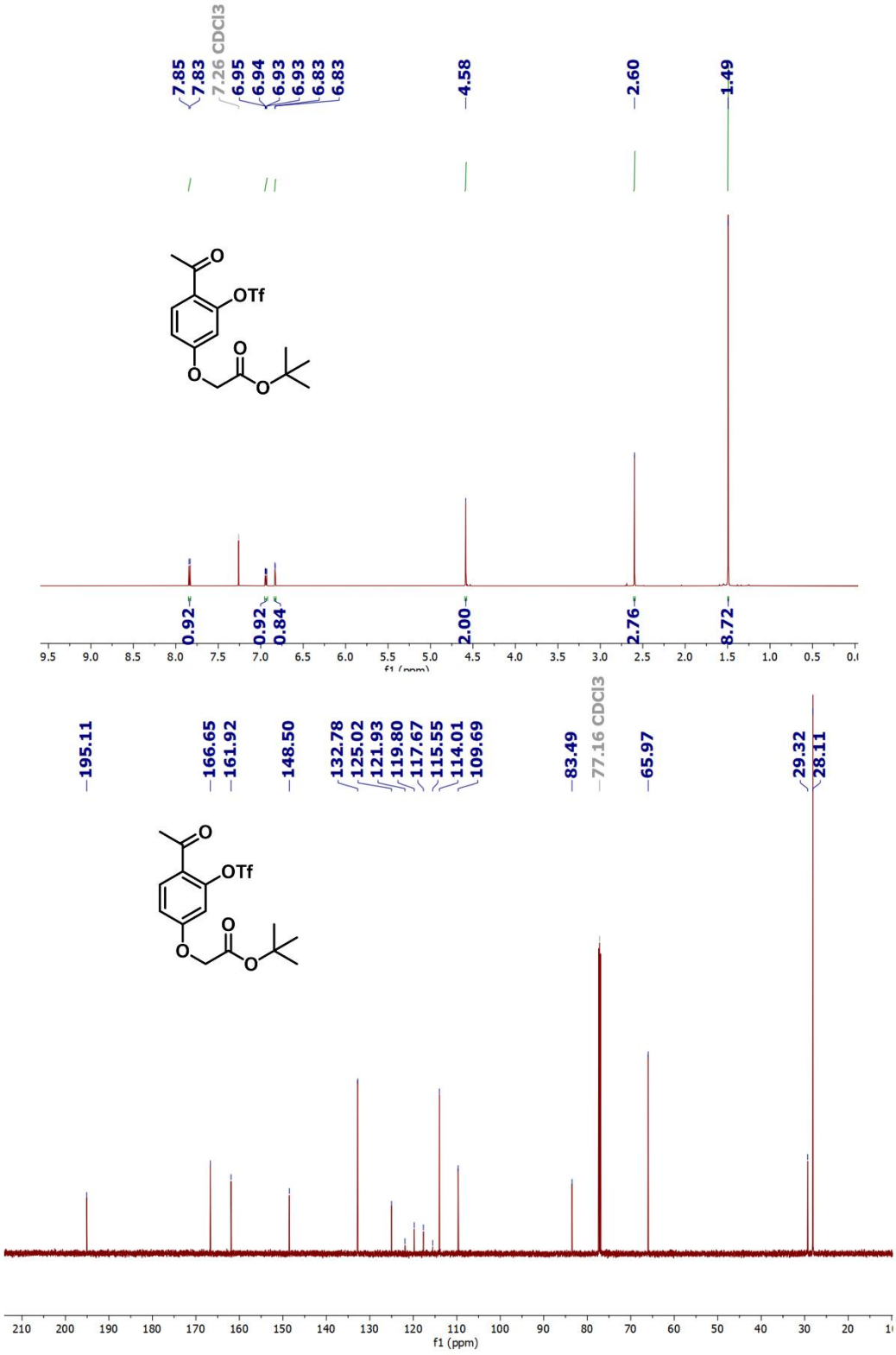
7.85
7.83
7.26 CDCl3
6.95
6.94
6.93
6.93
6.83
6.83
4.58
2.60
1.49
OTf
0.92
0.92
0.84
2.00
2.76
8.72
f1 (ppm)
195.11
166.65
161.92
148.50
132.78
125.02
121.93
119.80
117.67
115.55
114.01
109.69
83.49
77.16 CDCl3
65.97
29.32
28.11
OTf
f1 (ppm)

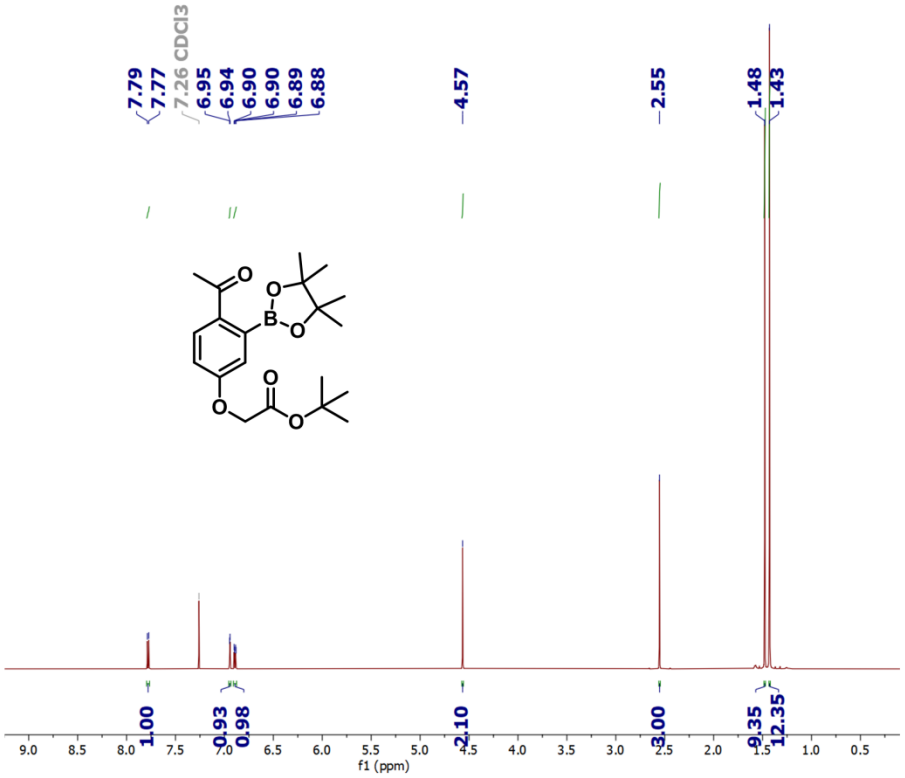
7.79
7.77
7.26 CDCl3
6.95
6.94
6.90
6.90
6.89
6.88
4.57
2.55
1.48
1.43
1.00
0.93
0.98
2.10
3.00
9.35
12.35
f1 (ppm)

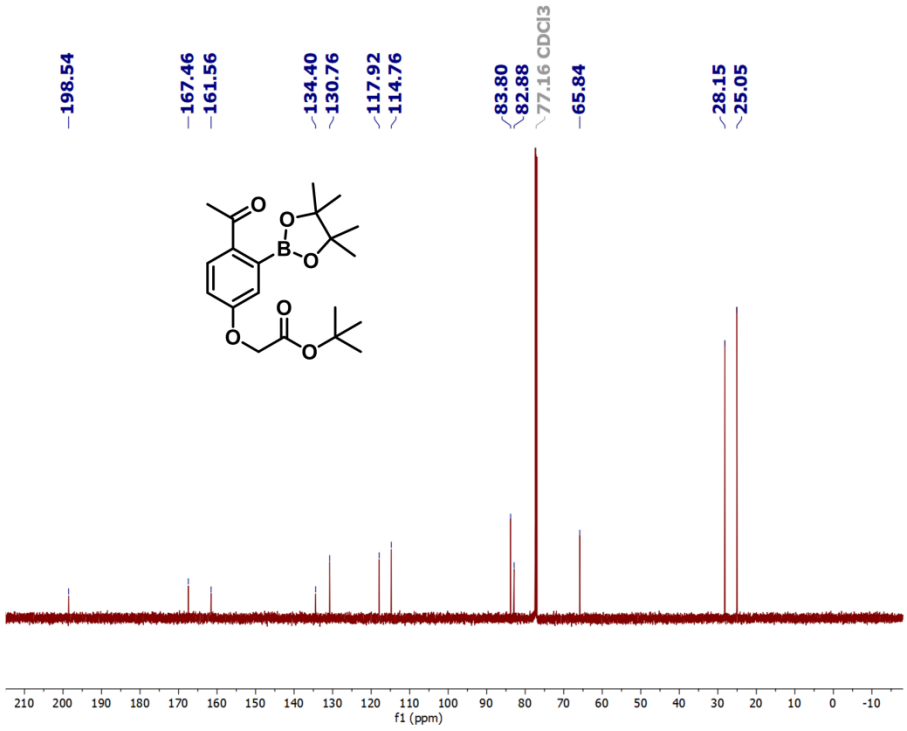
198.54
167.46
161.56
134.40
130.76
117.92
114.76
83.80
82.88
77.16 CDCl3
65.84
28.15
25.05
f1 (ppm)

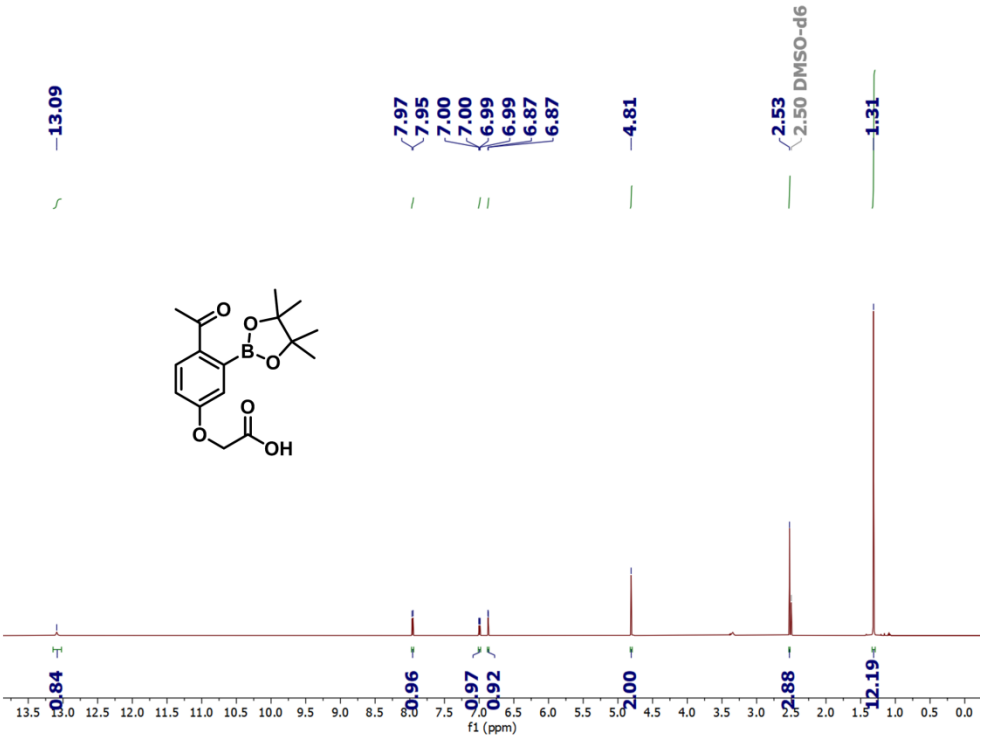
13.09
7.97
7.95
7.00
7.00
6.99
6.99
6.87
6.87
4.81
2.53
2.50 DMSO-d6
1.31
O
O
B
O
O
O
OH
0.84
0.96
0.97
0.92
2.00
2.88
12.19
f1 (ppm)

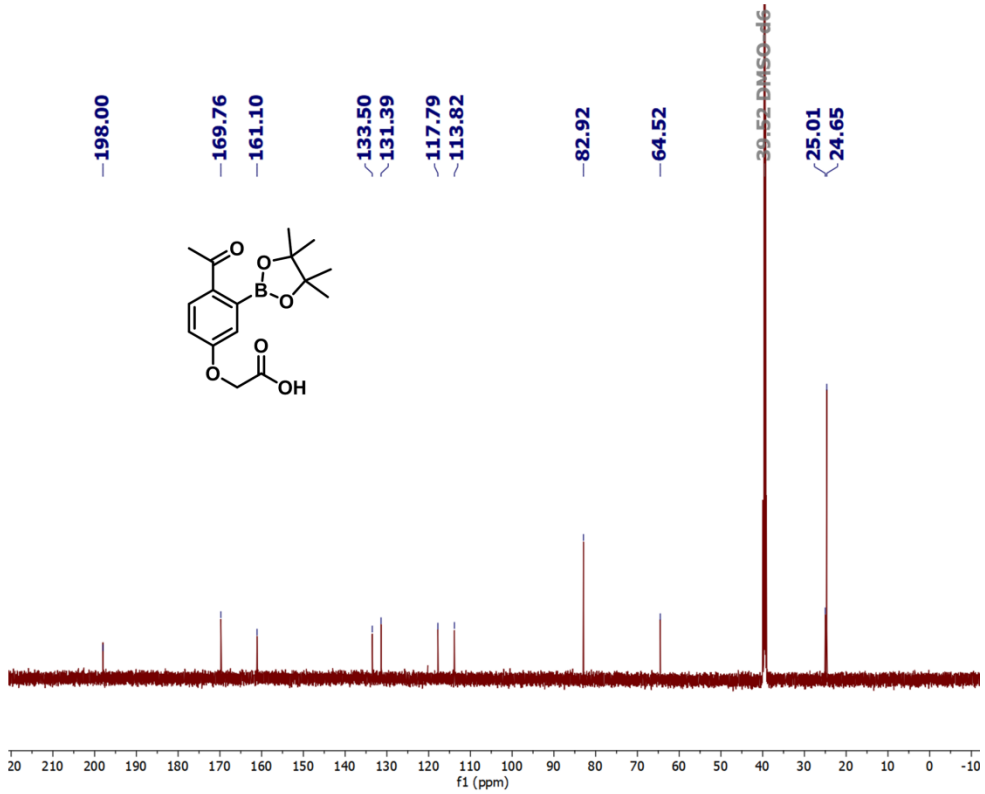
198.00
169.76
161.10
133.50
131.39
117.79
113.82
82.92
64.52
39.52 DMSO-d6
25.01
24.65
O
O
B
O
O
O
OH
f1 (ppm)

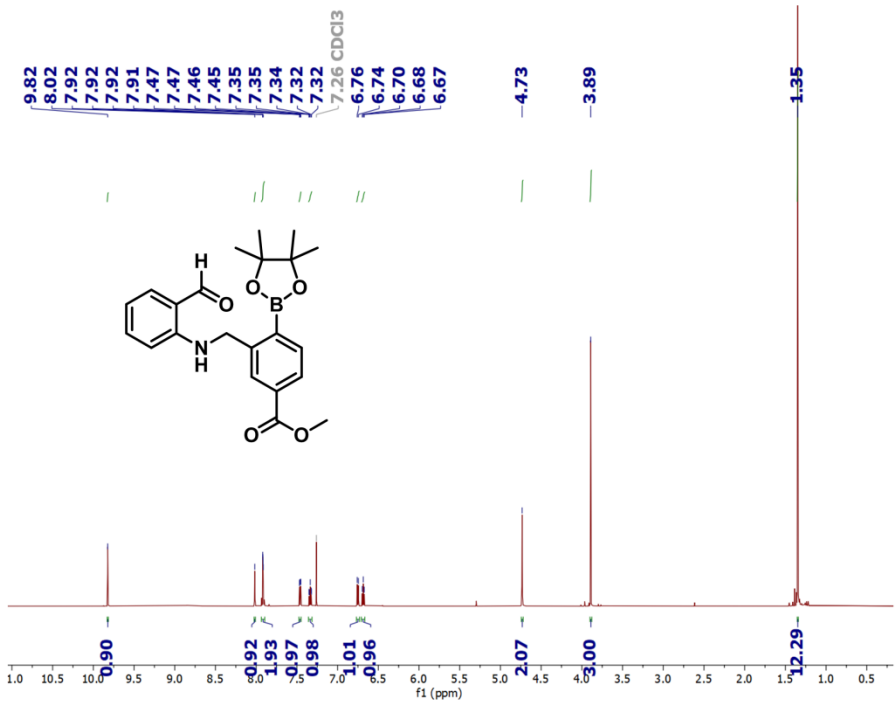
9.82
8.02
7.92
7.92
7.92
7.91
7.47
7.47
7.46
7.45
7.35
7.35
7.34
7.32
7.32
7.26 CDCl3
6.76
6.74
6.70
6.68
6.67
4.73
3.89
1.35
0.90
0.92
1.93
0.97
0.98
1.01
0.96
2.07
3.00
12.29
f1 (ppm)

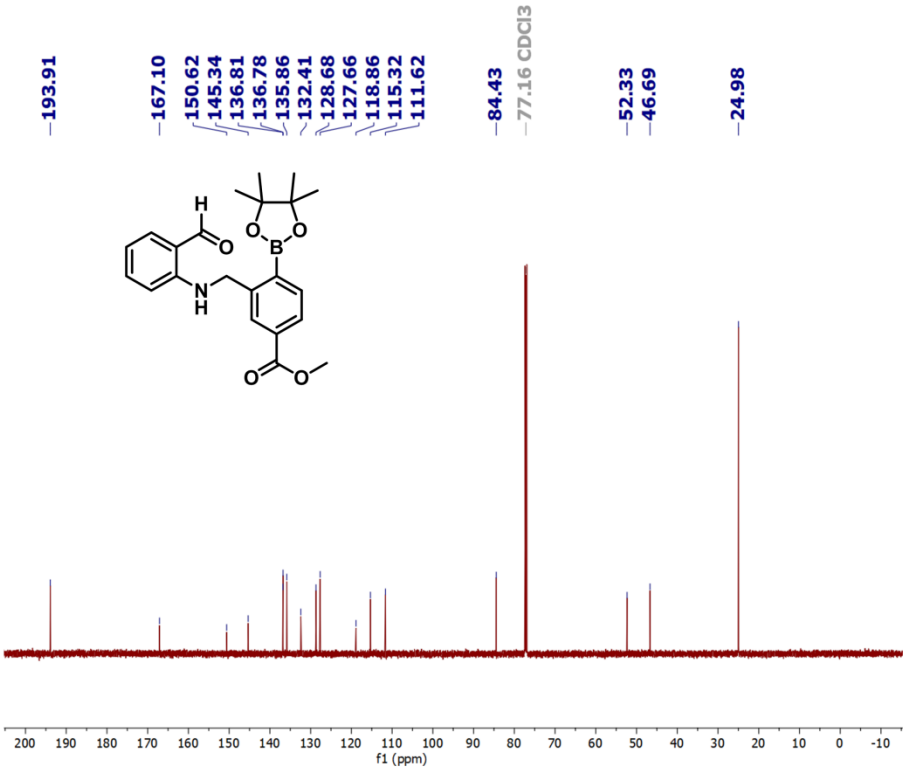
193.91
167.10
150.62
145.34
136.81
136.78
135.86
132.41
128.68
127.66
118.86
115.32
111.62
84.43
77.16 CDCl3
52.33
46.69
24.98
f1 (ppm)

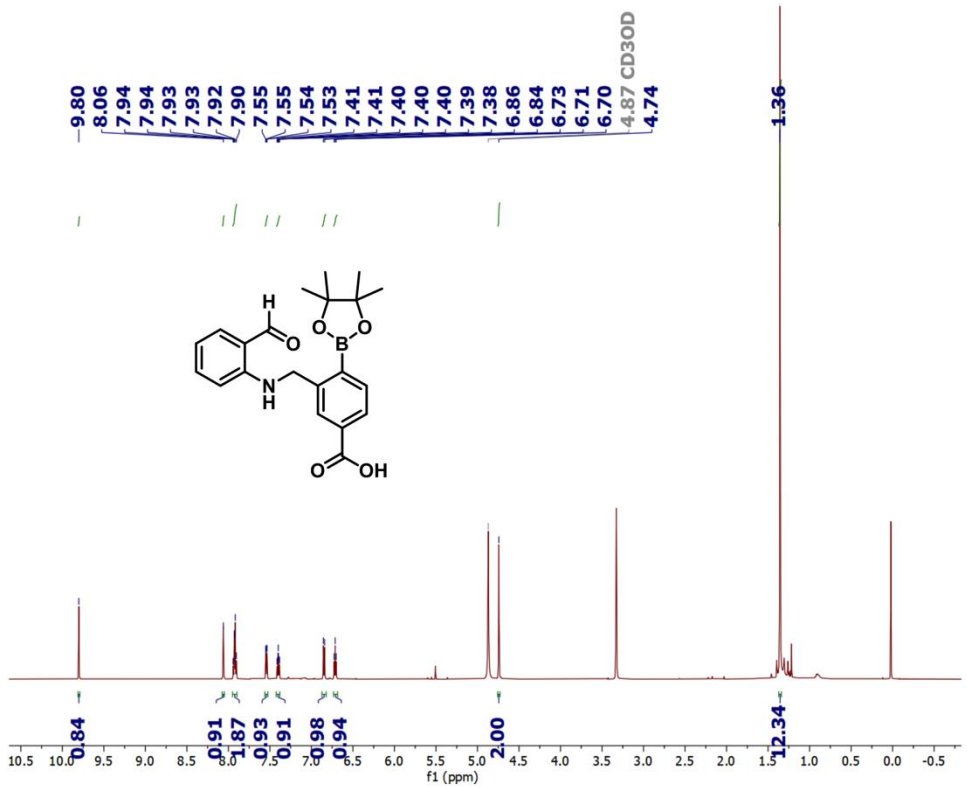
9.80
8.06
7.94
7.94
7.93
7.93
7.92
7.90
7.55
7.55
7.54
7.53
7.41
7.41
7.40
7.40
7.40
7.39
7.38
6.86
6.84
6.73
6.71
6.70
4.87 CD3OD
4.74
1.36
0.84
0.91
1.87
0.93
0.91
0.98
0.94
2.00
12.34
f1 (ppm)

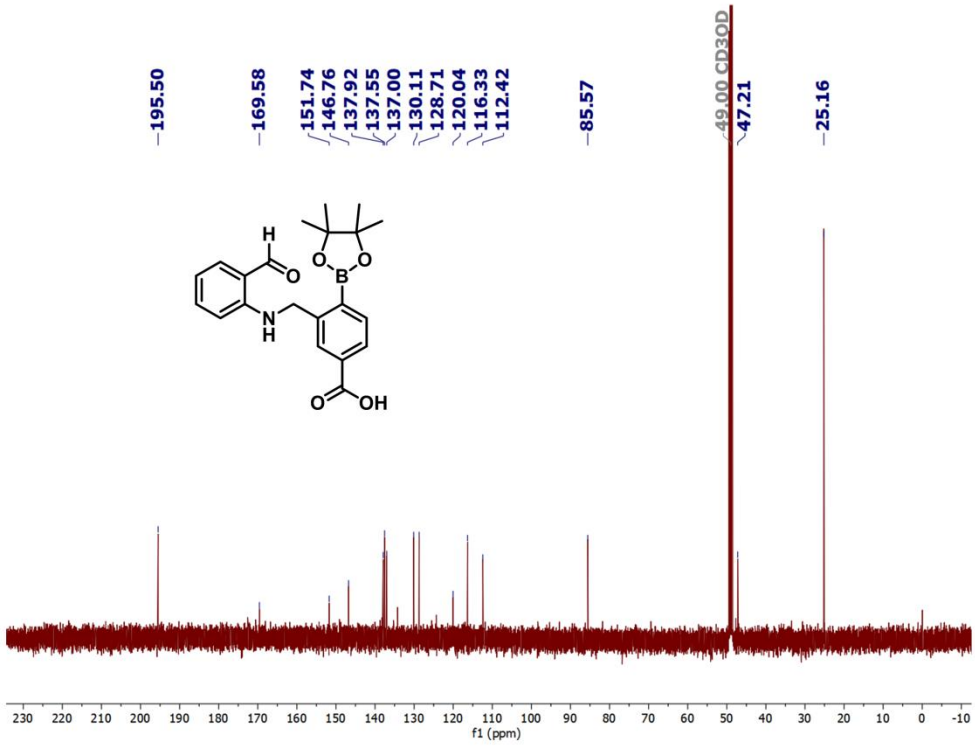
195.50
169.58
151.74
146.76
137.92
137.55
137.00
130.11
128.71
120.04
116.33
112.42
85.57
49.00 CD3OD
47.21
25.16
f1 (ppm)

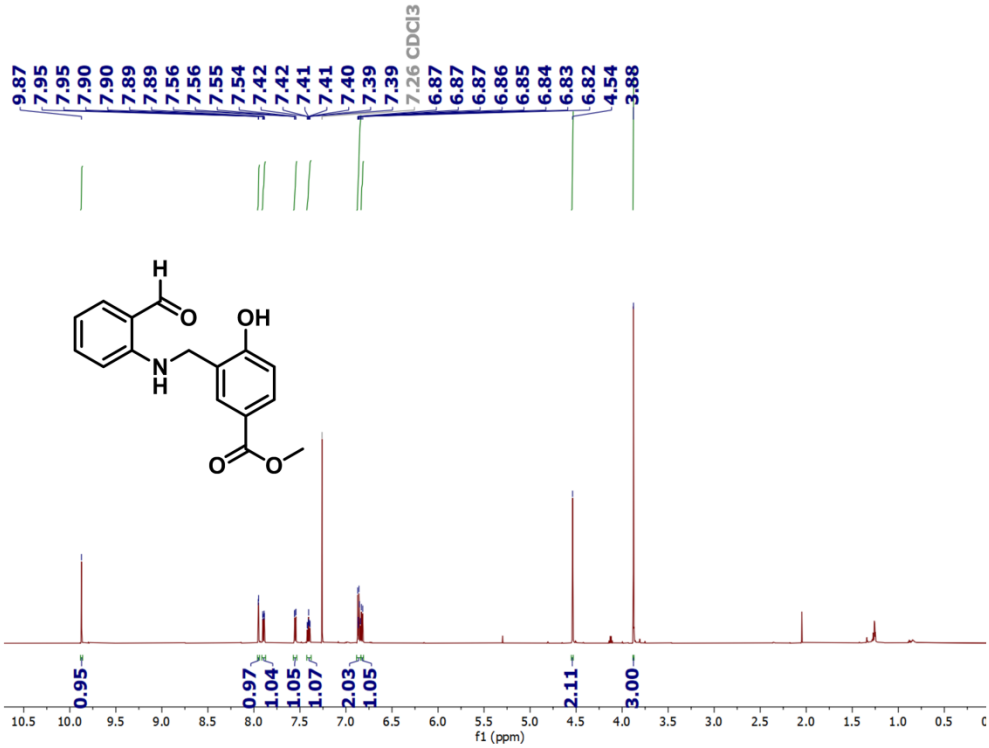
9.87
7.95
7.95
7.90
7.90
7.89
7.89
7.56
7.56
7.55
7.54
7.54
7.42
7.42
7.41
7.41
7.40
7.39
7.39
7.26 CDCl3
6.87
6.87
6.87
6.86
6.85
6.84
6.83
6.82
4.54
3.88
H
O
OH
N
H
O
O
0.95
0.97
1.04
1.05
1.07
2.03
1.05
2.11
3.00
10.5
10.0
9.5
9.0
8.5
8.0
7.5
7.0
6.5
6.0
5.5
5.0
4.5
4.0
3.5
3.0
2.5
2.0
1.5
1.0
0.5
f1 (ppm)

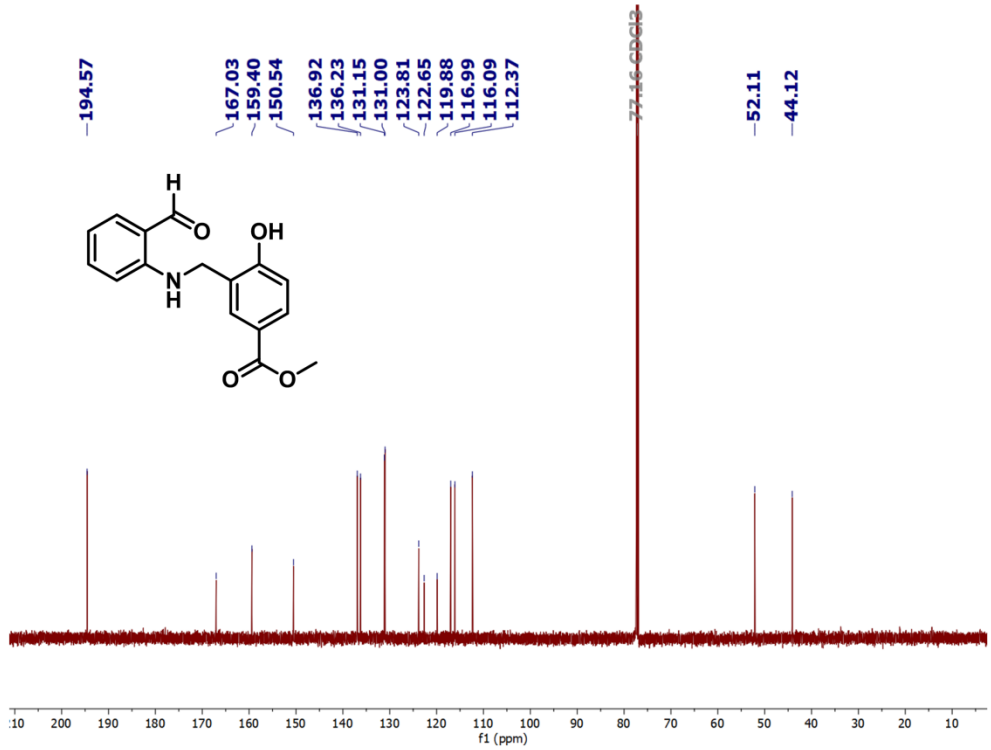
194.57
167.03
159.40
150.54
136.92
136.23
131.15
131.00
123.81
122.65
119.88
116.99
116.09
112.37
77.16 CDCl3
52.11
44.12
H
O
OH
N
H
O
O
210
200
190
180
170
160
150
140
130
120
110
100
90
80
70
60
50
40
30
20
10
f1 (ppm)

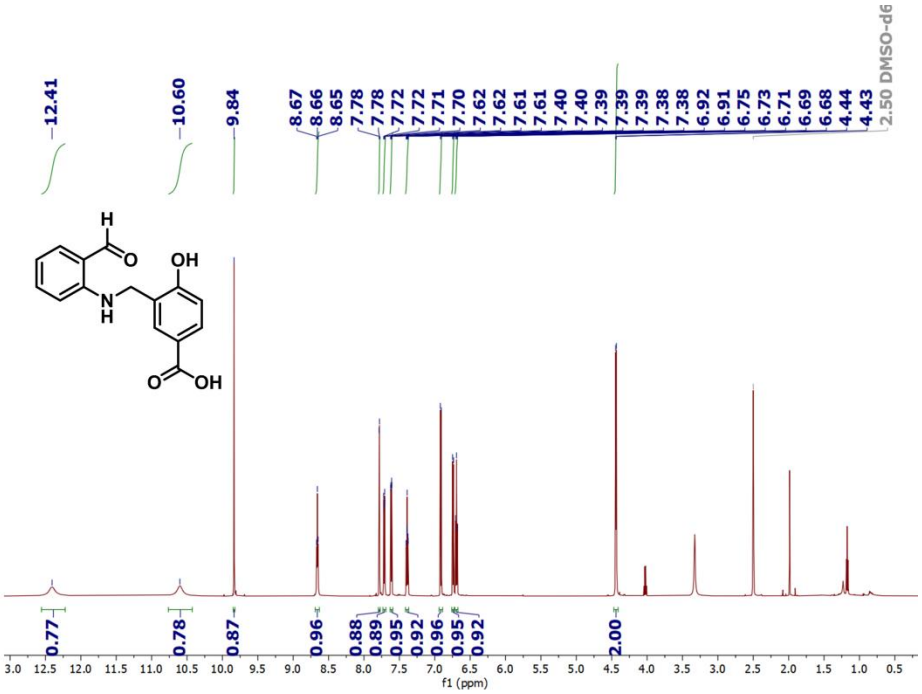
12.41
10.60
9.84
8.67
8.66
8.65
7.78
7.78
7.72
7.72
7.71
7.70
7.62
7.62
7.61
7.61
7.40
7.40
7.39
7.39
7.39
7.38
7.38
6.92
6.91
6.75
6.73
6.71
6.69
6.68
4.44
4.43
2.50 DMSO-d6
0.77
0.78
0.87
0.96
0.88
0.89
0.95
0.92
0.96
0.95
0.92
2.00
f1 (ppm)

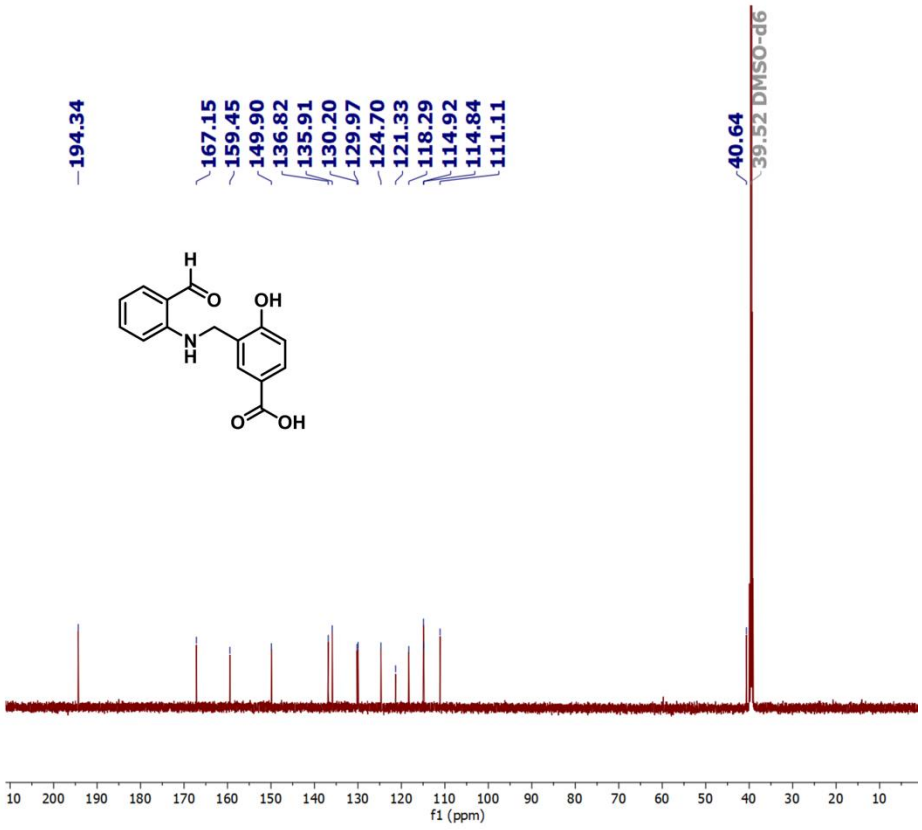
194.34
167.15
159.45
149.90
136.82
135.91
130.20
129.97
124.70
121.33
118.29
114.92
114.84
111.11
40.64
39.52 DMSO-d6
f1 (ppm)

20. SI References:

1. Li, K.; Wang, W.; Gao, J. *Angew. Chem. Int. Ed.***2020**, *59*, 14246.
2. Li, K.; Weidman, C.; Gao, J. *Org. Lett*. **2018**, *20*, 20.
3. Gaussian 16, Revision A.03, Frisch, M. J.; Trucks, G. W.; Schlegel, H. B.; Scuseria, G. E.; Robb, M. A.; Cheeseman, J. R.; Scalmani, G.; Barone, V.; Petersson, G. A.; Nakatsuji, H.; Li, X.; Caricato, M.; Marenich, A. V.; Bloino, J.; Janesko, B. G.; Gomperts, R.; Mennucci, B.; Hratchian, H. P.; Ortiz, J. V.; Izmaylov, A. F.; Sonnenberg, J. L.; Williams-Young, D.; Ding, F.; Lipparini, F.; Egidi, F.; Goings, J.; Peng, B.; Petrone, A.; Henderson, T.; Ranasinghe, D.; Zakrzewski, V. G.; Gao, J.; Rega, N.; Zheng, G.; Liang, W.; Hada, M.; Ehara, M.; Toyota, K.; Fukuda, R.; Hasegawa, J.; Ishida, M.; Nakajima, T. ; Honda, Y.; Kitao, O.; Nakai, H.; Vreven, T.; Throssell, K.; Montgomery, Jr. J. A.; Peralta, J. E.; Ogliaro, F.; Bearpark, M. J.; Heyd, J. J.; Brothers, E. N.; Kudin, K. N.; Staroverov, V. N.; Keith, T. A.; Kobayashi, R.; Normand, J.; Raghavachari, K.; Rendell, A. P.; Burant, J. C.; Iyengar, S. S.; Tomasi, J.; Cossi, M.; Millam, J. M.; Klene, M.; Adamo, C.; Cammi, R.; Ochterski, J. W.; Martin, R. L.; Morokuma, K.; Farkas, O.; Foresman, J. B.; Fox, D. J. Gaussian, Inc., Wallingford CT, **2016**.
4. Wang, L.; Dai, C.; Burroughs, S. K.; Wang, S. L.; Wang, B. *Chem. - Eur. J*. **2013**, *19*, 7587
5. Bandyopadhyay, A.; Gao, J. *Chem. - Eur. J*. **2015**, *21*, 14748.
6. Trott, O.; Olson, A. J. *J. Comput. Chem.* **2010,** *31*, 7587.
7. Rentero Rebollo, I.; McCallin, S.; Bertoldo, D.; Entenza, J. M.; Moreillon, P.; Heinis, C. *ACS Med. Chem. Lett.* **2016**, *7*, 606-611.